



In situ ellipsometry studies on swelling of thin polymer films: A review



Wojciech Ogieglo ^{a,*}, Herbert Wormeester ^b, Klaus-Jochen Eichhorn ^c,
Matthias Wessling ^d, Nieck E. Benes ^a

^a Inorganic Membranes, MESA+ Institute for Nanotechnology, University of Twente, Drienerlolaan 5, P.O. Box 217, 7500 AE Enschede, The Netherlands¹

^b Physics of Interfaces and Nanomaterials, MESA+ Institute for Nanotechnology, University of Twente, Drienerlolaan 5, P.O. Box 217, 7500 AE Enschede, The Netherlands²

^c Leibniz Institute for Polymer Research, Hohe Str. 6, P.O. Box 120 411, D-01069 Dresden, Germany³

^d DWI – Leibniz-Institute for Interactive Materials, Forckenbeckstrasse 50, 52074 Aachen, Germany⁴

ARTICLE INFO

Article history:

Received 11 April 2014

Received in revised form 3 September 2014

Accepted 22 September 2014

Available online 2 October 2014

Keywords:

In situ ellipsometry

Swelling

Thin polymer films

ABSTRACT

The properties of a thin polymer film can be significantly affected by the presence of a penetrant. This can have potential implications for many technological applications, such as protective and functional coatings, sensors, microelectronics, surface modification and membrane separations. *In situ* ellipsometry is a powerful technique for the characterization of a film in contact with a penetrant. The main advantages of ellipsometry include the very high precision and accuracy of this technique, combined with the fact that it is non-intrusive. Recent advances in the speed and automation of the technique have further expanded its application.

This article provides an overview of the research that has been done with *in situ* UV-vis ellipsometry on penetrant-exposed polymeric films, in the last 15–20 years. The focus is predominantly on films that are not attached covalently to a substrate. Polymer brushes and grafts are therefore excluded. This review addresses a variety of topics, covering instrumental aspects of *in situ* studies, approaches to data analysis and optical models, reported precision and repeatability, the polymer-penetrant systems that have been studied, the kind of information that has been extracted, and other *in situ* techniques that have been combined with ellipsometry. Various examples are presented to illustrate different practical approaches, the consequences of the optical properties of the ambient, and the various ways that have been employed to bring polymer films in contact with a penetrant, ranging from simple *ex situ*-like configurations (i.e., drying studies) to complex high pressure cells. The versatility of *in situ* ellipsometry is demonstrated by examples of the distinctive phenomena studied, such as film dilation, penetrant diffusion mechanisms, film degradation, electrochemical processes, and the broad variety of polymer-penetrant systems studied (glassy and rubbery polymers, multilayer stacks, etc.). An outlook is given on possible future trends.

© 2014 Elsevier Ltd. All rights reserved.

* Corresponding author.

E-mail addresses: w.ogieglo@utwente.nl (W. Ogieglo), h.wormeester@utwente.nl (H. Wormeester), kjeich@ipfdd.de (K.-J. Eichhorn), matthias.wessling@avt.rwth-aachen.de (M. Wessling), N.E.Benes@utwente.nl (N.E. Benes).

¹ Tel.: +31 53 489 2859.

² Tel.: +31 53 489 3148.

³ Tel.: +49 0351 4658 256.

⁴ Tel.: +49 0241 80 23179.

Contents

1.	Introduction and structure of the review	43
2.	Theory and instrumentation	45
2.1.	Ellipsometry – theory	45
2.2.	Ellipsometry – data interpretation and optical modeling	46
2.2.1.	Analysis of bulk samples, substrates and ambients	46
2.2.2.	Analysis of thin, transparent and absorbing films	47
2.2.3.	Optical models and modeling aspects	48
2.3.	In situ configurations	51
2.3.1.	No in situ sample cell	51
2.3.2.	Near-atmospheric pressure in situ cells	51
2.3.3.	High-pressure cells	53
3.	Types of polymeric materials studied	53
3.1.	Simple glassy polymers	53
3.2.	Simple rubbery polymers	54
3.3.	Random and block copolymers	54
3.4.	Multilayer films	55
3.5.	Other systems	56
4.	Types of polymer-penetrant phenomena studied	56
4.1.	Penetrant uptake from dry state	56
4.1.1.	Liquid water	57
4.1.2.	Water vapor	57
4.1.3.	Organic solvents, liquids and vapors	58
4.1.4.	High-pressure gases	59
4.2.	Drying processes	60
4.3.	Thermally, pH, and ionic strength induced transitions	61
4.4.	Reactions at interfaces, depositions and formations	62
4.5.	Dissolution or degradation	63
4.6.	Electrochemically induced swelling changes	64
5.	Types of information extracted with the use of in situ ellipsometry	64
5.1.	Dynamic studies	64
5.1.1.	Simple dynamic phenomena	64
5.1.2.	Complex dynamic phenomena	65
5.2.	Penetrant volume fraction calculations	67
5.3.	Thermodynamic parameters	68
6.	Ellipsometry combined with other techniques	69
6.1.	Ellipsometry concurrently combined with other techniques in situ	69
6.2.	Ellipsometry complemented with other in situ techniques	69
6.2.1.	Quartz crystal microbalance (QCM)	70
6.2.2.	Atomic force microscopy (AFM)	70
6.2.3.	Neutron and X-ray reflectivity	70
6.2.4.	Electrochemical methods	72
6.2.5.	Gravimetric methods	72
6.2.6.	Contact angle measurements	72
6.2.7.	UV-vis spectroscopy	72
6.2.8.	IR spectroscopy	73
6.2.9.	Surface plasmon resonance (SPR)	73
6.2.10.	Methods to determine mechanical properties	73
7.	Concluding remarks and outlook	73
	Acknowledgments	74
Appendix	74	
Appendix B. Supplementary data	75	
References	75	

1. Introduction and structure of the review

Thin and ultra-thin polymer films in contact with penetrants are very relevant systems in many areas, including protective and functional coatings, sensors, microelectronics, surface modifications and membrane separations. Spectroscopic ellipsometry (SE) is a well-established optical technique that has been used for many years mainly in the semiconductor research and industry. Due to advances

in instrumentation in the recent years ellipsometry has been increasingly used in the field of thin polymer film characterization. In particular, the large advantages of the technique are apparent when the studied films are exposed to various ambients that affect the film properties. The reasons for the increasing interest in the use of ellipsometry for such studies are that the technique retains its very high precision and accuracy, non-intrusive character, and high temporal resolution even in the presence

List of abbreviations

Chemical names

BSA	bovine serum albumin
CF _x	fluoropolymer
DMPC	dimyristoylphosphatidylcholine
DNA	deoxyribonucleic acid
HA	hyaluronic acid
Matrimid	polyimide of 3,3',4,4'-benzophenone tetracarboxylic dianhydride and diamino-phenylidene
p(HEMA- <i>co</i> -EGDA)	poly[(2-hydroxyethyl methacrylate)- <i>co</i> -(ethylene glycol diacrylate)]
p(NIPAM- <i>co</i> -AA)	poly(<i>N</i> -isopropyl acrylamide- <i>co</i> -acrylic acid)
PAA	poly(acrylic acid)
PAArVBA	poly(acrylic acid- <i>ran</i> -vinylbenzyl acrylate)
PAH	poly(allylamine hydrochloride)
PANI	polyaniline
PC	phosphorylcholine
PDADMAC	poly(diallyldimethylammonium chloride)
PDMAEMA	poly(2-dimethylaminoethyl methacrylate)
PDMS	poly(dimethyl siloxane)
PEBAX	poly(amide-6- <i>b</i> -ethylene oxide)
PEG	poly(ethylene glycol)
PEI	poly(iminoethylene), poly(ethylene imine)
PEO	poly(ethylene oxide)
PES	poly(ethersulfone)
PFOMA	poly(1,10-dihydroperfluoroctyl methacrylate)
PGA	poly(L-glutamic acid)
PHEMA	poly(2-hydroxyethyl methacrylate)
PLL	poly(L-lysine)
PMMA	poly(methyl methacrylate)
PNIPAM	poly(<i>N</i> -isopropyl acrylamide)
PNVP	poly(<i>N</i> -vinyl pyrrolidone)
Posimca50	poly(methylcarboxypropyl siloxane)
PPO	poly(<i>p</i> -phenylene oxide)
PS	poly(styrene)
PSF	polysulfone
PSS	poly(styrenesulfonate)
PVME	poly(vinyl methyl ether)
PVP	poly(2-vinylpyridine)
PVS	poly(vinyl sulfonate)
SPEEK	sulfonated poly(ether ether ketone)
SSEBS	polystyrene- <i>block</i> -poly(ethylene- <i>ran</i> -butylene)- <i>block</i> -polystyrene

Other abbreviations

AFM	atomic force microscopy
EMA	effective medium approximation
iCVD	initiated chemical vapor deposition
MOFs	metal-organic frameworks
OWS	optical waveguide spectroscopy
P _g	penetrant induced glass transition

QCM	quartz crystal microbalance
RH	relative humidity
RSD	relative standard deviation
sc-CO ₂	supercritical carbon dioxide fluid
SE	spectroscopic ellipsometry
SPR	surface plasmon resonance
T _g	glass transition temperature
VOCs	volatile organic compounds

of various fluids, including high-pressure gases and vapors.

This article provides a review of the research that has been done in the last 15–20 years, involving *in situ* ellipsometry studies of thin films exposed to penetrants. The focus is predominantly on polymer films that are not attached covalently to the substrates.

In Section 2, the theoretical basis and experimental aspects of ellipsometry are outlined. The precision and repeatability of the analysis of typical thin film polymeric samples are illustrated with examples. The examples are based on already published data, as well as on some unpublished data. Practical approaches to analysis of samples in contact with various penetrants are highlighted and the accurate determination of ambient and substrate optical constants is addressed. The paragraph also provides a survey of the optical models employed in the literature, illustrated with some noteworthy examples. The various means employed to bring thin polymer films in contact with penetrants are described, ranging from simple *ex situ*-like configurations (i.e., drying studies) to complex high-pressure cells.

Further paragraphs focus on the particular studies presented in the literature. The technique has been applied to a very broad range of different polymeric systems that can be classified as relatively simple (glassy/rubbery polymers) and more complex ones (copolymers, multilayers and composites). A wide range of investigated phenomena demonstrates the versatility of the technique. These are not limited to determination of film swelling by the penetrant, but also address complex diffusion mechanisms, polymer degradation, glass transitions, and electrochemical processes. Often penetrant concentrations and thermodynamic parameters describing polymer-penetrant mixtures are extracted from the analysis. The various approaches to these calculations found in the literature are presented and their applicability is discussed.

In the majority of studies, especially in the more recent ones, ellipsometry has been combined with other *in situ* techniques. This has been done concurrently, using the same sample and experimental cell, or non-concurrently, where the measurements are done on separate samples but yield complementary information. Examples of studies in both categories are shown with particular focus on the complementarity of the information gathered with the combined techniques.

All *in situ* ellipsometry studies that are discussed are presented in an extensive reference table (supplementary information) that summarizes the most important

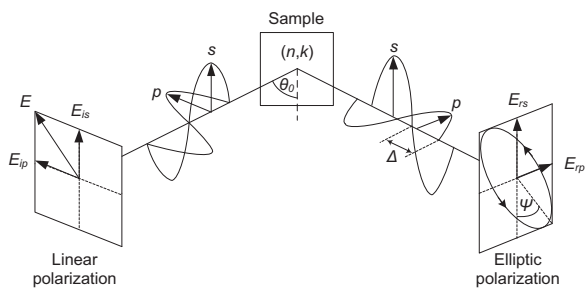


Fig. 1. Schematics of ellipsometric measurement principle [6]. Copyright 2007. Adapted with permission from John Wiley & Sons Inc.

information with regard to the contents of 80 publications on in situ swelling studies. The table categorizes the publications with respect to the polymer-penetrant systems studied, in situ set-up used, information extracted, etc.

Finally, conclusions are given and an outlook for the possible future trends is provided.

2. Theory and instrumentation

2.1. Ellipsometry – theory

Ellipsometry is a non-destructive optical technique that allows for very precise and accurate analysis of the optical properties of various thin film systems, including film thickness and dielectric constants. Ellipsometry relies on the changes in the polarization state of light upon reflection from, in general, multilayer systems. The first experiments employing the change in polarization of light upon reflection and refraction were conducted as far back as the early nineteenth century, by Sir David Brewster and later Jules Jamin. These experiments led to formulation of the respective laws of Brewster and Jamin. Hendrik Antoon Lorentz made important contributions to the mathematical formulation of Maxwell's equations, applied to light [1]. These developments allowed quantitative physical interpretation of light reflection and transmission. Much of the development of the theory, instrumentation and application of ellipsometry can be ascribed to the pioneering contributions of Paul Drude [2–4], although others made important contributions much before him [5]. A rapid growth of the use and the applicability of ellipsometry has been observed within the past 15–20 years, due to the significant progress in speed and automation of measurements and data analysis.

In a typical ellipsometry configuration, Fig. 1, light from a light source passes through a polarizer unit that sets the incident polarization state. Typically, this incident polarization state is linear for older SE instruments with only a polarizer on the incident beam, or elliptic for more modern devices that possess fixed or rotating compensators or photoelastic modulators. The probing light can be monochromatic (most commonly a He-Ne laser at 632.8 nm) or spectroscopic (incandescent or arc discharge lamps). Upon reflection from a sample, at a certain angle, the polarization state is changed. In general, the polarization state of the reflected light is elliptic, evincing the name of the technique.

The change in polarization state is measured by a second polarizer coupled with a detector, the analyzer. The reflected light polarization state can be described in terms of the two angles: psi (Ψ) and delta (Δ). For a linear polarization of the incident light, that is when $E_{ip} = E_{is}$:

$$\tan(\Psi) \cdot e^{i\Delta} \equiv \frac{r_p}{r_s} \equiv \frac{E_{rp}}{E_{rs}} \equiv \rho(N_0, N_1, \dots, N_m, h_1, \dots, h_{m-1}, \theta_0) \quad (1)$$

The subscripts p and s refer to parallel and perpendicular (in German: senkrecht), with respect to the plane of incidence, and r_p and r_s represent the reflection coefficients. E denotes the electric field and subscripts i and r denote the incident and reflected light respectively. As such, Ψ represents the angle determined from the amplitude ratio between p - and s -polarizations, while the Δ represents the phase difference between the two components. The complex reflectance ratio, ρ , is a complex function of the optical structure of the sample and includes information about its physical properties. The polarization state of the reflected light depends on the angle of incidence, θ_0 , the thicknesses of the $m - 1$ layers, h , and the complex refractive indices ($N = n + ik$) of all of these layers, the ambient (N_0), and the substrate (N_m). This signifies the richness of information contained in the probing light.

In the early relatively simple instruments only the polarizing elements between the light source and the detector were used. The subsequent addition of a compensator allowed working with partially depolarizing samples, thereby extending the applicability of ellipsometry to samples with non-uniform thickness. This is particularly important for polymer samples that are obtained via spin coating or dip coating. A compensator contributes to higher flexibility of the ellipsometry technique, because it allows including non-idealities in an optical model of the sample. More detailed information on the principles of optics relevant for SE, on the optical elements used in typical configurations, as well as on the historical record of developed instruments can be found in textbooks [6–8].

In the case of monochromatic ellipsometry, the measurable parameters include only a single pair of Ψ and Δ for the single wavelength of the light, at a single angle of incidence. This means that at maximum two parameters can be simultaneously determined from the measurement, for example the film thickness, h , and the refractive index n . In the case of some thin film samples this can be enough information. In SE a measurement generates a pair of Ψ and Δ for each employed wavelength. The optical dispersion can usually be modeled with an expression using much less parameters than the number of determined Ψ and Δ pairs (for instance, Cauchy dispersion). Consequently, the number of sample parameters that can be independently determined increases significantly. This opens possibilities for the characterization of complex samples, where light absorption, optical anisotropy, density gradients, roughness, and other features of the probed layers can be determined in addition to film thickness and refractive index.

For ellipsometry, a clear distinction between precision and accuracy is important. Accuracy relates to the proximity of measurement results to the true value. Precision

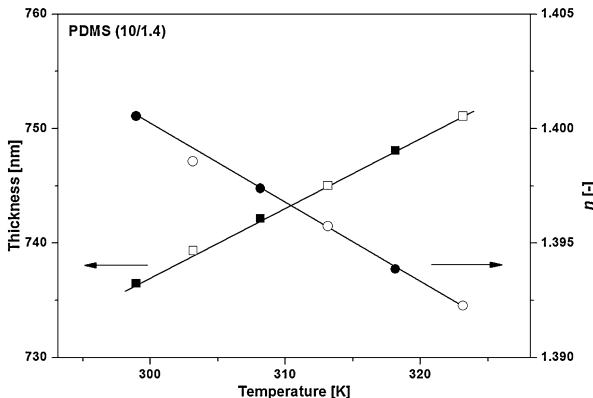


Fig. 2. Demonstration of the ellipsometry precision for the determination of film thickness and refractive index of ~ 730 nm poly(dimethyl siloxane) (PDMS) film supported on a glass slide [9], closed and open symbols represent the heating and cooling modes respectively; lines are linear fits through the data [9].

Copyright 2013. Adapted with permission from Elsevier Science Ltd.

relates to the repeatability, or reproducibility of the measurement. The accuracy of ellipsometry depends very much on the validity of the assumptions related to the sample and is discussed in Section 2.2.3. The very high precision of ellipsometry originates from the fact that modern optical devices enable very precise quantification of changes in the polarization state of light. This is accomplished by the measurement of *p*- and *s*-polarization light intensity ratios, Eq. (1), instead of the absolute intensities. This approach is especially beneficial for *in situ* measurements, because the introduction of a fluid ambient usually causes losses in the absolute intensity. Typically, the instrumental standard deviations in Ψ and Δ are on the order of 0.01–0.02°. For an optically uniform and transparent polymer film on a polished silicon wafer this translates into a precision in thickness determination on the order of 0.1 nm. Fig. 2 shows an example of the precision of the ellipsometric measurements for a thin polydimethyl siloxane (PDMS) film, exposed to increasing and decreasing temperature [9]. In the temperature range studied, PDMS can be considered an equilibrium liquid polymer. For such a polymer the observed linear dependence of thickness and refractive index, and the absence of hysteresis, are expected. The experimental data agree within 10% with literature data for thermal expansion coefficient of bulk PDMS. Such a difference is reasonable given the true differences in materials properties that will exist between different PDMS samples. The very small deviation from linearity, or scatter, allows estimating the thickness precision to be in the fraction of a nanometer. For the refractive index the precision is around ~ 0.0005 .

As another example three data sets are shown in Fig. 3, which have been measured with a light spot-size of about 2 mm in diameter for a thin polystyrene (PS) film spin coated on a 1.5 cm \times 1.5 cm silicon wafer. The sample has been annealed above its glass transition temperature, to relax post-preparation stresses and to remove any remaining solvent. Squares correspond to measurements of 15 different spots on the sample. Circles correspond to data measured by placing the sample on the ellipsometer stage,

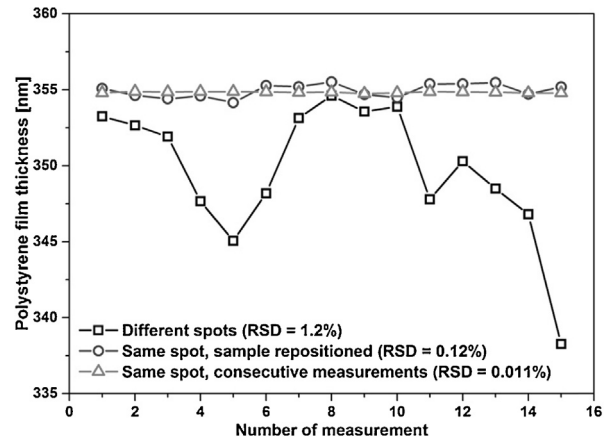


Fig. 3. Ellipsometry repeatability and precision: squares represent measured values from 15 different spots on the same 1.5 cm \times 1.5 cm sample; circles represent measured values when the sample is repeatedly placed on the ellipsometer stage, aligned, measured, taken off and re-positioned again on approximately the same spot as before; triangles represent consecutive measurements done on the same spot without sample repositioning. RSD indicates the relative standard deviations for the respective 15 measurement points. Data has been collected with an M-2000X spectroscopic ellipsometer of J.A. Woollam Co., Inc. at 70° angle of incidence and a PS film spin-coated on a crystalline silicon wafer.

aligning, measuring, and taking the sample off the stage again, followed by repeating this whole procedure. The measurement spot is kept approximately the same as before. Triangles correspond to data measured on the same spot but without repositioning the sample. Scatter in the data is quantified in terms of the relative standard deviation (RSD) in 15 measurements. The RSD decreases by approximately 1 order of magnitude going from squares to circles, and another order of magnitude when going from circles to triangles. The scatter in the dataset represented by the triangles corresponds solely to the precision of the measuring device and the modeling algorithm. The extremely low $RSD = 0.011\%$ signifies the very high precision of ellipsometry and the potential to study changes in film thickness within a fraction of a nanometer. The dataset represented by the circles, with $RSD = 0.12\%$, corresponds roughly to the operator error, related to the repeatability of placing the sample in the same spot. The highest $RSD = 1.2\%$ for the squares corresponds to thickness non-uniformity within the sample and is related to its preparation process. The value of 1.2% is typical for a spin-coated PS film. Other polymers can be characterized by much worse thickness uniformity after preparation. This will especially be the case for high-performance polymers, with a high glass transition temperature.

2.2. Ellipsometry – data interpretation and optical modeling

2.2.1. Analysis of bulk samples, substrates and ambients

In certain cases the Ψ and Δ can be directly used to calculate the properties of simple samples (n and k) from the reflection at the sample/ambient interface, Fig. 4. This is useful when the interest is in the characterization of a complex refractive index of a bulk material, for example: (i)

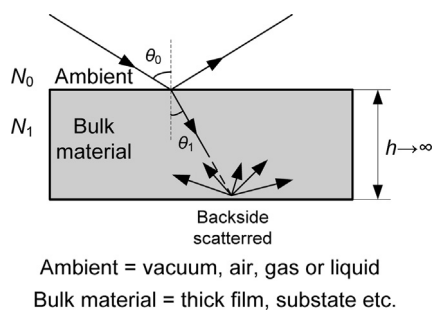


Fig. 4. Reflection from a very thick, bulk film or a substrate with backside reflection eliminated by scattering.

a particular polymeric substance, (ii) a substrate intended for further thin film analysis, or (iii) an experimental ambient (N_0) for the in situ measurements. For the latter case the optical properties of the bulk film need to be known in advance. In addition, the influence of the experimental ambient on the optical properties of the bulk material should be negligible. This is for instance the case for a glass slide immersed in pure water. For these types of measurements the sample is often assumed to be perfectly polished (negligible roughness) and the light reflection from the backside is disregarded. The last assumption can be fulfilled by analyzing a relatively thick sample (several mm) or by mechanically roughening the backside surface of the substrate. Alternatively, adhesive tape can be applied at the backside to scatter transmitted light. Elimination of the backside reflection has been found to be the best method for dealing with thick substrates [R. Synowicki of J.A. Woollam Co. Inc., private communication].

Quantitative information about refractive index of the ambient, N_0 , in a range of experimental temperatures, is of particular importance for in situ applications. Many in situ ellipsometry measurements are done in liquid water for which optical properties are very well known [10]. Applications do exist that involve a different ambient. These include aqueous solutions of simple and complex compounds, organic solvents, ionic liquids, compressed gasses, etc. Accurate knowledge of the optical dispersion of the particular ambient, at the experimental conditions, is an absolute prerequisite for accurate determination of the optical properties of the analyzed film. This is in particular the case for the determination of the optical dispersion of a swollen film. In that case the ambient fluid is also present in the analyzed film, where it contributes to the optical properties of the swollen film.

In the case of the single wavelength ellipsometry, the measurement of the Ψ and Δ enables determination of two parameters of the system. For example, with a known θ_0 :

- If the ambient is air ($n_0 = 1, k_0 = 0$), then n_1 and k_1 (at the wavelength of measurement) of the sample material can be determined.
- If the substrate complex refractive index is known (n_1 and k_1), then the ambient properties, n_0 and k_0 , can be determined. This is only valid assuming that the presence of the ambient does not alter properties of the substrate,

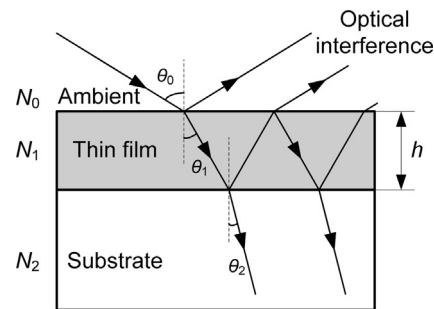


Fig. 5. Optical structure of a typical in situ ellipsometric sample [6]. Copyright 2007. Adapted with permission from John Wiley & Sons Inc.

for example by preferential adsorption of the dissolved species, etc.

In SE, the complete optical dispersions (n and k as a function of light wavelength) can be determined in the same way. Details of these calculations can be found in ellipsometry textbooks [6–8], and are briefly outlined in Appendix. As an alternative method to determine the ambient dispersion, a minimum deviation approach employing a prism-shaped experimental cell can be used [11].

2.2.2. Analysis of thin, transparent and absorbing films

In in situ ellipsometry studies, the samples are in general thin polymer films on top of supporting substrates, Fig. 5. When light enters such a sample it reflects and transmits at each of the interfaces. The rays leaving the sample interfere with each other and produce spectral oscillations in Ψ and Δ . A more detailed mathematical description can be found in Appendix.

Fig. 6a and b shows SE Ψ and Δ spectra simulated for a 1000 nm film of an optically transparent PDMS polymer supported on a polished crystalline silicon wafer. The spectra have been generated based on realistic input parameters regarding optical dispersion of PDMS [9]. The bare substrate spectra are also shown. The optical dispersion of PDMS, $n(\lambda)$, is shown in Fig. 6c; note that over the full wavelength range $k_{PDMS} = 0$.

The minima of the oscillations in Ψ , in Fig. 6a, coincide with the spectrum of the bare silicon substrate, which is referred to as the so-called spectral envelope. This feature of the Ψ spectrum holds for any transparent film/substrate system. The Δ spectrum oscillates around its value for the substrate. The number of oscillations in both Ψ and Δ is related to the optical thickness of the film, $n \cdot h$, and increases with increasing film thickness h and refractive index n . For most of the typical polymeric materials the refractive index (at 632.8 nm) varies in a relatively narrow range ($n = 1.4\text{--}1.6$), therefore, the number of oscillations in a certain wavelength range (for instance 380–1000 nm) can be treated as a rough estimate of the polymer film thickness, see for examples Table 1.

As the film thickness increases an increasing number of oscillations needs to be covered within the spectral resolution of an ellipsometer. This implies, that for thicker films the accuracy of the spectrum representation decreases. In practice, measurements on samples thicker than about

Table 1

Approximate number of spectral oscillations for 4 different thicknesses and 3 different refractive indices (given at 632.8 nm) in a visible range typical for most common polymeric materials.

Film thickness [nm]	$n = 1.4$	$n = 1.5$	$n = 1.6$
500	2	2	3
1000	4	4	4
2000	8	8	9
5000	19	20	23

2000–3000 nm may be considered relatively inaccurate. For the same reason, the spectral representation of a film with a certain thickness is also worse in the shorter wavelength range, where the oscillations are more densely distributed. Additionally, for short wavelengths the effects of a finite spectral bandwidth become apparent. In the simulations presented in Fig. 6a a finite bandwidth of 4 nm is considered at each wavelength, rather than using an exact single wavelength value. In the UV range this spectral bandwidth results in deviations between the minima in Ψ and the envelope.

Fig. 7 shows similar data simulated for a 1000 nm film of a sulfonated poly(ether ether ketone) (SPEEK), which is a light absorbing polymer. Its optical dispersion is plotted in Fig. 7c. As can be seen from the figure, in a transparent region (above about 400 nm) the Ψ and Δ spectra show a similar behavior as for the PDMS, Fig. 6, with the oscillations being limited by the substrate envelope. In the range where the polymer absorbs light this is no longer the case. When the light is almost completely absorbed by the material there is no interference of light and no oscillations are apparent in the spectra in the near-UV

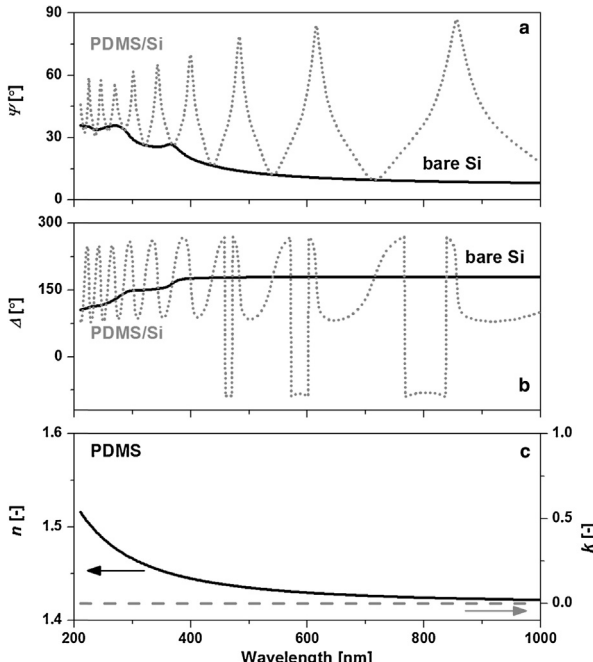


Fig. 6. Simulated Ψ (a) and Δ (b) spectra of a 1000 nm transparent poly(dimethyl siloxane) (PDMS) film on a silicon wafer; (c) optical dispersion of PDMS.

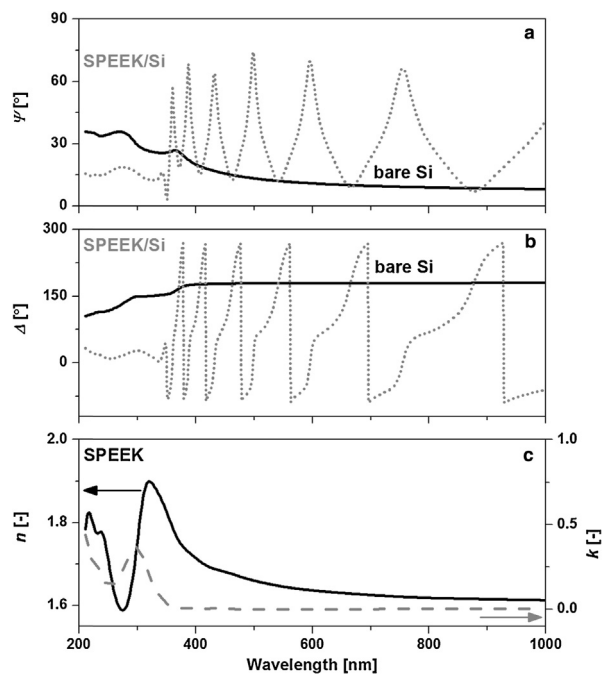


Fig. 7. Simulated Ψ (a) and Δ (b) spectra of a 1000 nm absorbing sulfonated poly(ether ether ketone) (SPEEK) film on a silicon wafer; (c) optical dispersion of SPEEK.

region. This qualitative feature of the spectra is often a strong indication that the polymer absorbs light.

It can clearly be seen that for more complex samples (multilayers, absorbing, anisotropic, etc.) the direct deconvolution of the sample properties from the measured Ψ and Δ can become very difficult. This is the reason why optical models are utilized.

2.2.3. Optical models and modeling aspects

2.2.3.1. Types of optical models used in the literature. In the examples provided in Section 2.2.2 Ψ and Δ spectra are generated based on known optical properties of the film. Analysis of experimental ellipsometry data analysis is done in the opposite manner: the Ψ and Δ spectra are measured and the optical properties of the film are to be derived from these data. For this, an optical model of the system is introduced. Ideally, an optical model should include all information about the sample that is known prior to the measurement. Most importantly, the type of substrate (see Section 2.2.3.2) should be known. In some cases also an approximate layer thickness or refractive index of the film material are known. Fig. 8 shows the most commonly utilized optical models that represent sample systems.

Most of the studies, about 85% of the literature included in this review, consider both dry and swollen samples as uniform films. The corresponding optical model is depicted in Fig. 8a. This Uniform model assumes little or no roughness of the interfaces, and a homogeneous materials density throughout the isotropic film. To limit the scope of this review, polymer brushes or grafts are not included. In these cases the Graded optical model, depicted in Fig. 8b, is more often used. Typically, the density of the

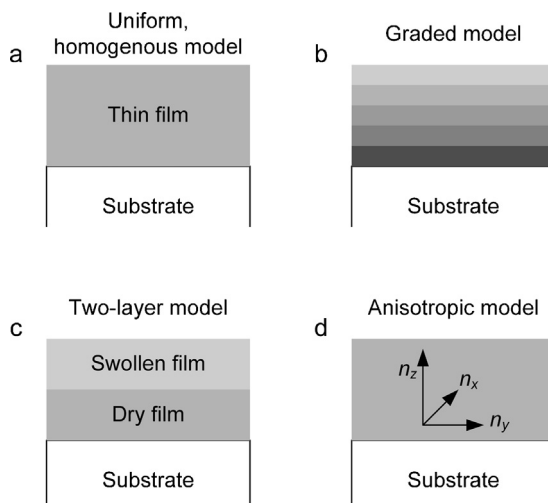


Fig. 8. Optical models used in typical *in situ* ellipsometry measurements of swollen polymer films.

polymer material in swollen brushes is larger close to the substrates, and decays more or less exponentially toward the ambient. The distribution in mass density corresponds to refractive index distribution and may be modeled with a graded refractive index. Interested readers are referred to one of the reviews on polymer brushes in which also the ellipsometry technique for this particular application is discussed [12–14]. Density gradients within the non-covalently attached films, Fig. 8b, have been considered during dynamic swelling measurements of zwitterionic films in water [15,16]. In these cases the researchers have concluded the gradients not to be adequately captured with a Graded model. In another investigation on swelling of zwitterionic supported films in an electrolyte solution, the physically realistic density gradients have been obtained by the Graded model [17]. Contrary to the situation in brushes, in the polyzwitterions density gradients are only apparent during the penetrant diffusion process; at equilibrium swelling no significant gradients have been observed.

Some studies employ the two-layer model, where one layer in the film is swollen with the penetrant while the other layer is essentially dry, Fig. 8c. These studies describe the anomalous Case II diffusion of solvent in a film, where the timescale of polymer relaxation at a sharp diffusion front determines the kinetics of the process. Case II diffusion has been investigated with *in situ* ellipsometry for poly(methyl methacrylate) (PMMA) dissolution in various organic solvents [18–23], and for the diffusion of n-hexane into PS thin and ultra-thin films [24,25]. In these studies, ellipsometry has been proven able to resolve the temporal progress of the penetrant front within thin films, and to probe the surface polymer mobility of ultra-thin films [25]. More complex multilayer models have also been found in the literature [26], in which the problems of swelling and protein adsorption are discussed.

Ellipsometry allows the study of optical anisotropy, Fig. 8d. This has been demonstrated for dry films [27–32]. Studies where optical anisotropy is investigated in detail during swelling of polymers are very rare [17]. One

interesting study uses Mueller matrix polarimetry to study swelling induced anisotropy in swollen hydrogels [33]. Mueller matrix polarimetry is an advanced form of Ellipsometry. Optical anisotropy in dry and swollen high performance polymer layers is considered in [34]. Whether the swollen layers have been modeled with a Uniform or an Anisotropic model remains unclear. Anisotropic swelling has been suggested in the investigation of Kleinfeld et al. [35], although the Uniform optical model has been used in that study.

2.2.3.2. Substrates utilized for *in situ* studies. By far the most commonly utilized substrate is a silicon wafer with a native oxide of about 1.5–2 nm thickness. The temperature dependent optical dispersion of this substrate is very well known [36] and does not change upon immersion in most experimental ambients. In addition, the surface roughness of a silicon wafer is very small. Therefore, it can be considered an ideal substrate for *in situ* ellipsometry. The high real part of the complex refractive index of crystalline silicon ($N_{Si} = 3.874 + 0.015i$ at 632.8 nm [36]) assures very good optical contrast between the polymer film and the substrate, even when the ambient index is much larger than 1 (e.g., liquid water $n_{water} = 1.332$). For glass substrates ($n = \sim 1.5$) the optical contrast in liquid water may not be enough for accurate measurements. The complex refractive index of silicon substrates weakly depends on the degree of doping, at least at low to moderate levels, especially in the visible region, where most studies on swollen polymers are conducted. For heavily doped Si substrates the appropriateness of the utilized complex refractive index of the substrate needs to be verified [37]. In some cases silicon wafers with thick, thermally grown, oxide layers are utilized. This is done predominantly to improve the accuracy of the measurements, in particular when layers below 50 nm are studied [38–40]. Other examples include studies like the one done by Kleinfeld et al. [35]. These researchers used an oxide layer in the range 1.4–216 nm, with atop a multilayer composite film with thickness in the range 16–223 nm, while keeping the total thickness approximately the same (~ 230 nm). This has allowed determining the approximate depth of rapid water penetration within these potential sensor materials, and overcoming the limited temporal resolution of the used device.

When ellipsometry measurements are combined with other techniques, in particular with the QCM or electrochemical methods, often gold-coated quartz crystals are used [41–44]. A gold film of 200 nm can already be treated as bulk for light in the visible range. As a consequence, gold-coated crystals can be considered as bulk substrates for ellipsometry. The additional advantage of metal substrates is that they are compatible with total internal reflection ellipsometry (TIRE) [45], albeit the thicknesses of about 50 nm need to be used. However, the surface roughness in the case of metal substrates can be much larger and less controllable as compared with silicon wafers. Gold and other metals (titanium, platinum) are also utilized in the case of electrochemically deposited or responsive films, where they serve as electrodes [46–48]. Less frequently than silicon wafers, glass slide substrates are used [9,49–54]. Glass slides provide much lower optical contrast,

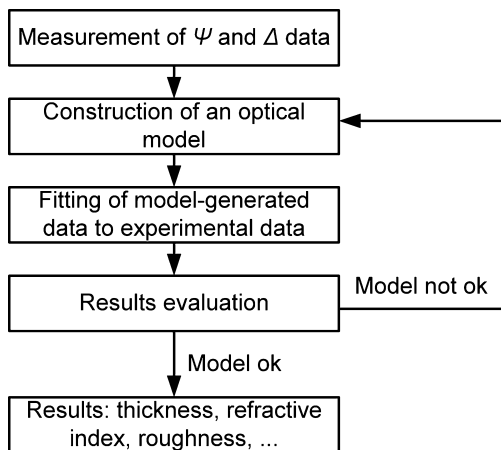


Fig. 9. General scheme of ellipsometry data analysis and sample properties extraction.

because the refractive index of glass ($n_{\text{glass}} \sim 1.5$) is typically very close to that of the polymer film of interest.

Occasionally other less common optical substrates have been employed, including surface modified wafers. Richardson et al. [55] have used octyl trichlorosilane grafts on silicon wafers to study the impact of surface interactions in structural relaxation of PMMA films during solvent loss. Ogieglo et al. have presented the applicability of the Graded model for polished porous membrane substrate [56]. Following up on this, they studied high pressure driven transport of n-hexane through supported 1–2 μm PDMS layers [9]. Sirard et al. [57], have studied the influence of replacing SiO_2/Si wafer with GaAs wafer on the anomalous maxima of sc- CO_2 sorption in PMMA films.

2.2.3.3. Optical modeling and limits of ellipsometry. Values for the film properties, such as film thickness and/or refractive index, are obtained from a numerical fit of the optical model to the experimental Ψ and Δ data. This approach is depicted schematically in Fig. 9. The most widely used measure for the quality of the fit is the (root) mean square error parameter, MSE . This parameter quantifies the error between the model-generated and measured Ψ and Δ values [58]. The iterative fitting is commonly done with the Marquardt-Levenberg algorithm [59]. Some authors suggest using a different measure of fit error, χ^2 , which overcomes various drawbacks of the MSE [60]. In any case it is important to be confident about the meaning and significance of the used fit quality parameter to avoid misinterpretations.

The fit parameters commonly include the layer thickness, the optical dispersion, and various other sample features such as sample roughness, sample uniformity, gradients, and anisotropy. Because most polymeric materials are simple transparent dielectrics, their optical dispersion can be modeled according to the relation proposed by Cauchy [61]:

$$n(\lambda) = A + \frac{B}{\lambda^2} + \frac{C}{\lambda^4} \quad (2)$$

In this equation A , B and C can serve as adjustable fitting parameters. For polymers that absorb light in the vicinity

of the UV spectral region, the wavelength range for the modeling is often limited to the transparent part. When the light absorption characteristics are of interest, these can be modeled with dielectric oscillator models, such as Gaussian or Tauc-Lorentz oscillators [6]. Alternatively, light absorption spectra can be represented with B-splines [62]. This approach yields good results provided that the underlying assumptions are appropriately accounted for.

For simple samples, such as <500 nm thick Cauchy-type polymer films deposited on silicon wafers, the MSE values representing very good fits are in the range 1–5. For thicker films MSE values of 10–20 are acceptable. Thicker films generate a larger number of oscillations. The limited experimental spectral resolution dictates to what extent this number of oscillations can be represented. This is discussed in Section 2.2.2.

If the obtained MSE value for a given optical model is not satisfactory, additional fit parameters can be included. This has to be done with care, to avoid over-parameterization. If the number of fitting parameters is too large, significant correlations between them may be introduced. As a result the physical meaning of some parameters may become difficult to establish and the description of a sample with such a model becomes meaningless. A proper data analysis should always include a parameter correlation assessment. Typically, the reduction of MSE after the introduction of an additional fitting parameter should be *significant*, that is roughly on the order of at least ~25% [63]. A significant reduction in the MSE reductions can often be considered as a strong indication of meaningfulness of the additional parameters. Examples include the large reduction of the MSE when the more complex two-layer model was used instead of the Uniform model for Case II diffusion [24], and the more than 5-fold reduction of the MSE with an Anisotropic model over a Uniform model in the study of swelling zwitterionic films [17].

Parameter correlations may also become an issue when film thickness and index need to be independently determined for very thin films, in the so-called ultra-thin region much below 100 nm. This is because for typical refractive indices of polymers ($n=1.4\text{--}1.6$) Ψ becomes a very weak function of the thickness below about 30 nm [6]. With state of the art ellipsometry instruments, the thickness range allowing a reasonably accurate determination of the independent thickness and index is thus ~30–3000 nm. However, if the refractive index of the polymer is known (can either be determined independently or does not change too much from its dry value during the *in situ* measurement) its value can be fixed and the thicknesses down to essentially fraction of a nanometer can be accurately measured.

The more complex optical models, such as those depicted in Fig. 8b-d, usually require sufficiently thick samples to work reliably. If more complex information is required on the density distribution within very thin films (a few nanometers), then ellipsometry may be complemented with techniques that use much shorter wavelengths, for instance neutron or X-ray reflectivity. Both of these techniques are applicable *in situ*. For complex optical models fit parameter correlation needs to be checked carefully. This is because these models comprise

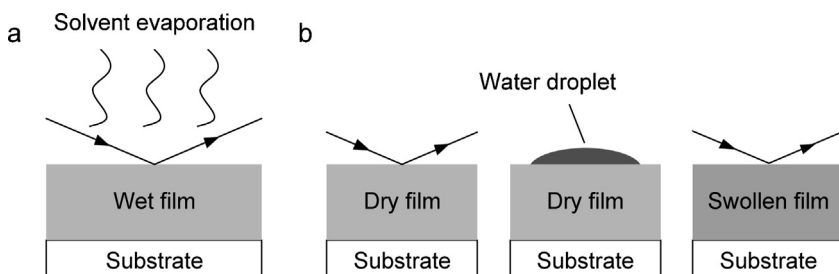


Fig. 10. In situ ellipsometry configurations without experimental cells; (a) [55,64,65] and (b) [66].

usually a large amount of fitting parameters. In some cases the validity of certain optical models over others can be assessed by additional measurements. For instance, comparing the graded model, Fig. 8b, and the anisotropic model, Fig. 8d, can be done by measuring several angles of incidence. Rotating the sample around a perpendicular axis can allow distinction between uniaxial and biaxial anisotropy. In the case of polymer film samples biaxial anisotropy is very unlikely.

2.3. In situ configurations

In situ ellipsometry requires that the sample is in contact with a penetrant. This has been realized in various ways. Some of the most frequently used configurations are briefly discussed in this paragraph.

2.3.1. No in situ sample cell

Interactions of the penetrant with the polymeric films have been studied, where the ambient was not confined in an experimental cell. The advantages of such a configuration are that the measurements can be performed at multiple angles. This may increase accuracy. The disadvantages include less control over experimental conditions related to the ambient, as compared to the in situ cells described in Section 2.3.2.

The no-cell configuration has been used for the observation of structural relaxations during solvent (toluene) evaporation from thin and ultra-thin PMMA films [55,64], Fig. 10a. The thin film samples have been simply transported from the spin coater pad onto the stage of spectroscopic ellipsometers. Measurements have been taken with relatively short time intervals (about 20 s), to dynamically observe simultaneous changes in film thickness and index. A similar methodology has been applied in the study of drying processes in the same polymer, with a solvent that provides relatively high optical contrast (bromobenzene) [65]. In a different configuration, Fig. 10b, the film has been brought in contact with a water droplet for a certain period of time, and the uptake of the penetrant has been measured with ellipsometry after the water droplet removal [66]. This approach has been used in the analysis of contact angle hysteresis of a polyimide film.

Also, controlled relative humidity conditions can be obtained without the application of an in situ cell, Fig. 11, for example as has been done in the study of swelling of ultra-thin cellulose Langmuir–Blodgett deposited films [38]. The ellipsometer stage is placed in a relatively big

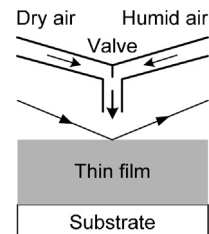


Fig. 11. Controlled relative humidity measurements without experimental cell [38].
Copyright 2003. Reproduced with permission from the American Chemical Society.

container (or even a plastic bag with cut holes as windows for the light beam) in which humidity is controlled [35,67]. An intermediate step between no sample cell, Section 2.3.1, and the utilization of such, is a trapezoidal sample cell with holes as windows. The advantage is good ambient gas or vapor flow repeatability combined with no impact of windows on the probing polarized light. This configuration of course cannot be used with liquid or compressed fluid ambients.

2.3.2. Near-atmospheric pressure in situ cells

Fig. 12 shows the schematics of a typical in situ ellipsometry trapezoidal flow cell equipped with a temperature control unit. Such a cell is used in most of the in situ ellipsometry investigations of thin swelling films and allows excellent control over the experimental conditions. Flow of the ambient is not always imposed; some investigations are done in static conditions. The body of the cell is most often made of glass or stainless steel. The windows need to be transparent in the measurement wavelength range and optically isotropic. This last condition may not always fully apply. However, protocols exist that allow correcting

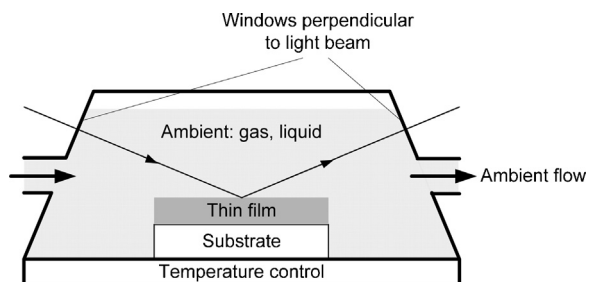


Fig. 12. Schematics of a typical in situ ellipsometry flow cell with temperature control option and windows at 70°.

for the birefringence of the windows (in particular for the in-plane component), which is most severe in the case of the Δ parameter determination. This can be done by running appropriate calibration procedures, for instance by measuring a sample (or pure substrate) with known optical constants inside of the cell and fitting for the Δ offsets [57,68].

Out-of-plane window offsets can often be sufficiently corrected for by the design of the instrument and internal calibration methods. If not corrected for, such offsets can lead to significant errors especially in the cases where liquid ambients (refractive index significantly larger than 1) are used. This is because when light enters from air ($n \sim 1$) to a liquid ($n > 1$) small deviations from the right angle between the beam and the window become amplified.

Windows are, in almost all cases, placed perpendicular to the light beam. This is not absolutely required when the measurements are done in vacuum, air or in fluids with index close to 1. It becomes crucial when an ambient with a refractive index significantly larger than 1 is placed inside of the measurement cell. This is because when the light enters the cell at a non-right angle, the whole cell becomes a prism in which the transmitted light travels at an angle given by the Snell's law (see Appendix, Eq. (A2)), which is different from the incidence angle. This in turn produces a different exit angle as well. In severe cases this deviation is so large that the light beam misses the sample or the detector entirely.

Typical angles of incidence found in literature are close to 70° (in a range from 65° to 75°), which is near the Brewster angle of the most commonly used crystalline silicon substrate, 73.7° at 632.8 nm . At the Brewster angle the reflectivity of p -polarized light as a function of incidence angle passes through a minimum [6–8]. This minimum is zero for non-absorbing substrates. Since ellipsometry measures reflection coefficients ratio (r_p/r_s) and the difference between r_p and r_s is maximized at the Brewster angle, an increased sensitivity for a bare substrate is found at that angle. However, precisely at the Brewster angle the Δ parameter becomes very noisy and the angle of incidence needs to be known very precisely. That is why actual measurements are performed close to, but no exactly at, Brewster angle. The common use of a 70° angle of incidence for in situ ellipsometry studies of polymers is largely due to historical reasons. In the past decades ellipsometry has been used extensively in semi-conductor research, where very thin films with relatively high refractive index (metalloid elements, their oxides and alloys) atop crystalline silicon substrates have been studied. In typical polymer studies the films are much thicker, from tens of nm to several microns, and have much lower refractive indices, 1.4 – 1.6 . In such cases the largest sensitivity may not necessarily be found around the Brewster angle of the substrate, but often closer to the Brewster angle of the film itself. This can be seen in Fig. 13, where a sensitivity calculation is shown for a 100 nm polymer film of a polymer ($n = 1.6$) supported on a silicon wafer, as a function of the angle of incidence. The sensitivity is defined as the change in the MSE when the film thickness changes 1 nm . For this particular polymer the largest sensitivity is obtained at a wavelength $\sim 550\text{ nm}$ and an angle of incidence of 60° . This angle

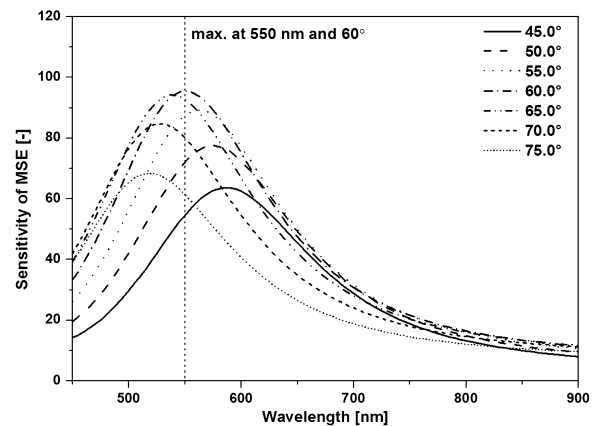


Fig. 13. Sensitivity of MSE to thickness variation by 1 nm for a 100 nm polymer film with refractive index of 1.6 supported on a silicon wafer for various angles of incidence; maximum sensitivity observed at 550 nm for 60° incidence angle which is closer to the Brewster angle of the film itself, rather than the Brewster angle of the supporting wafer.

is closer to the Brewster angle of the polymer, 58.2° , than to that of the wafer, 74.6° at that same wavelength (note that Brewster angle is wavelength-dependent). The sensitivity at 70° is still very good and this angle of incidence should give high quality results as well. However, to obtain the best sensitivity for a particular measurement problem, similar analysis should be done to determine the most optimal incidence angle. Consequently, a custom-made optical cell adjusted for that angle may be constructed.

Depending on the type of application the ambient may be stationary or continuously flown over the thin film sample. A flowing ambient is often applied in relative humidity measurements, to assure accurate control over the saturation level of water in the gas phase. Flow cells can be often used for simultaneous ellipsometry and QCM or electrochemical measurements [42,47,48,69]. Such applications greatly improve the amount of information that can be determined about the measured system. For example thickness/index changes within the swollen films can be observed simultaneously with viscoelastic changes within the films (QCM with dissipation, QCM-D) or redox transitions (electrochemical measurements). This is discussed in more detail in Section 6.

A backside configuration [53,54] is an alternative but less common approach to in situ liquid measurements, Fig. 14. A similar setup can be used to perform the TIRE experiments [70]. In this configuration the film is attached to a backside of a transparent substrate, usually a glass slide. The incident light (IL) comes from the topside of the

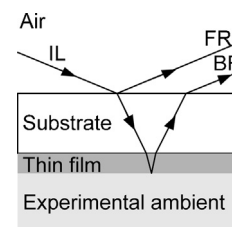


Fig. 14. Backside in situ ellipsometry configuration.

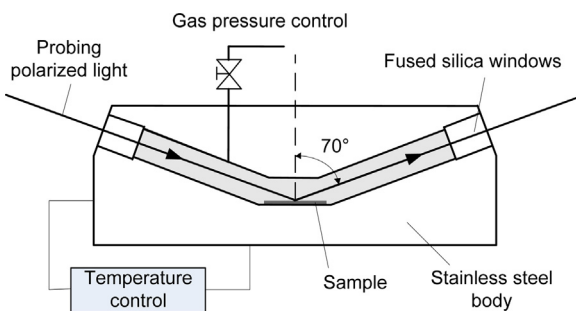


Fig. 15. Schematics of a high pressure in situ ellipsometry cell, first developed by Sirard et al. [68].

substrate. The first reflection from the top of the substrate (FR) carries no information about the sample: the reflections at the bottom of the substrate (BR) are of interest. The benefits of this configuration include the possibility for multiple angles of incidence and the simplicity of the cell, because no windows perpendicular to light beam are utilized. For a liquid ambient the disadvantages include the perquisite of a completely filled cell. Gas cavities between the thin film and the liquid disturb the experiment.

2.3.3. High-pressure cells

Sirard et al. have been the first to develop a high-pressure in situ ellipsometry chamber, for the measurements of supported thin PDMS films exposed to carbon dioxide [68]. Due to mechanical requirements the body of their cell has been constructed from stainless steel combined with thick fused silica windows (1.5 cm diameter, 1 cm thick), Fig. 15. A high-pressure can induce window birefringence, even if the windows are not birefringent at atmospheric pressure. That is why it is usually required to calibrate for these effects by running high-pressure measurements on calibration wafers (thermal SiO₂/Si), to determine the in-plane Δ offset. Pressure dependence of the dispersion of the ambient should be taken into account in the optical modeling. Data for several gases including CO₂, N₂, ethylene and ethane can be found in [71–73].

High-pressure ellipsometry has also been shown to be a very powerful tool for the determination of swelling of thin and ultra-thin glassy films exposed to condensable gases, and for determination of sorption induced glass transition pressure, P_g [57,74–76]. In addition, the technique has been used to calculate concentrations of dissolved gas in thin films [50,77,78], investigations of anomalous maxima in swelling near critical conditions of CO₂ [57,79], and observations of order-disorder transitions in block copolymers in compressed CO₂ [80].

Recently, a new type of a high-pressure in situ ellipsometry cell has been introduced that allows for studying the behavior of selective layers of composite membranes during permeation, Fig. 16 [9]. The cell presented in the figure is to a large extent the same as the one from Fig. 15. The difference is that permeation of the species from the top to the bottom of the cell is possible. This allows for the convenient and non-invasive study of different transport phenomena that are important in membrane science,

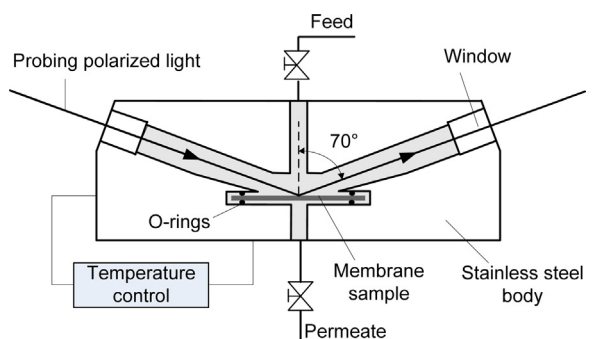


Fig. 16. Schematics of a high pressure in situ ellipsometry cell allowing for permeation experiments [9]. Copyright 2013. Reproduced with permission from Elsevier Science Ltd.

provided that an appropriate optical model for the porous substrate is available [56].

3. Types of polymeric materials studied

This paragraph is intended to provide a full picture on the different types of non-covalently attached polymeric films that have been investigated with in situ ellipsometry. Emphasis is put on the chemical structure of the material, the film fabrication methods, and the equilibrium (liquid) or non-equilibrium (glassy) characteristics of the films. All these aspects influence the behavior of a film upon exposure to a penetrant.

3.1. Simple glassy polymers

Glassy polymers are of tremendous importance in a range of technologically important areas. This originates from their good mechanical properties, dimensional stability, and chemical resistance at room temperature and at slightly elevated temperatures. For high performance polymers the application range can be extended to even higher temperatures. Exposure to penetrants very often strongly affects the non-equilibrium status of glassy polymers. In other words, penetrants often alter the kinetics of the slow relaxation of a glass toward its equilibrium state, referred to as physical aging [81]. In many applications, especially in coatings, barriers, and membranes, this long-term process has a large impact on the performance of the films. For experimental studies of the slow changes in density and thickness of (ultra-)thin films often very high (sub-nanometer) resolution is necessary. This is in particular true when physical aging concurs with slow penetrant induced secondary relaxations [78]. SE has been demonstrated to be an ideal tool in such studies.

Glassy polymeric materials studied by far the most with in situ ellipsometry are PS [24,25,78,79,82–85], and PMMA [18–21,55,57,64,65,77,85–87]. These materials constitute ideal model, amorphous, glassy polymers with easily accessible T_g ($T_{g,PS} \sim 100^\circ\text{C}$, $T_{g,PMMA} \sim 110^\circ\text{C}$). They are also easy to dissolve in common solvents (predominantly toluene, chloroform or acetone) and it is easy to tune the thickness of PS and PMMA films during spin coating by changing solution concentration. This aids systematic investigations

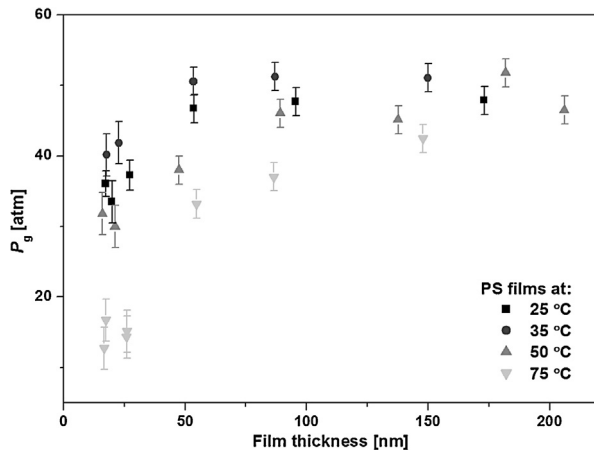


Fig. 17. Devitrification pressure (P_g) versus film thickness; isotherms for PS ($M_w = 590$ k) films at 25, 35, 50 and 75 °C [84]. Copyright 2004. Adapted with permission from the American Chemical Society.

on the effects of dry film thickness on penetrant induced effects [25,55,64,65,74,84]. An example of such an investigation is shown in Fig. 17, where pressure induced glass transition, P_g , is shown to vary with initial film thickness.

Other studies include investigations on the dimensional stability of high performance polymers used in microelectronics [34], water swelling in ultra-thin layers of cellulose [38,51,88], swelling of ion beam treated polyimide layers [89,90], contact angle hysteresis in polyimides [66], anomalous swelling of several high-performance polymers in supercritical CO_2 [79], and swelling of electrically conducting polymers [49]. In membrane science the sorption, relaxation, and plasticization in high pressure CO_2 has been investigated for various high T_g materials, including self-synthesised polyetherimides, polyimides, polysulfone (PSF), poly(phenylene oxide) (PPO) and SPEEK [50,75,76,78,91]. In most cases these polymer films have been prepared by spin coating from good solvents.

3.2. Simple rubbery polymers

Contrary to glassy polymers, sorption in rubbers usually proceeds very fast with quick equilibration of the system. This is manifested by a lack of apparent secondary and long-term relaxations. This makes PDMS and its derivatives very good candidates for volatile organic compounds sensing, where the material sorption response can be conveniently studied with in situ ellipsometry [92,93]. PDMS has also been investigated as a model system for sorption of CO_2 at higher pressures, Fig. 18 [68], and high-pressure in situ liquid solvent nanofiltration experiments [9]. Other rubbery systems investigated include poly(amide-6-*b*-ethylene oxide) (PEBAX) [50] and pH-responsive poly(methylcarboxypropyl siloxane) (Posimca50) [94]. The preparation of rubbery films may involve the use of a cross-linking agent [9]. This is done to ensure the dimensional stability of the rubbery material that otherwise possesses too low viscosity for practical use.

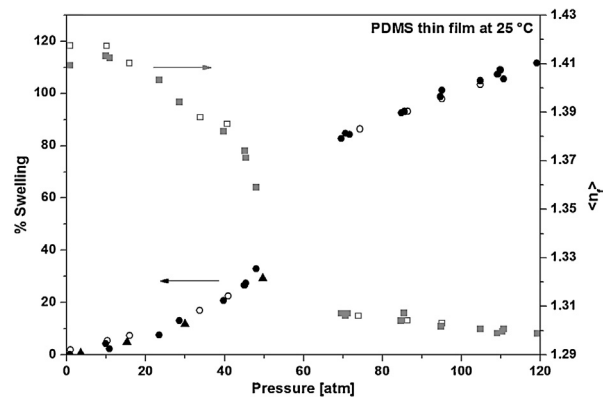


Fig. 18. Swelling isotherms for a PDMS thin film at 25 °C. The circles represent the equilibrium swelling and the squares represent the refractive indices of the swollen film. Filled circles and squares correspond to sorption measurements and open circles and squares correspond to desorption measurements. Triangles are from bulk measurements [68,138]. Copyright 2001. Adapted with permission from the American Chemical Society.

3.3. Random and block copolymers

Copolymers belong to a practically important class of polymers. For copolymers distinguishing between glassy or rubbery characteristics is difficult. Often multiple T_g values are found, especially in the case of block copolymers. However, penetrant plasticized copolymers often reside above the highest observed glass transition and can be considered rubbers. The broad range of copolymers investigated with in situ ellipsometry reflects a multitude of potential applications.

Chen et al. [41], have investigated swelling of various hydrophilic copolymers in humid environments. The polymers used are based on polyacrylates with low M_w poly(ethylene glycol) PEG side chains, and could be potentially used as coatings with tunable wettability and adhesive properties. The researchers have reported on the existence of a humidity induced phase transition within the materials. This has been confirmed by combining in situ ellipsometry and QCM. In their fundamental study, Elbs et al. have investigated the organic solvent (vapor) swelling of various homo- and related copolymers, Fig. 19 [83], and have extracted Flory–Huggins interaction parameters. Based on those data the researchers have been able to quantify solvent compatibility of polymers synthesized from different co-monomers.

Spin-coated thermosensitive coatings of cross-linked microgels of poly(*N*-isopropyl acrylamide-*co*-acrylic acid) (p(NIPAM-*co*-AA)) have been investigated by Schmidt et al. [95]. Aim of their study was to enable temperature tunable surface reflection properties. Chandler et al. [80] have investigated the scaling behavior of the order-disorder transition in PS-*block*-polyisoprene copolymers, in compressed CO_2 . For PS-*block*-PVP it has been observed that the solvent up-take by the polymer film is limited by molecular confinement to the dimension smaller than the characteristic lamella spacing, as well as to the non-equilibrium microstructures limits [96]. Confinement effects, manifested as a 10% increase of solvent uptake

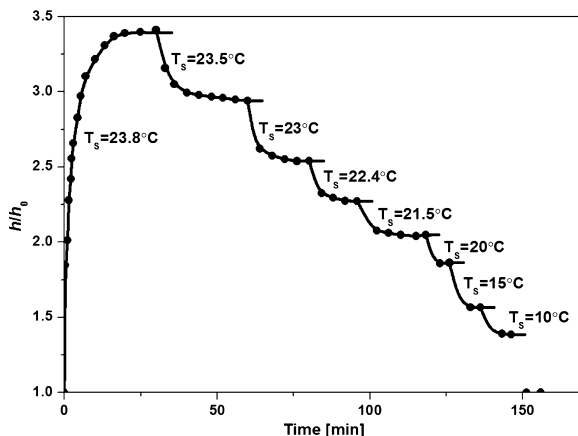


Fig. 19. Swelling behavior of a PtBMA film in decreasing activity of chloroform vapor ($T_p = 24^\circ\text{C}$, $h_0 = 150 \text{ nm}$). Activity of vapors is tuned by the saturation temperature [83].

Copyright 2004. Adapted with permission Elsevier Science Ltd.

with decreasing film thickness, have also been investigated in cylinder-forming PS-*block*-polybutadiene copolymers [97]. In spectroelectrochemical sensor applications partially sulfonated polystyrene-block-poly(ethylene-ran-butylene)-block-polystyrene (SSEBS) thin films have been evaluated toward sensing of Ru(bpy)₃²⁺, phenosafranine and rhodamine analytes in aqueous conditions [98]. Yagüe et al. [99], have shown the possibilities to control the mesh size in poly[(2-hydroxyethyl methacrylate)-co-(ethylene glycol diacrylate)] (p(HEMA-co-EGDA)) synthesized by initiated chemical vapor deposition (iCVD) during water swelling of the layers. iCVD prepared pH-responsive copolymers have also been investigated with respect to their drug release capabilities [100].

3.4. Multilayer films

A significant number of *in situ* ellipsometry studies have been dedicated to swelling of multilayer films. Such systems, in particular polyelectrolyte multilayers prepared by layer-by-layer (LbL) deposition [101], are known for their stimuli responsive characteristics. They can be used in sensor, electronic, separation, cell adhesion, and many other applications. In this section the multilayer systems investigated are outlined. More focus on the particular processes studied is given later in Section 4.

Kleinfeld et al. [35], have described composite films prepared by alternate adsorption of poly(allylamine hydrochloride) (PAH) and exfoliated sheets of Laponite RD that show very quick response toward changes in the ambient humidity. For ionic separation applications, PAH/poly(styrenesulfonate) (PSS) and PAH/poly(acrylic acid) (PAA) films have been shown to present pH dependent permeability of Fe(CN)₆³⁻ and Ru(NH₃)₆³⁺ [46]. LbL self-assembled osmium complex-derivatized PAH and glucose oxidase multilayers (PAH-Os)_n(GO_x)_n, change thickness and index in response to electrical potential changes, and have been investigated by Forzani et al. [47]. History dependent pH-responsive swelling behavior, and molecular conformational memory has been

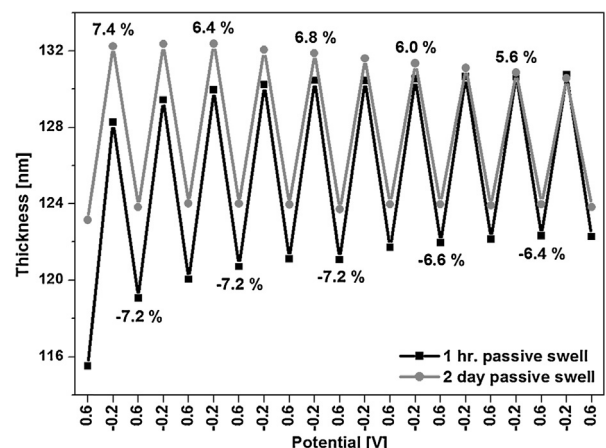


Fig. 20. Active swelling of two (linear PEI/Prussian Blue)₃₀ films subjected to 10 redox cycles after 1 h and 2 days. Swelling percentage values (calculated relative to thickness in the preceding redox state) are next to the corresponding data points; negative values represent shrinking [69].

Copyright 2009. Adapted with permission from the American Chemical Society.

demonstrated in PAH/PSS incorporated into multi-layer films [102]. A multilayer stack of Poly(L-glutamic acid) (PGA) layers and poly(L-lysine) (PLL) layers, on poly(ethylene imine) (PEI), has been shown to be a stable drying/dewetting system that is responsive to changes in temperature and pH [103]. The dynamic swelling of PAA and PAH under various pH conditions has been studied by Tanchak et al. [104]. Assemblies of PSS and PAH have been characterized with respect to thickness changes in humid environments and the odd-even effect (swelling dependence on the outer layer charge) has been investigated [105]. Swelling of biopolymer multilayers containing hyaluronic acid (HA) and PAH has been reported by Burke et al. [106]. pH-induced swelling/deswelling transition mechanism in multilayers containing PAH have been investigated by Itano et al. [107]. Permeability/swelling correlations of various polyelectrolyte multilayers have been investigated by Miller et al. [108]. Olugebefola et al. [109], synthesized and characterized a photo-cross-linkable weak polyelectrolyte based on poly(acrylic acid-ran-vinylbenzyl acrylate) (PAArVBA). Electrodes modified by layer-by-layer-assembled redox-active polyelectrolytes have been investigated by Tagliazucchi et al. [48]. Schmidt et al. [69], investigated electrochemical swelling control capabilities in nanocomposite thin films comprising linear PEI and Prussian Blue nanoparticles, Fig. 20. As can be seen from the figure, these multilayers showed excellent stability and swelling-deswelling reproducibility. Hysteretic swelling in PAH and PAA multilayers has been investigated by Secrist et al. [67].

The effects of cross-linking in bioreducible poly(2-dimethylaminoethyl methacrylate) (PDMAEMA) and deoxyribonucleic acid (DNA) have been investigated with respect to their biologically active properties [110]. Electric-field-controlled orientation of bilayers containing gramicidin and dimyristoylphosphatidylcholine (DMPC) has been described by Fiche et al. [111]. Temperature-induced swelling of multilayer triblock copolymers has

been investigated by Tan et al. [112]. Diblock copolymer micelles with thermo-sensitive cores have been characterized by Xu et al. [113]. Ionic-strength effects on swelling of PSS and poly(diallyldimethylammonium chloride) (PDADMAC) have been investigated in depth by Dodoo et al. [114]. Cell migration through cell-cell interaction on polyelectrolyte multilayers has been characterized by Han et al. [115].

3.5. Other systems

Other larger groups of polymeric systems, investigated with *in situ* ellipsometry, included zwitterionic films based on PC [15,16,116,117], and polysulfobetaine [17]. In contrast to the polyelectrolyte multilayers described in Section 3.4, zwitterionic polymers contain both positively and negatively charged groups within a single monomer unit. This strongly affects their properties, in particular with respect to cell adhesion and biofouling. Cyclic oligomeric molecules of calixarenes have been characterized for sensing of organic vapors by several groups [43,44,118]. Hydrogel behavior under aqueous conditions has also been characterized by *in situ* ellipsometry [52,119–121]. Swelling of hyperbranched polyesters has been investigated in several cases [26,39,122,123]. Swelling of adsorbed latex particles has been studied by van der Zeeuw et al. [124,125] by reflectometry. This detailed study has focused on the determination of size changes of the adsorbed particles during swelling.

Other less common polymeric systems include electrochemically grown polyaniline (PANI) [42], 200 nm Pd-fluoropolymer ($\text{Pd}-\text{CF}_x$) sputtered films [126], sol-gel processed polyelectrolyte-silica composite films [54], iCVD deposited, cross-linked systems [127], chemical reactions of ferrous ion within thin Nafion films [53], MOFs [128], Nafion nanomembranes [129] and dendritic macromolecule films of oligosaccharide-modified PEI [130].

4. Types of polymer-penetrant phenomena studied

In situ ellipsometry has been applied to study a wide range of polymer-penetrant phenomena. In the most common experiments a dry polymeric thin film sample has been exposed to a penetrant and the change in its properties has been recorded. These types of investigations constitute about 50% of *in situ* ellipsometry studies on polymer swelling. They are outlined in Section 4.1 where also the distinction is made between the different types of penetrants used in the literature. In Sections 4.2–4.6, the other less commonly found groups of investigations are described.

4.1. Penetrant uptake from dry state

In this part the focus is on thin film samples that have been swollen with various penetrants from a dry state. These studies involved samples that have been prepared by spin coating or dip coating, or have been prepared *in situ*. After film formation, these samples are generally annealed under inert gas flow or vacuum to remove the solvent and relax post-preparation stresses. Fig. 21 shows

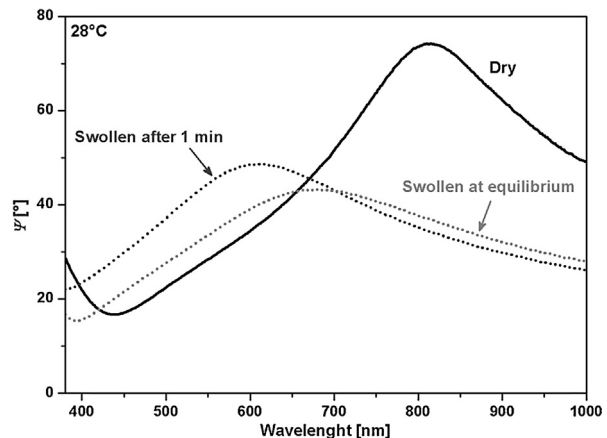


Fig. 21. Changes in the Ψ spectrum of ~ 150 nm PS film supported on a silicon wafer upon exposure to liquid n-hexane penetrant at 28°C [24]. Copyright 2013. Adapted with permission from Elsevier Science Ltd.

the change in the Ψ spectrum for a dry and liquid n-hexane swollen ~ 150 nm PS film [24]. As discussed by the authors, in this case the pronounced change in the amplitude going from a dry to a swollen film has been only weakly related to the change in the film index during swelling of about 20% ($n_{\text{dry}} = 1.585$, $n_{\text{swollen}} = 1.556$). Most of the amplitude dampening has originated from the replacement of the experimental ambient (air for the Dry spectrum, $n_{\text{air}} = 1.000$) with liquid n-hexane (for the Swollen spectrum $n_{\text{n-hex}} = 1.369$). This has caused a very significant reduction in the optical contrast between the layer of interest (PS film) and the ambient. This is a typical issue during *in situ* ellipsometry swelling experiments.

The loss of contrast contributes to an increase in the error in the values of the determined sample properties. A much smaller change in Ψ has to be detected, with the same resolution of the device. If the swollen system possesses refractive index very close to the experimental ambient (which is usually the case for polymers swollen much above 100%), the loss of contrast may even prevent accurate determination of the swollen film refractive index. The solution for the problem could be, in some cases, the assumption that the index of the film does not change too much during sorption. This may be especially helpful when only relative swelling or differences between similar samples are investigated.

For the experiments where only penetrant vapors are used, usually the index of the ambient can be assumed not to differ significantly from that of air, $n_{\text{air}} = 1.000$. The exceptions are high-pressure gas experiments where the departure may be significant already for moderate pressures. For example, at 50 bar $n_{\text{CO}_2,\text{gas}} = 1.027$. Changes in refractive index of the ambient can be expected in particular for highly polarizable molecules, such as VOCs or carbon dioxide. The effects are smaller for He or H₂.

Multilayer and responsive (pH, temperature, ionic strength, etc.) samples, highlighted already in Section 3.4, are often prepared and characterized *in situ* and dry properties are not known. Therefore, these samples are not discussed here, but in Section 4.3. The segregation of studies in the following subparagraphs is done on the

basis of the type of penetrant used (aqueous–non-aqueous, liquid–vapor–gaseous), and the examples are selected to give an as broad as possible picture of the various types of investigations.

4.1.1. Liquid water

Liquid water has a room temperature refractive index of $n_{\text{water}} = 1.332$ [10,131,132], which is lower than for most typical polymer systems. The value is also significantly lower than the indices of the most commonly utilized organic solvents ($n_{\text{n-hexane}} = 1.386$ [133,134], $n_{\text{toluene}} = 1.496$ [135], $n_{\text{chloroform}} = 1.446$ [136], $n_{\text{ethanol}} = 1.361$ [137]). That is why liquid water provides a reasonable optical contrast for not too highly swollen, relatively thick samples and an accurate swollen refractive index determination is possible. Water is also the most widely studied penetrant in the literature, mainly due to the obvious biological and environmental importance.

Swelling studies of a very wide range of polymeric materials in liquid water are available. The following examples represent some unique studies found in the literature. One of the first studies, dealing with dynamic *in situ* SE determination of swelling, has been conducted on a biocompatible zwitterionic polymer based on PC [15,16]. The focus has been put on the interplay between the hydrophilic and hydrophobic units of the polymer. This interplay results in formation of complex morphologies that determine the swelling characteristics of the films. These swelling characteristics are shown to possibly deviate from what is expected in the case of classical Fickian diffusion. The authors have found that Fickian diffusion and polymer relaxation both contributed to the total swelling of the material. Hennig et al. studied water-induced surface swelling of thin polyimide films by combined contact angle and ellipsometry measurements [66]. Polyimides are widely used in electronic devices where the impact of humidity may cause reliability problems. In the study of Hennig et al. ellipsometry has been used to correlate the swelling of the layers upon contact with a water droplet to the observed contact angle hysteresis. The impact of layer annealing at high temperature has been reported. Chan et al. reported contact angle hysteresis of iCVD synthesized hydrogels intended for use in drug release [127]. The hysteresis has been attributed to surface reconfiguration of the films. The authors have used ellipsometry to study the effects of the hydrogel cross-linking on the water uptake and found a significant decrease of the water fraction with increasing cross-linking and decreasing incorporation of the hydrophilic monomer. Cross-linking effects on water uptake of electron beam irradiated hydrogels based on PNVP have been reported by Burkert et al. [120].

The hydrogels show very high swelling degrees, defined as $h_{\text{swollen}}/h_{\text{dry}}$, Fig. 22, that reduce with increasing temperature. The figure shows that the higher swelling degrees come with a reduced precision of the ellipsometry data. This lower precision is due to the low optical contrast, resulting from the extremely large water fraction in the films. The authors have also reported on an irradiation threshold necessary to fix the material to the silicon substrate. Swelling of iCVD synthesized, cylindrical-shape copolymer hydrogels with controllable mesh sizes has been

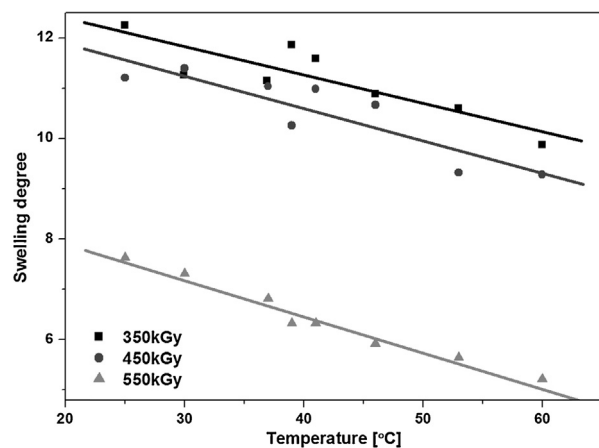


Fig. 22. Swelling degree of hydrogels as a function of temperature for different irradiation doses. Ellipsometry precision decreases for the highest swelling degrees due to reduction of the optical contrast related to extremely high saturation of the films with experimental ambient [120]. Copyright 2007. Adapted with permission from Elsevier Science Ltd.

reported by Yagüe et al. [99]. They derived the degree of cross-linking and mesh size from the extent of swelling.

4.1.2. Water vapor

Water vapor *in situ* ellipsometry measurements have mostly dealt with humid inert gases close to atmospheric pressures. Swelling and index changes of polymeric samples have been measured as a function of the Relative Humidity (RH). Similarly to the studies described in Section 4.1.1, here also the range of both investigated systems and experimental approaches is very wide.

One of the earliest RH swelling studies has been reported by Kleinfeld et al. [35]. They investigated water penetration into composite films of PAH and sheet-silicate mineral, Laponite RD. Control of the relative humidity was achieved by placing the ellipsometer stage in a plastic bag with small holes serving as windows for the polarized laser beam. The researchers have been able to rule out surface condensation as a dominant mechanism for the rapid water sorption in the films. For this, they devised a very elegant approach for fabrication of composite films of variable thickness, on top of a thermal silicon oxide variable thickness, while keeping the total thickness constant, Fig. 23. The authors have also discussed the possibility to semi-quantitatively correlate the changes in color of the films to their swelling magnitude as a result of a change in light interference at the outer film interface (so called interference color).

Mathe et al. [40] have reported a study on water sorption in films of the biologically relevant polysaccharides HA and dextran. They have found significant differences in the swelling behavior at high RH. The differences have been correlated with internal pressures related to the rearrangement of the sorbed water molecules. The forces within the films have been calculated from the disjoining pressure. This disjoining pressure is the negative derivative of Gibbs energy with respect to film thickness, and is a function of the swelling. The hydration forces in ultra-thin (below 20 nm cellulose films) have been investigated by Rehfeldt et al. [38]. The authors have found no effect of

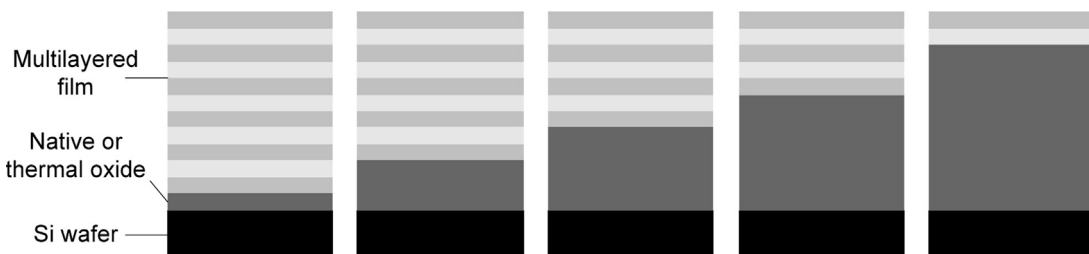


Fig. 23. Preparation of multilayer composite films on top of variable thermal silicon oxide thickness layers, while keeping the total film thickness constant. Such a sample configuration gives different changes in color upon exposure to the same relative humidity and helps to rule out surface water condensation [35]. Copyright 1995. Adapted with permission from the American Chemical Society.

the dry thickness of the films, down to several nm, on the swelling degree or the corresponding disjoining pressure. Eichhorn et al. [89,90] have reported water vapor swelling of thin films of aromatic polyimides, modified by B^+ bombardment. The produced partially carbonized material has been shown to be characterized by a very small (2%) and completely reversible water vapor sorption, making it very interesting in sensor applications. Rowe et al. [91] have reported a study on the impact of humidity on the changes of refractive index and thickness of thin polyimide films. The polyimide films have been obtained from 3,3',4,4'-benzophenone tetracarboxylic dianhydride and diamino-phenylidene (Matrimid). The researchers considered two limiting cases for the refractive index versus RH dependence: one where the glassy sample volume does not change with sorption (implying sorption into the microporosity, or excess free volume of the polymer), and a second one where volume additivity is obeyed (Henry-type sorption).

As can be seen in Fig. 24, the data falls in-between the limiting cases, but lies closer to the constant volume line which suggests the pronounced hole-filling sorption mechanism in this material. The implications from this study are important for the fundamental understanding

of the operation of the glassy membranes. Water vapor sorption in flexible MOFs (MIL-89) has been reported by Horcajada et al. [128]. The researchers have shown the possibility of tunable and remarkably reversible sorption properties with relatively high swelling degrees of these network structures. Abuin et al. [129], have demonstrated substrate effects on the swelling of Nafion nanomembranes with dry thicknesses in a very broad range (17–1000 nm). It has been found that the water uptake for the thin films is much smaller than in the case of the bulk, and also that an effect of the supporting substrate is significant.

4.1.3. Organic solvents, liquids and vapors

In contrast to water as a penetrant, the studies involving sorption of non-aqueous liquids or vapors into dry polymer films are less common. A variety of topics can be found.

The need for the ability to detect VOCs has stimulated a significant effort in the development of selective sensors. Because these very often involve polymeric thin films able to swell in contact with VOCs, *in situ* ellipsometry has proved to be a very useful technique in these types of investigations [92,93,96,97,126]. Spaeth et al. [92,93], have focused on the most widely used VOCs sensing polymer PDMS, as well as its derivatives. The authors have also characterized a polyurethane type material. Their choice of organic vapors included toluene, tetrachloroethane, and cyclohexane. The use of relatively thick films (several hundred nm) has allowed independent observation of the changes in thickness and refractive index. The polymers have shown a linear dependence of swelling on vapor concentration. The highest sensitivity has been found for the penetrant with the refractive index deviating most from that of PDMS ($n_{PDMS} = 1.400$) – tetrachloroethane ($n_{TCE} = 1.505$). As a result, the largest changes in refractive index upon swelling are found, Fig. 25. Conversely, a polymer with similar refractive index as the solvent of interest is not suitable as sensor material for that particular organic compound. The findings of studies of Spaeth et al. can be used to choose the sensing material that is very sensitive toward some analytes and not toward others.

Linear swelling of nanostructured composites for sensing applications (Pd- and Au- CF_x) toward vapors of acetone, chloroform and 2-propanol has been reported by Cioffi et al. [126]. Swelling of calixarenes, potential candidates for organic vapor sensing with fast and reversible sorption, in several organic vapors has been reported by

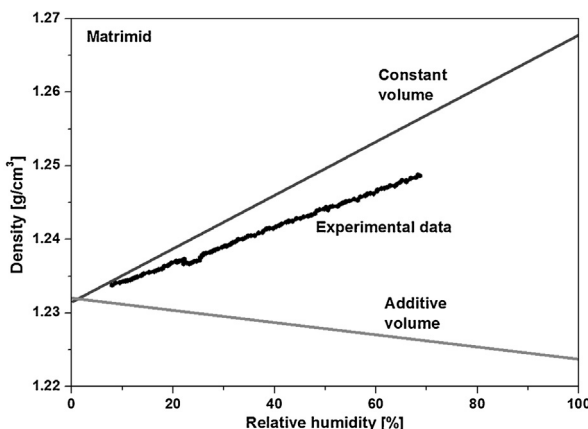


Fig. 24. Density changes in thin Matrimid films as a function of RH. The limiting cases assume either exclusive sorption into microporosity of the glassy polymer (constant volume) or perfect additivity of volumes of the polymer and sorbed water (additive volume) [91]. Copyright 2007. Adapted with permission from the American Chemical Society.

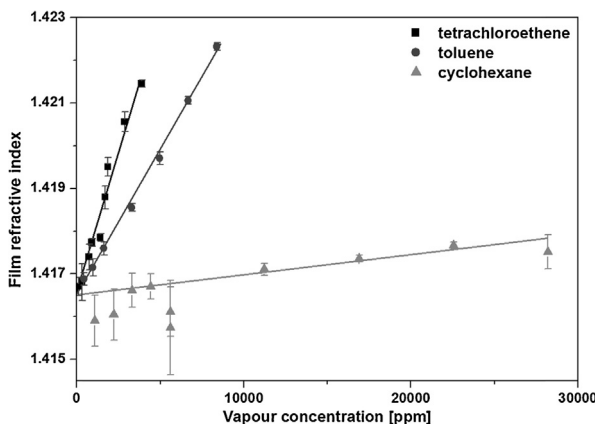


Fig. 25. Change in PDMS refractive index when exposed to organic vapors; the largest response seen in the case of tetrachloroethane indicating good sensitivity toward this compound [93].

Copyright 1997. Adapted with permission from Springer.

Nabok et al. [43,44]. Other studies in the field of sensors include swelling of nano-confined block copolymer films [96,97].

Filippov [86] and Filippova [82] have presented theoretical and experimental studies on organic solvent diffusion into thin polymer films. In another fundamental study of Elbs et al. [83], the Flory–Huggins interaction parameters for various glassy polymers in common vapor solvents have been determined. The researchers have measured the sorption in homopolymers, as well as in copolymers. This allowed them to study the compatibility between the different monomers in the presence of different solvents. Buchhold et al. [34], have reported on swelling of various high performance glassy polymers in vapors including water, ethanol, methanol, and 2-propanol, for the applications in microelectronic devices. Crossland et al. [49] have investigated the nucleation density in poly(3-hexylthiophene) thin films. Control has been achieved by a two-step approach. In the first step the films are swollen in a good solvent with high vapor activity, to completely remove crystallites. In the second step the vapor partial pressure is reduced to induce re-crystallization within the films. Depending on the conditions the re-crystallization results in different crystalline structures. Ogieglo et al. [24,25] investigated fundamentals of n-hexane sorption into thin and ultra-thin PS films. They have shown that a temperature-induced transition in the diffusion mechanism occurs in a narrow temperature range close to room temperature. In addition, their experiments reveal the existence of a distinct ~14 nm thin surface region that is instantaneously swollen upon contact with the solvent.

Recently, in situ ellipsometry has revealed the swelling behavior of a thin cross-linked PDMS layer atop a porous ceramic support, during pressure induced permeation of liquid n-hexane [9]. The dilation of the swollen film, exposed to a hydrostatic pressure difference, is in excellent agreement with the theoretical predictions of the so-called Solution-Diffusion model. This study demonstrates the applicability of ellipsometry to directly observe

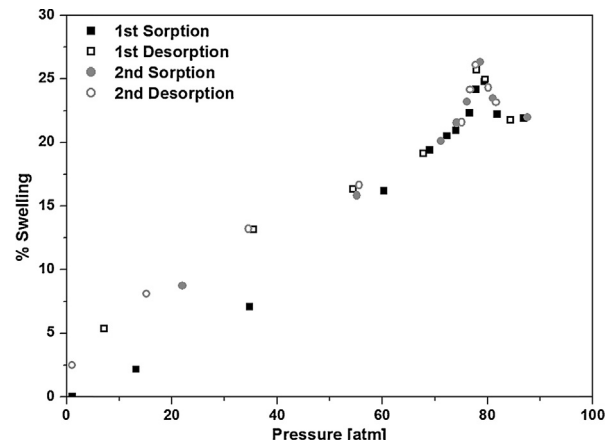


Fig. 26. Anomalous swelling maxima around 75 bar reported during high pressure CO_2 sorption in thin PMMA films. Onset of sorption–desorption hysteresis visible around 60 bar [57].

Copyright 2002. Adapted with permission from the American Chemical Society.

the behavior of thin selective layers of membranes during permeation.

4.1.4. High-pressure gases

There are only a handful of in situ ellipsometry studies involving high-pressure gases. All of them focus exclusively on sorption of CO_2 , mainly due to the use of this gas as an environmentally friendly solvent and its importance in membrane separations. Sirard et al. [68], have been the first to develop a high pressure ellipsometry cell, described in Section 2.3.3, and show data on the swelling of cross-linked PDMS films in CO_2 up to pressures of about 120 bar. The results for these rubbery thin films have been shown to correspond very well with gravimetrically determined swelling of bulk films [138]. Considerable attention has been devoted to the investigations of the unexpected swelling maxima (anomalies) reported first for PMMA [57], in vicinity of the critical point of CO_2 , Fig. 26.

The anomalous swelling is not observed in bulk swelling, and is more pronounced at 35 °C as compared with 50 °C. Distinct behavior close to the critical temperature is also observed for the physical properties of CO_2 , for instance the compressibility factor. The swelling maxima are not affected when a GaAs wafer instead of silicon wafer is used as substrate. The maxima in the swelling factors increase proportionally with the dry film thickness in the range from 85 to 325 nm. This suggests that the maxima cannot be solely explained by surface effects, but must be related to the swelling in the entire films. The anomalies have been further studied by Li et al. [79] for several other polymers, including PS, poly(ethylene oxide) (PEO), PDHFOMA, and the diblock copolymer PS-*b*-PDHFOMA. All of the polymers have shown the anomalous maxima, and their occurrence has again been found to be related to swelling within the whole volume of the films, rather than to an excess of CO_2 at the interfaces.

Wind et al. [75,76], have studied the relaxation dynamics in thin and thick polyimide films, intended as membrane selective layers. These authors have focused on the effects

of annealing on the CO₂ sorption and relaxation. Thin polyimide films were shown to relax much faster than thick films. The departures of the behavior of thin films from the bulk, and the impact on the gas sorption properties have been further systematically studied with *in situ* ellipsometry by Horn et al. [78]. These authors have been able to conclusively establish the large deviations in behavior of thin films from bulk behavior with respect to permeability of the thin layer membranes, reported in [139]. The long-term dynamic ellipsometry measurements have revealed refractive index minima in glassy films exposed to penetrant over large timescales (~ 100 h), suggesting a competition between plasticization and physical aging. For the longer timescales the aging has been shown to be dominant.

In situ high-pressure ellipsometry has also been used to study the effects of confinement on the glass transition of penetrant swollen polymers. Below the glass transition temperature polymers are not in their thermodynamic equilibrium, which has consequences for instance in their gas sorption behavior. Common features related to this include a slightly concave swelling versus pressure isotherm, as well as the existence of sorption–desorption hysteresis. The interactions with highly plasticizing gases, like CO₂, can significantly bring down the glass transition temperature of a polymer. Above glass transition the polymer–penetrant the system resides in a rubbery state with a linear (or slightly convex) sorption curvature and no sorption–desorption hysteresis. The first application of *in situ* high pressure ellipsometry to observation of the penetrant induced glass transition (P_g) has been done by Sirard et al. [57], in their study on anomalous maxima in CO₂ sorption in PMMA. Due to sufficiently high accuracy of ellipsometry, it has been possible to detect a pressure point at which the onset of sorption–desorption hysteresis occurred, Fig. 26, hence quantifying the P_g . More detailed studies of this phenomenon in highly plasticized PS and PMMA have been done by Pham et al. [74,84]. In these studies the authors utilized the change of swelling curvature (linear to concave) upon going from rubbery to glassy state. They have been able to determine the dependence of dry film thickness on the P_g even in very thin films, Fig. 17, by looking at changes of the Ψ parameter at several wavelengths. This approach has been chosen because the change in curvature associated with P_g could be seen in the raw data and the modeling has not been necessary. The thinner films have been shown to be plasticized at significantly lower pressures than the thicker ones. Additionally, the signature of a retrograde vitrification in PS/CO₂ system has been found. This phenomenon is not observed for bulk PS [84]. High-pressure *in situ* ellipsometry of highly plasticized glassy polymers has also been used by Carla et al. [77,140,141], in their development of a non-equilibrium sorption model. The technique has been used to determine sorption data, by application of the Clausius–Mossotti equation (discussed in more detail in Section 5.2 of this review). The sorption data have been compared with predictions of their non-equilibrium model. SE experiments were also conducted to locate the P_g from the intersection of linear fits from the rubbery and glassy regions, similar to the studies of Pham et al.

The other high pressure ellipsometry studies include those of Simons et al. [50], reporting CO₂ swelling and concentration data for several glassy polyetherimides and rubbery PEBAX, and the investigations on order–disorder transition in block copolymers by Chandler et al. [80].

4.2. Drying processes

A few studies focused on the details of solvent removal from a film. In most cases these studies do not require any experimental cell and can be done in a configuration presented in Fig. 10a. The dynamic changes in the film properties are followed during drying, usually immediately after film preparation.

The first studies of thin polymer film drying have been done by Filippov [86] and Filippova [82]. Their studies involve theoretical and experimental aspects. Based on dynamic film thickness changes, the authors have derived expressions for solvent diffusion. They determined the solvent diffusion coefficient and the corresponding energy of activation over a wide range of temperatures and solvent concentrations. At relatively high temperatures (55, 75, and 96 °C) the decrease in thickness is exponential with time. Further below the T_g of the pure polymer the temporal evolution of the thickness is more complex. The complex behavior of thickness versus time, during drying, is related to the fact that the system undergoes a glass transition. This has significant implications for technological applications. In the studies of Richardson et al. [55,64], for ultra-thin films of as spin-cast PMMA the vitrification of the polymer has been associated with the emergence of the glass compression energy barrier. This barrier opposes the thickness decrease during solvent loss. The manifestation of these effects results in a very slow relaxation of ~150 nm films (about 10 h) during drying, much slower than required if the process is governed solely by the diffusion of the solvent. The authors have investigated the effect of thickness on the slow relaxation. They found that the thickness of the drying films does not return to the thickness obtained by cooling an initially dry film from the melt. Also, thinner films relax much faster regardless of the used substrate, Fig. 27. The results have been discussed in terms of nano-confinement effects in the films manifested as an enhanced mobility within the polymer film closer to its top interface.

Drying of much thicker films of the same polymer, PMMA at ~300 nm, has been investigated by López García et al. [65]. In this case the researchers have chosen a solvent with high refractive index and high boiling point, bromobenzene. Use of this solvent allows to enhancing the optical contrast between the polymer and the solvent, and slowing down the rate of evaporation. This has been done to test several possible solvent evaporation scenarios, Fig. 28.

In scenario (i) the structural relaxation occurs together with the removal of solvent, in (ii) the solvent is lost long before the structural relaxation and in (iii) the solvent removal proceeds without any polymer relaxation. The calculated refractive index dynamics are shown in Fig. 28b. The conclusion is that some voids are indeed forming

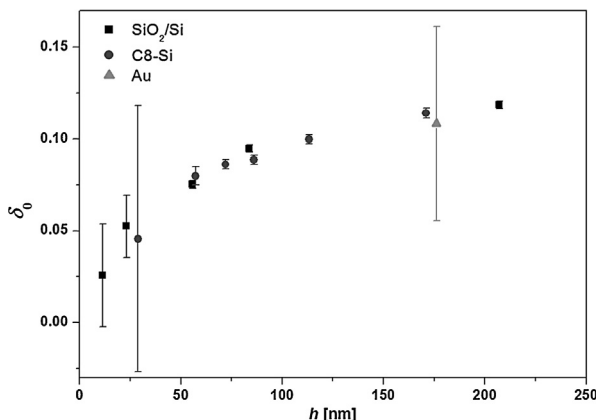


Fig. 27. Dry thickness dependence, h , of the structural relaxation parameter, δ_0 , defined as $(h_t - h_\infty)/h_\infty$, in drying of thin PMMA films. h_t and h_∞ represent film thicknesses at the beginning and end of drying. The data has been measured for several different substrates. The smaller values with decreasing thickness indicate significantly faster drying in the thinner films [55].

Copyright 2004. Adapted with permission from the American Physical Society.

during the solvent loss in the thin films. The loss of solvent in PMMA has also been investigated by Atarashi et al. [87], who showed a surprisingly significant impact of the produced morphology of as cast films on the subsequent water uptake. The effects have been explained in terms of the formation of unrelaxed pathways for water diffusion within the films. Annealing of the films after preparation would close the pathways, resulting in the swelling behavior expected solely from thermodynamics of polymer – solvent affinity.

4.3. Thermally, pH, and ionic strength induced transitions

In situ ellipsometry, especially in aqueous solutions, has been widely applied in studies of responsive polymers. Often, the layer preparation itself is carried out in situ and can be followed with ellipsometry. This is done, for example, in Ref. [103]. In this section, the representative examples for temperature, pH and ionic strength responsive polymeric materials investigated with ellipsometry are presented. As indicated before, polymer brushes and other covalently attached to substrate polymers are considered beyond the scope of this review, due to the specific physics and properties of these systems.

In a study of Harris et al. [46], in situ ellipsometry has been used to explain the changes in ion permeability of multilayer polyelectrolyte films as a function of pH. The authors observed that at acidic and neutral pH the swelling is significant (~40%), but stable in time. At alkaline pH the films swell to a similar magnitude, but continued to increase in thickness, and eventually delaminate. Correspondingly, at the same alkaline conditions the layers show dramatic increases in permeability. This indicates a much more solvent saturated structure. A pH responsive derivative of PDMS (Posimca50) has been shown to be able to detect of ammonia in air [94] and may provide a good alternative for the conventionally used dye-based

ammonia detectors. The changes in the optical thickness ($n \cdot h$) in response to water vapor containing ammonia have been the basis for the sensing mechanism, Fig. 29. The swelling changes have been primarily due to the interaction of ammonia with the carboxyl groups attached to the polymer matrix.

A general design strategy for the preparation of variable pH-responsiveness polyelectrolyte multilayer films has been presented by Hiller et al. [102]. Their material is based on PAH/SPS and has a history dependent swelling behavior. At low pH swelling is ~500%. Above neutral pH the film thickness is dramatically lower (~100%), and the film is in a collapsed state. The film swelling versus pH exhibits hysteresis. A hysteresis has also been observed for polypeptide multilayers, built by layer-by-layer deposition. This has been explained in terms of dynamic changes in charge density [103]. The films have been shown to be responsive to changes in temperature (swelling of 8% at 28 °C and 4% at 37 °C) due to conformational rearrangements. Small effects of ionic strength (concentrations of 1–6 mM NaCl) together with pH responsiveness of swelling and swelling kinetics in multilayers of weak polyelectrolytes have been found by Tanchak et al. [104].

Burke et al. [106], have investigated the effects of pH during assembly on the pH and ionic strength responsiveness in multilayers of HA and PAH. The swelling ratio has been found to increase with decreasing assembly pH and the swelling curves have revealed a minimum of swelling at around neutral pH, Fig. 30. The latter has been explained in terms of the acid–base chemistry of the layers; around neutral pH the majority of the free functional groups within the films are charged. Because of the polyampholytic nature of the films (presence of both acidic and basic groups), this leads to a partial collapse of the structure. On the other hand, for pH significantly different than neutral, chain extension due to like-charges repulsion dominates, causing increase in swelling. The authors have reported also on the swelling changes as a function of NaCl concentration. At higher salt concentrations the swelling has increased, which has been explained by the high salt concentration causing an irreversible weakening of the ionic bonds within the structure. Assembly pH responsiveness of polyelectrolyte multilayers has also been studied by Itano et al. [107] and Nerapusri et al. [119].

Temperature-sensitive hydrogels synthesized by electron beam irradiation of poly(vinyl methyl ether) (PVME) have been described by Hegewald et al. [52] in a combined ellipsometry, surface plasmon resonance (SPR) and optical waveguide spectroscopy study (OWS). Fully reversible swelling-deswelling process has been found with a phase transition temperature around 33 °C. In another study on hydrogels [95], thermo-responsive coatings of p(NIPAM-co-AA) on silicon wafers have been described. These coatings consisted of, instead a uniform film, a densely packed monolayer of spheres of 600 nm swollen diameter, which constituted a 10 times increase in dimensions from dry state. Despite the confinement effects the layers have been shown to still respond to temperature changes. Assuming a Uniform film model ellipsometry has been able to resolve these changes due to close packing in

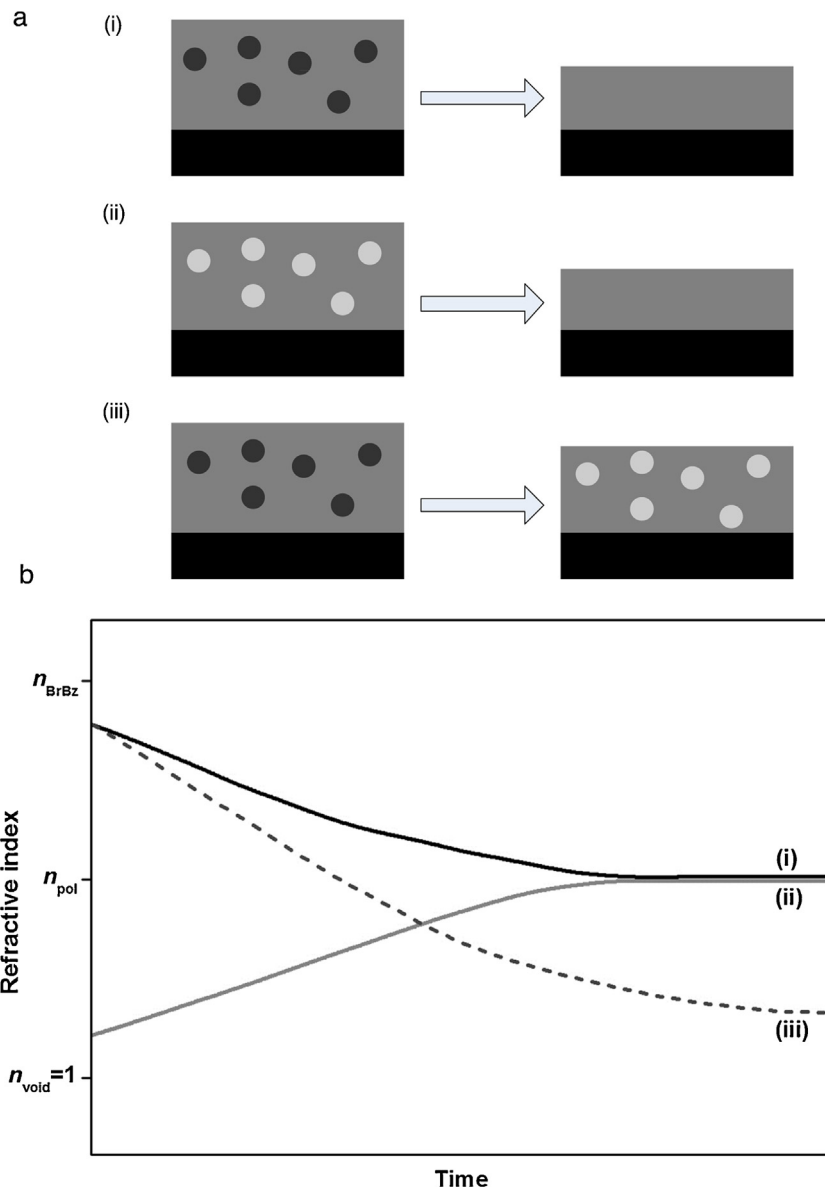


Fig. 28. (a) Three different scenarios of structural relaxation and removal of solvent molecules from drying PMMA films, (b) the corresponding dynamic refractive index changes [65].
Copyright 2011. Adapted with permission from John Wiley & Sons Inc.

the structure. Close-packed monolayers of hydrogels have also been investigated toward temperature, pH and ionic strength responsiveness by Nerapusri et al. [119].

A slightly different type of a responsive film investigation has been presented by Freudenberg et al. [88]. The authors have investigated the charging and swelling in thin cellulose films in water by combined streaming potential and ellipsometry measurements. It has been found that differences exist in the dissociation behavior of the carboxylic acid groups at the surface of the film and those within the films. The topmost groups have been able to dissociate completely, whereas for the rest only partial dissociation has occurred.

4.4. Reactions at interfaces, depositions and formations

In this section some of the examples of in situ ellipsometry studies of reactions at interfaces, depositions and film formations are described. Because such studies are quite common [142–144], especially in biological and protein research, here the focus is only on some examples where significant attention is dedicated to studying the properties of the swollen polymer layers with ellipsometry.

The study of adsorption of lysozyme and bovine serum albumin (BSA) on a surface of highly swollen hydrogel polymer based on PC has been presented by Murphy et al. [117]. This zwitterionic hydrogel, prepared by dip-coating, has been found to significantly reduce adsorption of the pro-

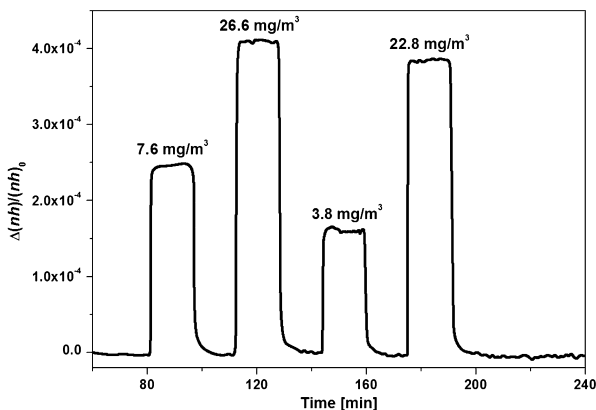


Fig. 29. Changes in optical thickness of a pH responsive polymer as a result of variable concentration of ammonia in water vapor at RH = 50% [94]. Copyright 2000. Adapted with permission from Springer.

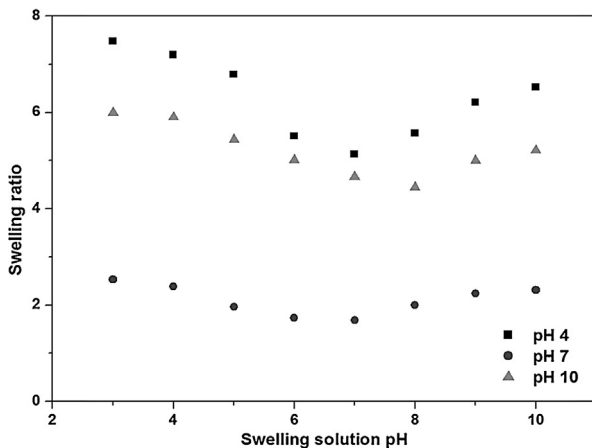


Fig. 30. Swelling ratio as a function of pH for HA/PAH multilayers assembled at different pH: 4 (■), 7 (●), 10 (▲) [106]. Copyright 2005. Adapted with permission from the American Chemical Society.

teins, which is important in many medical applications and in surfaces fouling. The spatial distribution of water within the swollen layers has been obtained by a combination of the neutron reflectivity and ellipsometry. It has been shown that the non-uniformly distributed density (gradient) within the films, with highly diffuse outer interface, is an important factor contributing to the control over protein adsorption. Protein adsorption on swollen hyperbranched polyesters has been investigated by Reichelt et al. [26]. Their focus has been on the systematic study on the effects of the degree of branching, backbone structure, flexibility and polarity of the materials. Various optical models have been evaluated that account for the adsorbed protein layer, the underlayer of the polyesters, and the ambient solutions. Upon careful evaluation of applicability of the chosen optical models, ellipsometry has been shown to be capable of the simultaneous study of swelling and adsorption. In addition, the IR-ellipsometry has provided chemical evidence for the formation of a thin protein layer on top of the polyester layers. An interesting use of in situ SE to track a reaction between ferrous ion and 2,2'-bipiridine

(bpy) in swollen Nafion films has been made by Pantelić et al. [53]. Here the basis has been the strong changes in optical absorption spectra upon formation of the complex ion, Fe(bpy)₃²⁺. The optical absorption of the swollen films has been modeled with Urbach and Tauc–Lorentz oscillator functions.

4.5. Dissolution or degradation

Studies on polymer dissolution with in situ ellipsometry have been one of the first applications of this technique to investigate highly swollen polymer systems. Already in 1987 Manjkow et al. [18,19] have investigated the kinetics of PMMA dissolution in various organic solvents with a “psi-meter”. The name of this device derives from the use of only the Ψ parameter for the determination of the sample properties. In such case the refractive index of the film needs to be known beforehand to calculate the thickness. The authors have investigated the influence of various parameters, such as temperature, molecular weight or aging time on the dissolution rate. They have also been able to identify conditions when the process of anomalous Case II diffusion governs the initial stages of dissolution. For Case II diffusion the rate of swelling is proportional to time, as a result of the progress of a sharp front separating a swollen and a dry layer within the film. Subsequently, the polymer dissolution of the swollen layer occurred, which has been limited kinetically by the presence of the longer polymer chains. It has been shown that both thermodynamics and kinetics of the processes in the system could be mapped out accurately with utilization of the technique. Later, Papanu et al. [20,21,23] have further developed the technique. They focused on the solvent mixtures, effects of molecular weight, and the temperature, on the dissolution kinetics by Case II penetration. The authors have been able to show that the evidence for Case II description is very clear upon analysis of the Ψ and Δ curves. The spectra could not be modeled accurately with the Uniform Film model that does not account for a sharp front within the film.

Dissolution of composite films of PDADMAC and silica particles used in sensor applications has been studied by Zudans et al. [54]. The authors have been able to identify the different stages of the film dissolution. The initial one when the film index approaches that of the surrounding solution while the thickness does not change much, the second one where the disintegration of the matrix occurs together with the large expansion of the polymer network, and the third one where slow dissolution of the swollen film occurs. During the initial exposure to the experimental ambient (0.1 M KNO₃) a decrease in thickness has been observed, inset in Fig. 31, after which the network expansion (thickness increase starting after about 36 h) and subsequent dissolution occurs. No definite cause for this initial thickness decrease has been given. It has been speculated that presence of water in the structure leads to the formation of hydrogen bonds, causing compaction of the structure.

In other studies, the dissolution of photoresist [145] and plasma-polymerized polyethylene glycol-like films for drug delivery applications [121] has been investigated in

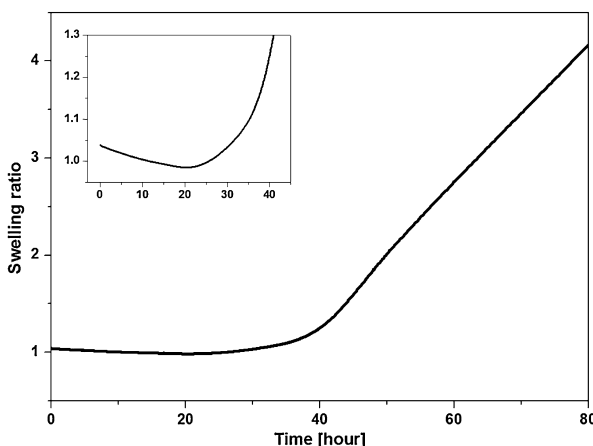


Fig. 31. Swelling ratio of composite sol-gel films upon immersion in 0.1 M KNO₃. Initial, very slight thickness decrease is observed, after which significant swelling and film dissolution occurs [54]. Copyright 2004. Adapted with permission from the American Chemical Society.

a similar manner. Enzymatic degradation of immobilized protein multilayer films has been investigated by Foose et al. [146], also using a dynamic in situ ellipsometry approach.

4.6. Electrochemically induced swelling changes

There exist several investigations that focus on the study of electrochemically induced changes in swelling of polymer and composite layers. In one of them a detailed electrochemical investigation on the PANI anodic pre-peak has been conducted in conjunction with in situ ellipsometry measurements of film swelling [42]. This anodic pre-peak had been previously found to occur in this important conducting polymer during cyclic voltammetry experiments, but the reason for its appearance has remained not investigated. The authors have been able to relate the appearance of this pre-peak to the changes in swelling of the polymer during electric potential scans. The either positive or negative shifts in the peak have been related to higher or lower water content within the polymer matrix (swelling differences). This water content could in turn be tuned by film annealing. Oxidation-reduction has been shown to change the optical properties in self-assembled osmium complex-derivatized poly(allylamine) and glucose multilayers, as investigated by Forzani et al. [47]. The swelling of the films has been shown to be correlated to redox transitions resulting in an exchange of anions and the solvent with the investigated film. Electrochemical swelling has also been investigated by Schmidt et al. [69], for nanocomposite films containing PEI and Prussian Blue nanoparticles. The incorporation of the particles has allowed electrochemical control over the swelling and mechanical properties of the films. Upon reduction the films have shown reversible swelling decrease and softening. These properties may have useful applications in responsive coatings and nanoscale devices. Oriented bilayer films of gramicidin and DMPC have been shown to respond to an electrical potential by a change in the

water content (swelling) and the resulting changes in circular dichroism of gramicidin molecules within the film [111].

5. Types of information extracted with the use of *in situ* ellipsometry

In about 40% of in situ ellipsometry studies on swollen polymers the technique is mainly used to determine static swelling and refractive index of the layers in contact with ambients. Many studies, however, include the kinetics of swelling. These kinetics may be relatively simple and sufficiently described by the Fick's law, or more complex. Studies on swelling kinetics are reviewed in Section 5.1. Ellipsometry data can also be used to calculate penetrant volume fractions, as is reviewed in Section 5.2. The extent of sorption can be used to determine thermodynamic parameters for the polymer-penetrant system, such as the Flory-Huggins interaction parameters, χ . This is reviewed in Section 5.3.

5.1. Dynamic studies

In many in situ ellipsometry studies no dynamic ellipsometry data is presented. The main reasons for this are the insufficient data acquisition rate of especially older equipment, or simply the lack of explicit interest in process kinetics. The significant recent advances in instrumentation for dynamic ellipsometry data acquisition allow data acquisition rates on the order of several seconds or less (depending on desired accuracy and precision) per full SE spectral scan. This has opened new possibilities to track even relatively fast processes with great accuracy. In this paragraph the focus is on these types of investigations.

5.1.1. Simple dynamic phenomena

This paragraph provides a few representative examples of dynamic ellipsometry studies of relatively simple diffusion phenomena. The technique has been used to study Fickian diffusion, in the absence of significant secondary relaxation phenomena. Secondary relaxations will be discussed in more detail in Section 5.1.2. Fickian type of dynamics can be observed for glassy films that are reversibly swollen to a relatively small degree, and in fully rubbery swollen films.

An example of the first case is the dynamic spectroscopic ellipsometry study of ion bombardment modified polyimides, presented by Eichhorn et al. [89]. In this study the spectra of about 500 nm glassy polyimide films have been recorded in time, while the relative humidity in the ambient air has been varied. The authors have been able to detect the small fully reversible swelling changes in the dilation of the film (see Fig. 32). This behavior makes the films interesting for sensor applications. Mikhaylova et al. have reported the very fast swelling toward equilibrium of hyperbranched polyester films in response to immersion in electrolyte solutions [39]. All their films exhibited similar kinetics. The extent of equilibrium swelling has been shown to depend on the annealing conditions. For longer annealing times the extent of swelling has decreased.

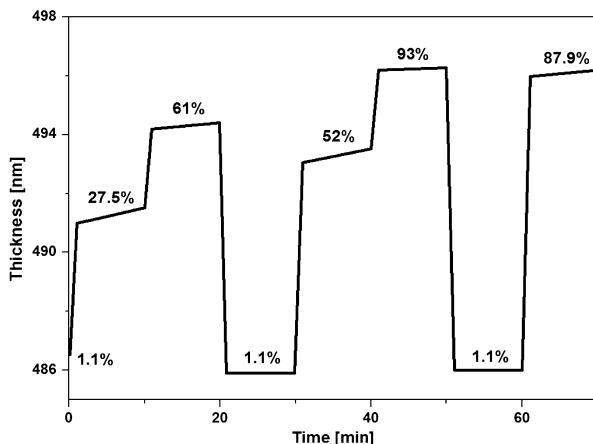


Fig. 32. Reversible dynamic response to changes in relative humidity in the ambient of ion bombardment modified thin polyimide film [89]. Copyright 2004. Adapted with permission from Elsevier Science Ltd.

This has been attributed to the formation of denser polymer structure, due to the formation of hydrogen bonding between–OH groups in the polymer network. Gensel et al. [96] and Zettl et al. [97] also investigated Fickian type of diffusion during the swelling of confined block copolymer films.

5.1.2. Complex dynamic phenomena

For glassy matrices often the assumption of purely Fickian dynamics does not hold. The diffusion may be accompanied by significant sorption induced relaxations of the polymer. These so-called secondary relaxations are due to structural reorganizations of the polymer network [147,148]. Usually, the timescale of Fickian diffusion is much shorter than that of the secondary relaxations. In a swelling experiment this is often manifested by an initial increase in film thickness due to diffusion of molecules into the polymer network, followed by slower changes in film thickness due to relaxations. Such processes can be fitted with the semi-empirical relationships established by Berens and Hopfenberg [149]. The extracted parameters are the concentration independent diffusion coefficient and relaxation time constants. Due to the infirm assumptions underlying the semi-empirical relation, the physical significance of these parameters needs to be treated with care.

Apart from thickness variation, in situ spectroscopic ellipsometry provides independent dynamic analysis of other sample properties such as the refractive index, film non-uniformity, anisotropy, density gradients), and light absorption. This enables very detailed studies of the dynamics of thin film swelling. The dynamic refractive index behavior may often bring even more insights than the thickness variations. In this section illustrative examples are discussed.

Tang et al. [15,16] have presented one of the first in situ spectroscopic ellipsometry studies on Fickian diffusion combined with polymer relaxation (see Fig. 33). They have investigated zwitterionic polymer films based on phosphorylcholine (PC), an important material in

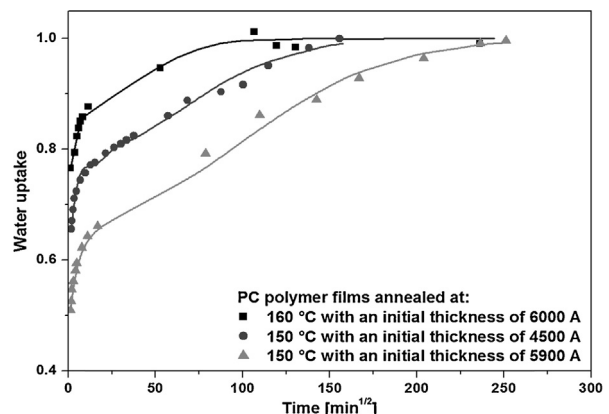


Fig. 33. Complex swelling of zwitterionic films in aqueous solutions. The initial fast swelling (Fickian) and the subsequent slower relaxation contribute approximately equally to the total swelling of the films [16]. Copyright 2002. Adapted with permission from the American Chemical Society.

biomedical applications. The temporal resolution of the used device was only ~40 s per scan, which was sufficient to resolve the slow swelling dynamics. The authors have found that Fickian diffusion and polymer relaxation contributed approximately equally to the final equilibrium solvent uptake. The annealing temperature has been shown to affect the equilibrium penetrant uptake. Annealing of the films significantly slows down the relaxational dynamics but has had little impact on the Fickian diffusion. The authors have used the Berens–Hopfenberg model and have indicated several inadequacies of this model. The model is valuable for comparing similar samples, and the extracted diffusion coefficients are similar to those determined with other methods.

In situ ellipsometry has been used to investigate pronounced relaxational behavior of glassy films upon exposure to plasticizing gaseous penetrants, over large timescales [75,76,78]. These studies benefit from the extremely high sensitivity of ellipsometry to small changes of both the thickness and the refractive index. Wind et al. [75,76] have correlated the dynamics of sorption and diffusion of CO₂ in polyimide membrane materials with permeation measurements, in particular with respect to the impact of annealing conditions. They have shown that thin polyimides films plasticize faster and at lower pressures than bulk films. This has important consequences for membranes for molecular separations. Such membranes generally comprise a thin selective layer that allows fast permeance of the species of interest. Horn et al. have investigated sorptive relaxations and simultaneous physical aging in ultra-thin films [78] (Fig. 34). The authors have systematically investigated various membrane related polymers, including Matrimid, poly(*p*-phenylene oxide) (PPO), poly-sulfone (PSF), and PS. The data obtained for thin films and bulk polymers reveals significant differences. The thin films sorb significantly less penetrant as compared to bulk polymer, and show greatly accelerated physical aging effects that dominate the sorption processes at longer timescales.

Sorption induced relaxations may dominate the dynamics of diffusion. If the relaxations limit the sorption

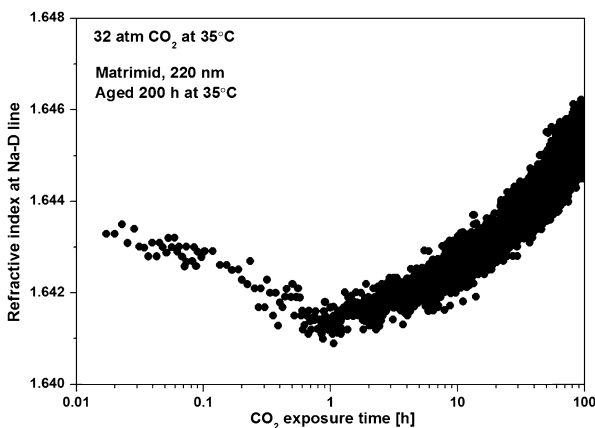


Fig. 34. Long term changes in the refractive index of Matrimid 220 nm film upon exposure to 32 bar of CO₂. Initially the index drops, being a sign of increasing penetrant uptake. In the later stages the structure densifies signifying an increasing impact of physical aging [78]. Copyright 2012. Adapted with permission from the American Chemical Society.

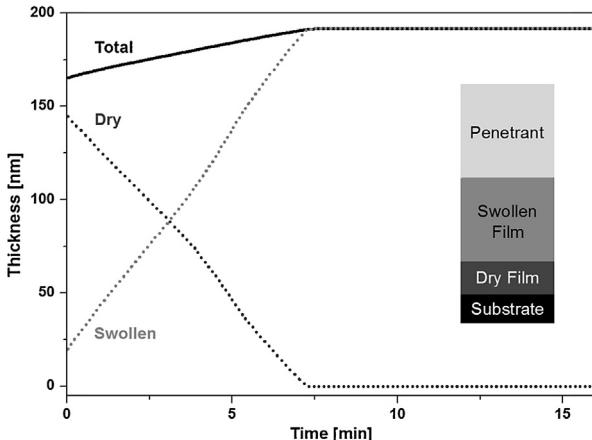


Fig. 35. Case II diffusion resolved in 150 nm PS film during swelling with liquid n-hexane. A sharp front existing between the swollen and the dry layers of the film allows application of a two-layer model enabling kinetics of the process to be accurately resolved [24]. Copyright 2013. Adapted with permission from Elsevier Science Ltd.

dynamics, anomalous diffusion can be observed, for instance Case II diffusion. This has been investigated with *in situ* ellipsometry in several studies, focused on dissolution of PMMA [18–21] and diffusion of n-hexane into PS [24,25]. The characteristic feature of Case II diffusion is the formation of a sharp front separating a swollen layer and a practically dry layer within the swelling film. This occurs when the diffusion through the swollen layer is much faster than the polymer relaxations at the diffusing front. In effect a uniform film is transformed into a stack of two films with dynamically changing thicknesses (see Fig. 35).

The overall dilation of the film proceeds linearly due to the limiting constant rate of polymer relaxation at the front. The multilayer can be represented by an appropriate optical model, assuming a stack of two distinct homogeneous layers (Fig. 8c). This approach has been used for the sorption of n-hexane into PS films of variable thickness [24,25].

The authors have shown that a temperature-induced transition from Fickian-Relaxation to Case II exists around room temperature. For Case II sorption the front velocity is strongly affected by the sample history. The front velocity is constant in the entire film, except for a ~14 nm outer surface region that is instantly swollen upon exposure to the solvent. The existence of such a region is technologically relevant in applications where films with thicknesses below 100 nm are utilized.

Significant deviations from Fickian diffusion have also been found in layer-by-layer-deposited polyelectrolyte films [104]. The authors have shown that the dynamics of water induced swelling of these films could be tuned by varying the assembly conditions. The diffusion mechanisms ranged from Case II (swelling linearly proportional to time) to Super Case II (sigmoidal swelling with time).

Application of more complex optical models aids more insights into the dynamic structural changes of swelling layers. An example is the study of swelling of zwitterionic films based on sulfobetaine and n-butylacrylate [17]. In this study several optical models have been compared and strong evidence is found for temporal optical anisotropy within the swollen films. An important indication for the existence of anisotropy is the very large reduction of the MSE when uniaxial anisotropy is included in the optical film model, is can be seen in Fig. 36.

The optical anisotropy is related to the chemical structure of the polymeric material. There is an orientation of the ionic crosslinks that are formed by the highly polarizable zwitterionic groups. The ellipsometry data indicate overshoot-swelling dynamics. The optical anisotropy emerges after the maximum swelling is observed, and the polymer relaxes to a denser structure. During relaxation the extent of anisotropy slowly decreases and an isotropic material is obtained when equilibrium swelling is reached. An optical model that combines a density gradient with anisotropy has revealed that the structural changes of the ware largest close to the substrate, where the immobilization of chains has been the strongest.

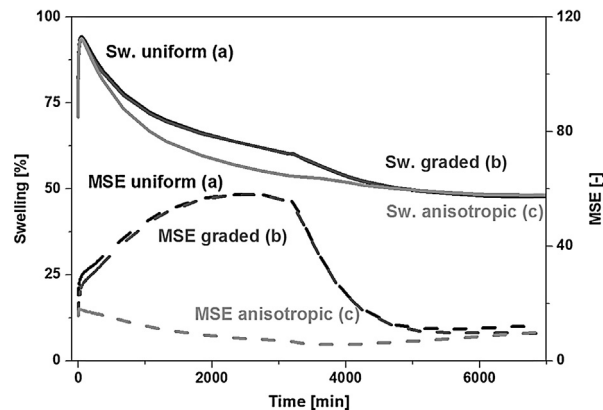


Fig. 36. Comparison of swelling of zwitterionic films exposed to 1 M NaCl modeled with various optical models. The large reduction of MSE, seen in the case of application of a uniaxial anisotropic model, strongly suggests the existence of anisotropic structure during swelling of the material [17]. Copyright 2013. Adapted with permission from Elsevier Science Ltd.

Toward the outer surface of the film the sample anisotropy diminishes.

5.2. Penetrant volume fraction calculations

From the change in the film dilation and refractive index penetrant concentration can be calculated. The simplest approach uses only the film dilation and is based on the assumptions of polymer-penetrant volume additivity and unidirectional swelling of the film. Unidirectional swelling implies dilation only in the direction perpendicular to the substrate. As a result, the penetrant volume fraction, $\phi_S^{dil.}$, can be calculated simply from film dilation:

$$\phi_S^{dil.} = \frac{h_{SP} - h_{DP}}{h_{SP}} \quad (3)$$

In this equation h_{SP} and h_{DP} represent the thicknesses of polymer films swollen with penetrant and dry, respectively. Such an approach has been used for the determination of the water volume fraction in hydrophilic polyacrylates [41], in zwitterionic polymer films [15,16], and in polyelectrolyte multilayers [114], as well as organic solvent fractions in block copolymers [97] and poly(3-hexylthiophene) [49].

Other approaches are based on the calculation of penetrant volume fraction from both the change of the film dilation and its refractive index. Such an approach is in particular beneficial when volume additivity is not proven. For polyelectrolyte multilayer films Miller et al. calculated the refractive index of swollen films from a linear combination of indices of pure constituents [108]:

$$h_{SP}n_{SP} = (h_{SP} - h_{DP})n_{SP} + h_{DP}n_{DP} \quad (4)$$

Because of the small refractive index differences between the polymer and water this simple relation has been shown to be quite accurate. The relation actually corresponds to the lower Wiener bound [150,151].

More frequently, two approaches are encountered that are based on treating the swollen polymer as an effective medium: the Clausius–Mossotti relationship and the Bruggeman Effective Medium Approximation (BEMA). The Clausius–Mossotti relation takes advantage of the dependence of the refractive index of a pure substance on its mass density [152]:

$$\frac{n^2 - 1}{n^2 + 2} = \frac{R}{M_w} \cdot \rho \quad (5)$$

where R is the molar refractivity and M_w is the molecular weight of the substance. The ratio of R/M_w is often assumed constant and denoted q . In a mixture of a polymer and a solvent the additivity of refractivity contributions can be assumed:

$$\frac{n_{mix}^2 - 1}{n_{mix}^2 + 2} = q_{solv.} \cdot C_{solv.} + q_{polym.} \cdot C_{polym.} \quad (6)$$

And the concentration of the polymer can be calculated from the dilation:

$$C_{polym.} = \rho_{polym.} \cdot \frac{h_{DP}}{h_{SP}} \quad (7)$$

When the mixture refractive index, n_{mix} , the polymer density $\rho_{polym.}$, the swelling, and $q_{solv.}$ for the pure solvent are known, the mass concentration of the solvent, $C_{solv.}$, can be calculated. The Clausius–Mossotti relation has been used for the determination of the volume fraction of high-pressure gaseous penetrants in glassy and rubbery polymers [50,68,75–78,91,153]. In these cases the procedure is somewhat flawed by the need of an assumption about the density of a penetrant dissolved in the polymer. For CO₂, Sirard et al. [68] took the supercritical densities of 0.95 g/cm³ and corresponding refractive index of 1.22 at room temperature to determine mass concentrations of CO₂ in PDMS. Whether the state of the dissolved penetrant at relatively low pressures can be assumed identical to that from its critical state is arguable, and the results of such calculations need to be treated as only estimate, as also indicated by the authors. In addition, the Clausius–Mossotti relation has been derived for polarizable molecules in vacuum, which further weakens the applicability of this procedure especially for highly pressurized gaseous penetrants (refractive index significantly larger than 1). In view of this other effective medium theories, such as Maxwell–Garnett or BEMA, are more advantageous. More information on the applicability and limitations of effective medium theories can be found in textbooks [6] and the work of Aspnes et al. [151].

The BEMA mixes the optical dispersions of the mixture components (designated as 1 and 2) in a self-consistent manner, treating the optical dispersion of the mixture as a host material:

$$\phi_1 \cdot \frac{n_1^2 - n_{mix}^2}{n_1^2 + 2n_{mix}^2} + \phi_2 \cdot \frac{n_2^2 - n_{mix}^2}{n_2^2 + 2n_{mix}^2} = 0 \quad (8)$$

This approach is advantageous when the volume fractions of the components are comparable. This is often the case for significantly swollen polymers. Similar to sorption analysis based on the Clausius–Mossotti relation, the dispersion of the penetrant is assumed to be known and unaffected by sorption in the polymer matrix. Examples of the use of the BEMA include organic solvent fraction determination in PDMS and its derivatives [9,93], water sorption in polyimides [66], polyacrylates [41], hydrated polysaccharides [40], hydrogels [100,127], block copolymers [98], and hyperbranched polyesters [26].

Chan et al. [127] have shown that for calculating the water fraction in hydrogels the dilation and EMA approaches are in very good agreement, Fig. 37. This confirms the unidirectional swelling of these films. Good agreement between the dilation and EMA approaches is mostly found for the sorption of penetrants in rubbery polymers. This indicates that for these systems the approximation of additive polymer and penetrant volumes is often reasonable. In glassy systems volume additivity often fails due to the existence of significant excess free volume. This excess free volume is kinetically trapped in the polymer during vitrification. Upon sorption, penetrant molecules may (partly) occupy this excess free volume. This causes a lower increase in volume of the swollen material as compared to the situation of volume additivity. An additional complication is associated with the non-equilibrium

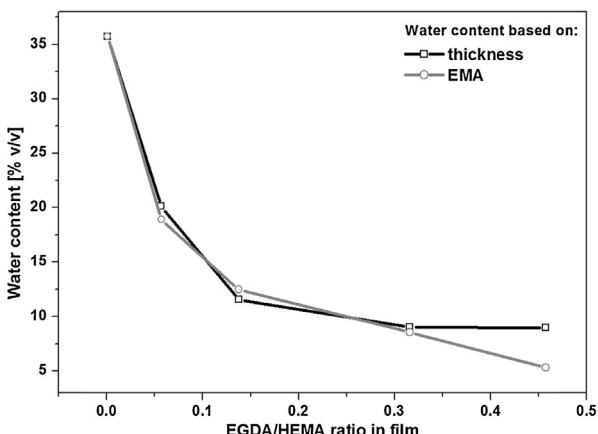


Fig. 37. EMA and dilation (thickness) approaches for the determination of water fraction in hydrogels shown to agree very well, confirming unidirectionality of swelling [127].

Copyright 2005. Adapted with permission from the American Chemical Society.

status of the excess free volume. A penetrant may significantly plasticize the glassy polymer to allow reduction of the excess free volume by polymer relaxation. As a result, the refractive index of the polymer in the penetrant-polymer mixture cannot be assumed equal to its refractive index prior to sorption. The presence of excess free volume complicates accurate calculations. For initially dry samples with significant excess free volume, the values derived for the penetrant concentrations are underestimations that depend on the method used as well as the sample history. These issues have been thoroughly discussed in the study of Ogieglo et al. [154]. They present an approach that is based on the extrapolation of the properties of a plasticized polymer from its rubbery state. For this approach the dilation and EMA approaches are shown to agree with each other and the underestimation of the penetrant concentration is avoided.

5.3. Thermodynamic parameters

The volume fractions calculated using one of the approaches, presented in Section 5.2, can be used to quantify the thermodynamic parameters of the polymer-penetrant systems. In investigations of swollen films the most popular approach is via the Flory-Huggins and Flory-Rehner theories [155,156]. The Flory-Huggins theory, written in terms of solvent volume fraction and its activity, uses the binary interaction parameter χ :

$$\ln(a) = \ln(\phi_S) + (1 - \phi_S) + \chi \cdot (1 - \phi_S)^2 \quad (9)$$

This parameter describes the interaction energy between the polymer and penetrant and is a useful measure of the strength of this interaction, due to simplicity of Eq. (9). When cross-linked thin film networks are considered the Flory-Huggins expression is modified by the elastic energy, Ω , yielding the Flory-Rehner expression by adding the following term to the right side of Eq. (9):

$$\Omega = \left(1 - \frac{2M_c}{M}\right) \frac{V_S E}{3RT} \left(\alpha - \frac{1}{2\alpha}\right) \quad (10)$$

In this expression M_c is the molecular weight between cross-links, M is the molecular weight of the polymer, V_S is the molar volume of the solvent, R is the gas constant, T is the temperature, E is the Young's modulus of the polymer, and α is the swelling factor defined as h_{SP}/h_{DP} . The use of the Flory Rehner expression instead of pure Flory-Huggins is of particular importance for cross-linked strongly swelling supported films. This is because, due to immobilization on the substrate, swelling can only occur in one direction perpendicular to the substrate. For unidirectional swelling the polymer network deformation is much larger than in the case where swelling occurs in all three spatial directions. In the case of unidirectional swelling the Ω contribution is usually quite significant and cannot be neglected [9].

There are several in situ ellipsometry investigations where the interaction parameters are calculated. In an interesting study of Elbs et al. [83] the Flory-Huggins interaction parameters have been determined for homo- and copolymers as a function of various organic vapor activities. The polymer films, of about 150 nm dry thickness, have been exposed to vapors at different saturations (p/p_{sat}) until stabilization. The volume fraction of the solvent has been calculated from polymer dilation, as described in Section 5.2, and then Eq. (9) has been used to extract the χ parameters. The authors have discussed the concentration dependence of the interaction parameters (which, according to Flory-Huggins theory should be concentration independent), Fig. 38. The effect is known to be related to the difference in densities between the polymer and the penetrant and concentration dependence of chain mobility or monomer interactions. Afterwards, the compatibility between different polymer components in block copolymer solutions has been estimated from a Scott-Flory-Huggins mean field approach. Ellipsometry has been shown to be a very consistent and convenient technique, which could be easily generalized for similar research problems. The interaction parameters for the non-cross-linked polymers have also been investigated in a scaling behavior study for block copolymers by Chandler et al. [80].

For the cross-linked materials the Flory-Rehner approach has been utilized in several cases [9,76,110]. Wind et al. [76], have used the expression to estimate the effect of cross-linking of thin polyimide and PDMS films on the sorption and relaxation behavior. They have found negligible effects in PDMS, whereas for the glassy polyimides the effect has been very significant. These effects have been related to much more pronounced relaxational behavior of glassy polymers in general, as compared to rubbery PDMS. Blacklock et al. [110], have investigated the impact of cross-linking on the behavior of bio-reducible polymers. The interaction parameters have been calculated with the Young's modulus determined from rubber elasticity theory ($E=3\nu_E RT$). An increase in the interaction parameter upon cross-linking has been correlated with an increased hydrophobicity of the network and formation of bulk water droplets within the films. The authors have found, in addition, an excellent agreement between results of QCM, AFM and ellipsometry. The impact of cross-linking density on the swelling and interaction parameters in PDMS-n-hexane system has been investigated with high-pressure

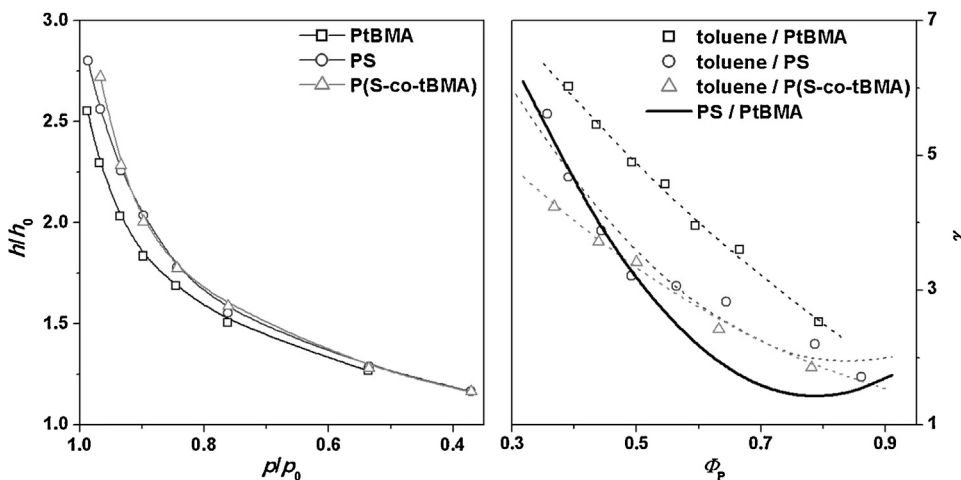


Fig. 38. Swelling of various polymers and a copolymer in toluene vapors (left), and the extracted Flory–Huggins interaction parameters (right). The concentration dependence of the interaction parameters clearly points to the breakdown of some assumptions in the simplest form of the Flory–Huggins relationship, Eq. (9) [83].

Copyright 2004. Adapted with permission from Elsevier Science Ltd.

liquid ellipsometry [9]. In this study the parameters have been compared that are calculated from the Flory–Huggins and Flory–Rehner equations, with and without the assumption of a perfect network. It has been concluded that the perfect network assumption does not hold for the lowest degree of cross-linking.

In several investigations also a different type of a thermodynamic parameter, the disjoining pressure, has been investigated [40,157,158]. This parameter, also calculable from swelling of the polymer, is a measure for the force per unit area within the wetting film. This pressure can be created by large macromolecules confined between cells in the extracellular matrix and result in emergence of hydrated pathways for the transport of molecules by separating the cellular barriers.

6. Ellipsometry combined with other techniques

More than half of the studies included in this review combine ellipsometry with other *in situ* techniques. There are two main reasons for that. One is the inherently indirect nature of ellipsometry. The extraction of useful film parameters requires the use of an optical model. It is difficult to assess *a priori* how physically realistic the optical model represents the sample, as is discussed in Section 2.2.3. On the other hand, optical models can include many sample features (roughness, gradients, anisotropy, etc.) that can yield additional information. A sensible balance needs to be found between sufficient details and overparametrization. This can be aided by confronting the ellipsometry results with those of other arguably more direct methods, such as QCM (at least for rigid, non-dissipating films) and AFM. These other techniques may also provide complementary information on the (non-)swollen polymer film. In most literature studies, the generation of complementary information is the main incentive for combining ellipsometry with other techniques.

6.1. Ellipsometry concurrently combined with other techniques *in situ*

Only a very few studies exist in which *in situ* ellipsometry measurements have been conducted concurrently with other methods. Dinh et al. have been combined electrochemical, QCM, and ellipsometry measurements in the study on the PANI anodic pre-peak [42]. For these three techniques the sample configuration is compatible; a special electrochemical/optical plastic (PMMA) cell with a working electrode consisting of AT-cut quartz crystal with evaporated Ti and Au layers, a Pt counter electrode is Pt, and reversible hydrogen reference electrode. This configuration allows observing the response of swollen films to electrochemical stimuli. A similar cell has been used in electrochemical and ellipsometry measurements done by Forzani et al. [47] and Tagliazucchi et al. [48] on swelling of polyelectrolyte multilayers during redox cycles (Fig. 39).

6.2. Ellipsometry complemented with other *in situ* techniques

A large variety of different *in situ* techniques have been used to complement *in situ* ellipsometry data. A very common technique is QCM, often with dissipation (QCM-D), for obtaining mass changes and viscoelastic properties of swollen films. Another frequently used technique is AFM, which provides a measurement of the film thickness and the top-view morphology. Both of these techniques are quite well established in *in situ* measurements of swollen polymers. Some prominent examples may be found in [159–161] for AFM and in [162,163] for QCM. In this paragraph the combination of *in situ* ellipsometry with other techniques is described. The principles of these techniques are introduced briefly, more details can be found in specialized literature.

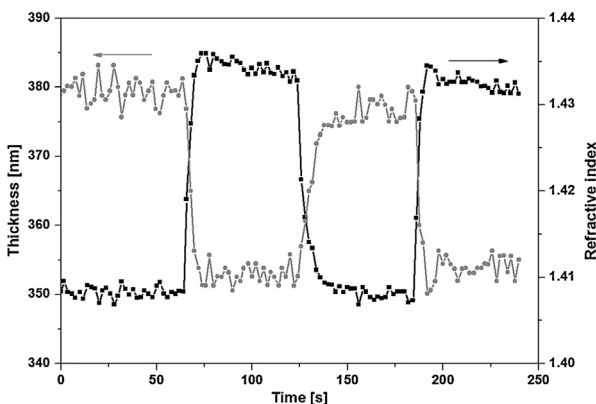


Fig. 39. Thickness (closed symbols) and refractive index (open symbols) changes induced by alternating electrical potential steps of 0 V and 0.5 V, measured by concurrent ellipsometry and electrochemical measurements [47].

Copyright 2002. Adapted with permission from the American Chemical Society.

6.2.1. Quartz crystal microbalance (QCM)

A quartz crystal microbalance measures very precisely changes of resonant frequencies of metal-coated (e.g., gold, titanium) quartz crystals. Atop such a crystal a polymer film can be present, or such a film can be formed during the measurement. A change in the mass of the polymer film will affect the resonant frequency of the crystal. This allows accurate measurement of penetrant mass uptake. The overtones of the resonant frequency can be related to viscoelastic properties of the films. A QCM that allows characterization of viscous dissipation is denoted QCM-D. The data obtained by a QCM-D is very complementary to SE data. SE gives access to the volumetric and optical density changes in the films, and calculations are required to relate these to changes in mass, as is discussed in Section 5.2. Extraction of mass changes from SE data is very problematic if the swelling ambient has a refractive index close to that of the film, or for films thinner than ~ 25 nm. QCM-D may remain sensitive for such systems, because it is based on a completely different principle as compared to SE. In addition, changes in the viscoelastic properties of the films cannot be derived from SE in a straightforward manner. For a comprehensive reference of a combinatorial QCM and ellipsometry studies the reader is referred to the work of Rodenhausen et al. [164] or Richter et al. [165].

QCM and ellipsometry have been used to study water uptake in hydrophilic polyacrylates [41]. Dynamics of swelling obtained from both techniques are in agreement, provided that the shape of the QCM resonance peak is not affected by the presence of the water. Minor changes in the shape of the resonant peak imply that minor changes in the viscoelastic properties of the swollen films occur. Kleinfeld et al. [35], have studied water uptake in composite multilayer films by combined QCM and ellipsometry measurements (Fig. 40). The observations are rationalized by an initial filling the void spaces within the films. This is manifested by limited dilation (SE) and significant mass uptake (QCM). Subsequently the films swell to a larger extent by combined dilation and mass uptake.

Abuin et al. have investigated similar sorption features in Nafion nanomembranes, with combined QCM and SE [129]. Rouessac et al. have demonstrated the complementarity of QCM and SE porosimetry in a very thorough study of supported inorganic glassy membrane films [166]. The authors have discussed in detail the advantages and disadvantages of all the techniques they used. Blacklock et al. combined QCM-D, AFM, and SE for characterization of the effect of crosslinking on mechanical properties of bioreducible swollen multilayer films [110]. SE combined with QCM and other techniques has also been used for organic vapor sorption in calixarene films [43], the absorption of supercritical gases in bulk glassy polymer films [77], and in the electrochemically modulated film thickness and mechanical properties of swollen nanocomposite layers [69].

6.2.2. Atomic force microscopy (AFM)

AFM belongs to the most direct methods to determine film thickness and top-view morphology. In AFM a nanometers scale tip on a cantilever scans the surface of the sample, and the forces between the sample and the tip are measured. These forces may include van der Waals forces, capillary forces, and electrostatic forces. The displacement of the tip is typically measured by reflecting a laser on the top surface of the cantilever, and detected the angle of reflection by a photodiode. The film thickness can be obtained by making a small scratch on the sample surface with a sharp tool. The local removal of the film exposes the bare substrate and an AFM scan perpendicular to the scratch provides the height difference between the substrate and the top surface of the film [102].

SE and AFM provide complementary data on surface topology and surface roughness [38,69,95,106,107,110,123,128]. In SE the probing light spot size is usually relatively large, ranging from hundreds of microns to several millimeters. SE data represents the average of the properties of the probed films over spot size area. AFM can provide nano-scale information on surface morphology, roughness, and homogeneity. In situ AFM allows for direct observation of film dilation and morphological changes upon exposure to penetrants [69,107,110]. For example, Blacklock et al. [110] have combined in situ AFM and SE to study the morphology changes in thin bioreducible layer-by-layer films as a function of number of layers, the extent of cross-linking, and extent of degradation (Fig. 41). Lee et al. have used in situ AFM to visualize pore closing in polyelectrolyte multilayers by [167].

6.2.3. Neutron and X-ray reflectivity

The wavelength of neutrons and X-rays is much shorter than that of visible light. This short wavelength allows neutron and X-ray reflection techniques to access information on small length scales, in the order of sub-Å to several nm.

In neutron reflection measurements, the intensities of the incoming and exiting beams are measured at very low angles (grazing incidence). The reflection is usually expressed as a function of the scattering length density, which is related to the chemical composition. The scattering length density is a relatively strong function of isotopic

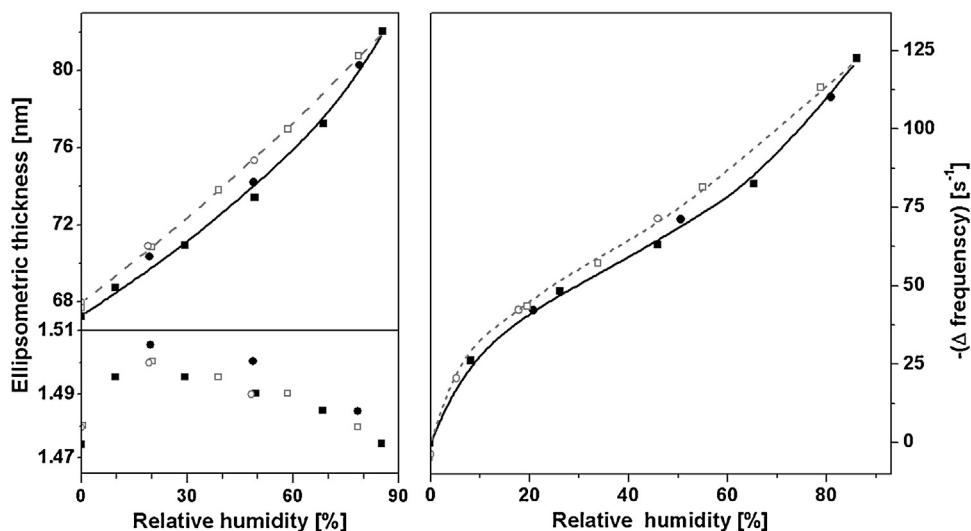


Fig. 40. Ellipsometry (left) and QCM (right) data on sorption of water vapor in composite multilayer films [35]. At lower humidity the mass uptake dominates without much swelling of the film (little thickness change, but significant index and mass increase). At higher humidity more pronounced swelling as results from mass uptake [35].

Copyright 1995. Adapted with permission from the American Chemical Society.

composition of the material. This allows distinguishing between, for instance, D_2O and H_2O in so-called contrast variation measurements. A mixture of 1 mol D_2O and 2 mol of H_2O has a specular neutron reflectivity that is very close to that of a silicon substrate. By using this mixture as swelling ambient for a polymer film on a silicon substrate, the neutron contrast is caused predominantly by the polymer film. In this way the spatial distribution of the polymer

density within the swollen film can be resolved with high precision, for layers of several nm thickness. SE studies on composition gradients require films that are at least an order of magnitude thicker. Murphy et al. [116,117] and Tang et al. [15] combined SE and neutron reflection in protein adsorption studies to obtain the spatial variation in polymer concentration in very thin (down to ~5–10 nm) zwitterionic films swollen in water. They have shown that

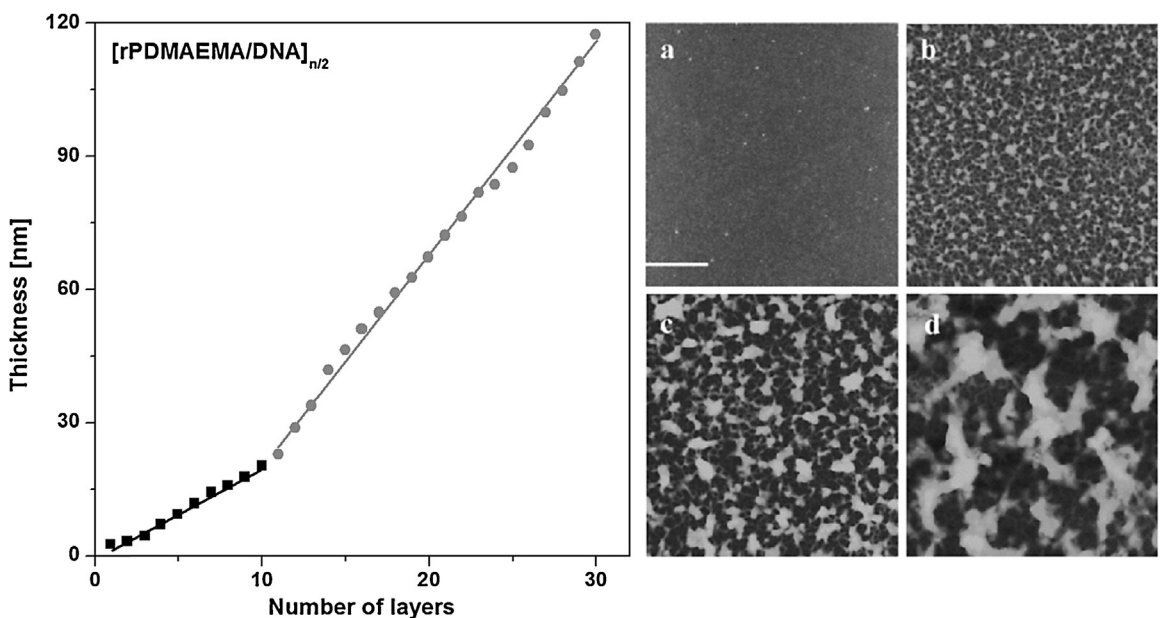


Fig. 41. Ellipsometry thickness data (left) and the corresponding changes in morphology of the layer-by-layer films by in situ AFM (right). Going from a to d (right) the numbers of layers are increasing from 2 (a), 10 (b), 20 (c), 30 (d). The bar in graph is a 1 μm long. In ellipsometry data, two linear regimes of deposition are visible, one from 1 to 10 layers (~2 nm per layer) and the second from 11 to 30 layers (~5 nm per layer) [110].

Copyright 2010. Adapted with permission from the American Chemical Society.

SE is practically insensitive to gradients in such very thin films. Neutron reflection combined with SE has also been used by Atarashi et al. [87] to study the density profiles of as-spun PMMA thin layers in their water.

X-ray reflection measurements are sensitive to electron density variation in the films. These variations can be correlated with the mass uptake of microporous systems. The technique can also provide information about a nanometer scale pore size distribution. Rouessac et al. have presented a thorough comparison of results obtained with SE, QCM, and X-ray reflection measurements, and have addressed the complementarity of the techniques [166].

6.2.4. Electrochemical methods

Electrochemical methods require preparation of films on a metal substrate that serves as an electrode. Examples of such substrates include gold, titanium, and platinum. The sample can often also be used for QCM measurements [69]. In a cyclic voltammetry experiment the electric potential is increased linearly in time until a certain value is reached and the potential ramp is inverted [46]. In impedance spectroscopy sinusoidal voltages, within a range of frequencies are imposed on a sample. Harris et al. [46], combined cyclic voltammetry and impedance spectroscopy with SE to assess the stability and ion permeability in of layer by layer polyelectrolyte films, at different pH. Cyclic voltammetry and impedance spectroscopy have shown dramatic increases in ion permeability in alkaline solutions, as compared to neutral and acid solutions. The observations can be rationalized from distinct swelling behavior of the films at alkaline conditions.

Ellipsometry has also been combined with streaming potential measurements in the study of close-packed monolayers of micro-gel particles [119] and swollen cellulose films [51,88].

6.2.5. Gravimetric methods

Gravimetric sorption (micro) balances allow direct measurement of the sample mass, but require more pronounced mass changes as compared to QCM(-D) and SE. The sensitivity of micro-gravimetric balances is several orders of magnitude lower than QCM. For example, Buchhold et al. have presented a relatively simple and direct approach, based on weighing the spin-coated samples on 3-in. diameter silicon wafers [34]. They have reported a precision on the order of 15% with an accuracy of 30 µg.

Gravimetry has been used in conjunction with SE to compare thick and thin films [64,91]. Rowe et al. have measured the changes in dilation of a quartz spring to which ~30 mg of a polymer sample was attached [91]. The mass uptake of several high glass transition polymers has been calculated from the displacement of the spring. At low pressures similar uptake was found for ~500 nm and 10 µm films. Richardson et al. have investigated the kinetics of drying of ~150 nm thin films and ~50 µm thick films [64], and the impact of vitrification on residual solvent remaining in these films. For all films the time required for drying is much larger than that calculated assuming Fickian diffusion. This has been rationalized by the occurrence of a glass transition during drying. Horn et al. have compiled SE and gravimetry data for CO₂ sorption in Matrimid, to elucidate

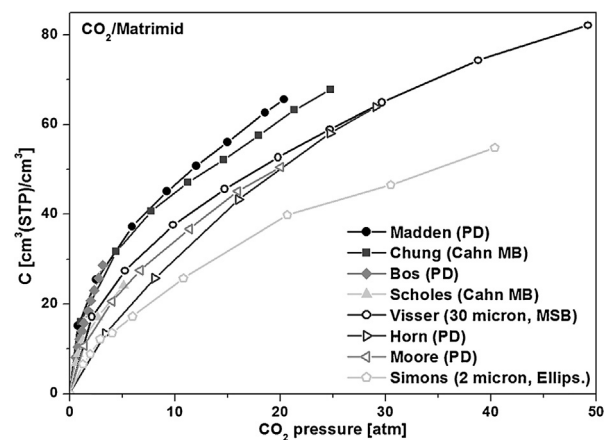


Fig. 42. CO₂ sorption data in Matrimid from several microbalance (MB), pressure decay (PD), and magnetic suspension balance (MSB) studies of bulk films compared with ellipsometry data for thin films [78]. Copyright 2012. Adapted with permission from the American Chemical Society.

difference in plasticization and relaxation of thin and thick films (Fig. 42) [78]. The ~100 nm thin films were shown to behave distinct from bulk films. This is in contrast to the findings of Rowe et al., who used ~500 nm thick films [91]. Wind et al. have measured carbon dioxide sorption, induced plasticization, and permeability of polyimides and compared thick and thin films [75,76].

6.2.6. Contact angle measurements

Contact angle hysteresis has been investigated for polyimide films [66] and hyperbranched aromatic polyester films [39]. Contact angle hysteresis can give information on the swelling induced dynamic changes in the hydrophilic–hydrophobic balance of the films. Such information is not accessible by SE.

Hennig et al. has measured the advancing and receding contact angles in dynamic cycling contact angle measurements [66]. The observed changes of the wetting behavior over various cycles are attributed mainly to swelling and/or liquid retention, as determined with ellipsometry. Curing at high temperatures has been found to reduce the water uptake, causing faster stabilization of the wetting behavior. Mikhaylova et al. have found no dependence of the contact angle on the thickness of hyperbranched aromatic polyester films. For the same samples the refractive index increases for thinner films [39]. These results imply a similar surface hydrophilicity of films of varying thickness, whereas the density of thinner films is higher.

6.2.7. UV-vis spectroscopy

Crossland et al. have used ellipsometry and UV-vis spectroscopy for the study of crystallization of conjugated polymers that display π–π interactions [49]. Single-wavelength *in situ* ellipsometry has been used to determine swelling changes, whereas UV-vis spectroscopy allowed tracking the changes in the optical absorption. The optical absorption is related to two types of molecular states, as is depicted in Fig. 43.

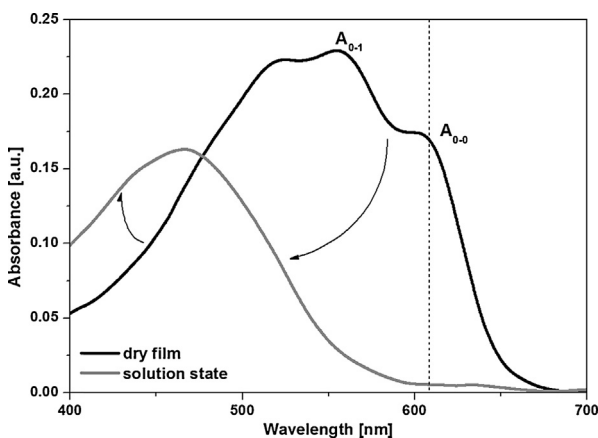


Fig. 43. UV-vis spectra of dry and significantly swollen $\pi-\pi$ conjugated films. The change in the absorption spectrum is related to dissolution of crystallites going from dry to swollen polymer. At the same time ellipsometry derived film thickness has been observed (not shown) [49]. Copyright 2011. Adapted with permission from John Wiley & Sons Inc.

The long wavelength absorption has been attributed to chains in a crystalline state: linearized π -stacked chains. The short wavelength absorption has been attributed to interchain states of isolated chains. The changes in the UV-vis spectrum could be used to quantify crystallinity changes within the swollen films. In principle, similar data could be gathered with in situ SE, provided that the optical absorption of the material is not too strong and the films are not too thick. UV-vis absorption measurements have also been used by Yagüe et al. [99] to track marker (fluorescein) emission signal depending on the mesh size in iCVD deposited hydrogels.

6.2.8. IR spectroscopy

IR spectroscopy is able to probe the properties of the swollen films with much longer wavelengths than UV-vis SE. IR spectroscopy is particularly sensitive to chemical changes of the investigated materials, giving rise to its complementary nature with respect to ellipsometry. Combined SE and IR spectroscopy has been used to study ammonia sensing of Posimca50, a derivative of PDMS containing carboxyl acid groups. The changes in IR transmission in a particular region of the spectrum have been interpreted as clear evidence of the acid-base reaction of the analyte (ammonia) with the sensing material. At the same time the changes in swelling of the material upon exposure to ammonia have been detected with ellipsometry. In another study Fourier Transform IR has been employed by Chan et al. [127] to investigate chemical changes related to cross-linking in iCVD deposited films. In situ ATR-IR (attenuated total reflectance – infra red spectroscopy) has been combined with in situ ellipsometry for the study of protein adsorption on oligosaccharide-modified hyperbranched poly(ethylene imine) films [130].

IR ellipsometry is a technique that is rarely employed in situ. It has been used together with VIS ellipsometry to study chemical changes and swelling occurring during the formation of protein adsorption layer on top of hyperbranched polyesters, in a study of Reichelt et al.

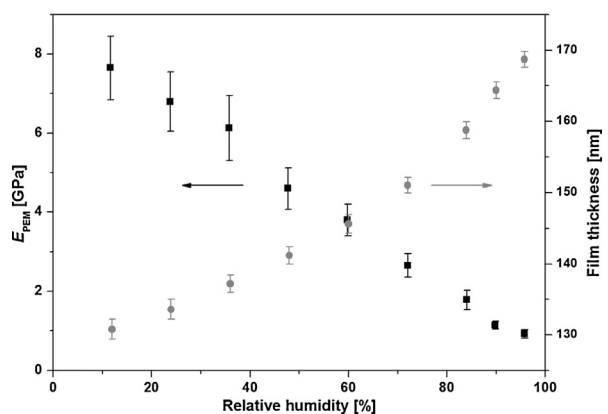


Fig. 44. Young's modulus (buckling) and film thickness (ellipsometry) obtained for polyelectrolyte multilayer films as a function of relative humidity [85]. Copyright 2008. Adapted with permission from the American Chemical Society.

[26]. Recently, in situ IR ellipsometry has been developed for the studies of polymer brushes [168]. Correlation of VIS-ellipsometry with IR-ellipsometry contributed to a significant improvement of water fraction determination in these highly swollen systems.

6.2.9. Surface plasmon resonance (SPR)

Surface plasmons are coherent electron oscillations at an interface. Excitation of a surface plasmon by incident light at resonance conditions can be used to visualize the response of a polymeric material to adsorbing species. The excitation can be done with a single wavelength *p*-polarized He-Ne laser light [43] and can be performed in an in situ arrangement [43,52,118]. The relative response in calixarene films, studied with SPR by several groups, has been shown to be correlated with saturation vapor pressure of penetrants [43,118]. SPR measurements have been treated as complimentary to ellipsometry; they give a more direct measure of the mass adsorption of the vapors, and are in this sense similar to QCM.

6.2.10. Methods to determine mechanical properties

Young's moduli of thin polymeric films can be extracted by analyzing strain induced buckling patterns [85]. These simple and elegant measurements have been shown to be applicable in situ (in controlled relative humidity) for PS, PMMA and polyelectrolyte multilayers. The collected data have allowed correlating changes in swelling (ellipsometry) with the changes of the mechanical properties of the investigated materials, see Fig. 44.

7. Concluding remarks and outlook

Based on the analysis of the studies described in this review several conclusions and future projections can be made. Undoubtedly, ellipsometry has established itself as a very useful technique in investigations of thin films interacting with penetrants. It offers a very balanced combination of precision, accuracy, non-intrusive character, and high temporal resolution. It is also relatively

inexpensive and well applicable to analysis of films with thicknesses in a practically important range, from nanometers to several microns. The high versatility of ellipsometry is signified by a large variety of the different processes studied, starting from penetrant uptake from dry state, via drying processes, pH, temperature, ionic strength or electrochemically induced transitions, ending with dissolutions, degradations and complex diffusion phenomena. All of the advantages of the technique have contributed to the situation, where in many studies ellipsometry suffices as the only characterization technique.

A gradual progress in instrumentation has been noticeable in the timeline of the studies, where a shift from single wavelength to spectroscopic ellipsometry going from older to more recent investigations has been well visible. At the same time the type of information extracted with the technique has changed from relatively simple static swelling studies to more complex dynamic ones. However, this trend has certain exceptions, like the early studies of complex dissolution phenomena in PMMA [18–21]. The improvement in the speed of data acquisition and analysis has made possible investigations of processes occurring on the timescales from seconds to weeks. The introduction of a compensator allowed dealing with samples with complex, depolarizing morphologies. In these cases the various non-idealities like roughness or thickness non-uniformity could be included in the analysis. A significant extension of applicability of ellipsometry has been made by the introduction of high pressure static [68] and permeation cells [9] that opened entirely new possibilities related to fundamental research in, for example, membrane technology. In this area, it is possible to notice that the research attention has been gradually shifting from fundamental studies to investigations on the behavior of practically applied systems.

In situ ellipsometry has been proven very successful in fundamental studies on the nature of interactions of glassy and rubbery polymers with liquids and condensable gases. Its potential has also been explored significantly in more complex polymeric materials, such as multilayers and composites. It can be expected that also other emerging classes of macromolecular materials will attract attention in the future. These may include nano- and bio-composites, or hybrid organic–inorganic materials, including metal organic frameworks. The characterization of these more complex systems may benefit especially from combination of ellipsometry with other in situ techniques. In particular, concurrent ellipsometry – QCM-D studies seem highly complementary, but are not extensively represented in thin polymer film research yet.

Acknowledgments

The authors acknowledge comments and helpful discussions with Michiel Raaijmakers and Emiel Kappert from Inorganic Membranes group and Beata Koziara from Membrane Science and Technology group at the University of Twente.

The authors gratefully acknowledge the permissions granted to reproduce the copyright material in this

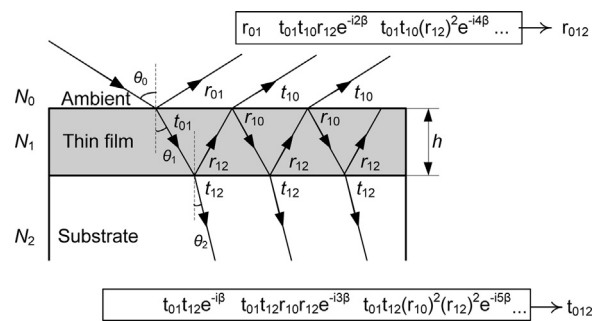


Fig. A1. More detailed scheme of light reflection and transmission at the thin film sample [6].
Copyright 2007 Adapted with permission from John Wiley & Sons Inc.

Review. The material is used in the present work under fair use, non-profit, review conditions.

Appendix.

In this section, the selected mathematical formulae utilized in the conversion of ellipsometric parameters, Ψ and Δ , into sample properties (and vice versa) are briefly presented. The detailed derivation can be found in Ref. [6]. The complex reflectance ratio for the sample shown in Fig. 4 can be written, using the well-known Fresnel relationships, as:

$$\rho = \frac{r_p}{r_s} = \frac{N_1 \cos \theta_0 - N_0 \cos \theta_1 / N_1 \cos \theta_0 + N_0 \cos \theta_1}{N_0 \cos \theta_0 - N_1 \cos \theta_0 / N_0 \cos \theta_0 + N_1 \cos \theta_1} \quad (\text{A1})$$

The transmission angle can be calculated from the Snell's law using the usually known incidence angle, θ_0 :

$$N_0 \sin \theta_0 = N_1 \sin \theta_1 \quad (\text{A2})$$

Eq. (A1) represents a complex number, because $N_0 = n_0 + ik_0$ and $N_1 = n_1 + ik_1$.

Ψ and Δ are then directly calculated as:

$$\Psi = \arctan(|\rho|) \quad (\text{A3})$$

$$\Delta = \begin{cases} \tan^{-1} \left[\frac{\text{Im}(\rho)}{\text{Re}(\rho)} \right] & \text{for } \text{Re}(\rho) > 0 \\ \arctan \left[\frac{\text{Im}(\rho)}{\text{Re}(\rho)} \right] + 180^\circ & \text{for } \text{Re}(\rho) < 0, \text{Im}(\rho) \geq 0 \\ \arctan \left[\frac{\text{Im}(\rho)}{\text{Re}(\rho)} \right] - 180^\circ & \text{for } \text{Re}(\rho) < 0, \text{Im}(\rho) < 0 \end{cases} \quad (\text{A4})$$

When light enters a thin film sample it reflects (reflection coefficient, r) and transmits (transmission coefficient, t) at each of the interfaces. The rays leaving a sample (r_{01} – reflection from topmost interface, t_{10} – transmittance after reflection from second interface, etc.) interfere with each other and produce spectral oscillations in the Ψ and Δ . Fig. A1 presents in more detail the light reflection and transmission occurring at the thin film sample.

The complex reflectance ratio is expressed as:

$$\rho = \frac{r_p}{r_s} = \frac{r_{01,p} + r_{12,p} \exp(-i2\beta) / 1 + r_{01,p} r_{12,p} \exp(-i2\beta)}{r_{01,s} + r_{12,s} \exp(-i2\beta) / 1 + r_{01,s} r_{12,s} \exp(-i2\beta)} \quad (\text{A5})$$

With:

$$\beta = \frac{2\pi h N_1 \cos \theta_1}{\lambda} \quad (\text{A6})$$

Calculation of Ψ and Δ can be performed using again Eqs. (A3) and (A4). However, for the measured Ψ and Δ values the determination of film thickness and its optical constants is usually done with an optical model, Section 2.2.3, due to mathematical complexity of Eq. (A5).

Appendix B. Supplementary data

Supplementary data associated with this article can be found, in the online version, at <http://dx.doi.org/10.1016/j.progpolymsci.2014.09.004>.

References

- [1] Lorentz HA. Over de theorie der terugkaatsing en breking van het licht: academisch proefschrift. Arnhem: K. van der Zande; 1875, 181 pp.
- [2] Drude P. Optische Eigenschaften und Elektronentheorie. *Ann Phys* 1904;319:677–725.
- [3] Drude P. Ueber Oberflächenschichten. II. Theil. *Ann Phys* 1889;272:865–97.
- [4] Drude P. Ueber Oberflächenschichten. I. Theil. *Ann Phys* 1889;272:532–60.
- [5] Hall AC. A century of ellipsometry. *Surf Sci* 1969;6:1–13.
- [6] Fujiwara H, Wiley I. Spectroscopic ellipsometry principles and applications. Hoboken, NJ: John Wiley & Sons; 2007, 369 pp.
- [7] Tompkins HG, Irene EA, editors. Handbook of ellipsometry. Norwich, NY/Heidelberg: William Andrew Inc./Springer-Verlag; 2005, 870 pp.
- [8] Azzam RMA, Bashara NM. Ellipsometry and polarized light. Amsterdam: North-Holland Pub Co.; 1977, 529 pp.
- [9] Ogieglo W, van der Werf H, Tempelman K, Wormeester H, Wessling M, Nijmeijer A, Benes NE. n-Hexane induced swelling of thin PDMS films under non-equilibrium nanofiltration permeation conditions, resolved by spectroscopic ellipsometry. *J Membr Sci* 2013;437:313–23.
- [10] Hale GM, Querry MR. Optical constants of water in the 200-nm to 200-μm wavelength region. *Appl Opt* 1973;12:555–63.
- [11] French RH, Yang MK, Lemon MF, Synowicki RA, Prbil GK, Cooney GT, Herzinger CM, Green SE, Burnett JH, Kaplan SG. Immersion fluid refractive indices using prism minimum deviation techniques. *SPIE Proc* 2004;5377:1689–94.
- [12] Barbuy R, Lavanant L, Paripovic D, Schuwer N, Sagnaux C, Tugulu S, Klok HA. Polymer brushes via surface-initiated controlled radical polymerization: synthesis, characterization, properties, and applications. *Chem Rev* 2009;109:5437–527.
- [13] Edmondson S, Osborne VL, Huck WTS. Polymer brushes via surface-initiated polymerizations. *Chem Soc Rev* 2004;33:14–22.
- [14] Hinrichs K, Eichhorn KJ, editors. Ellipsometry of functional organic surfaces and films. Berlin: Springer-Verlag; 2014, 363 pp.
- [15] Tang Y, Lu JR, Lewis AL, Vick TA, Stratford PW. Swelling of zwitterionic polymer films characterized by spectroscopic ellipsometry. *Macromolecules* 2001;34:8768–76.
- [16] Tang Y, Lu JR, Lewis AL, Vick TA, Stratford PW. Structural effects on swelling of thin phosphorylcholine polymer films. *Macromolecules* 2002;35:3955–64.
- [17] Ogieglo W, de Groot J, Wormeester H, Wessling M, Nijmeijer K, Benes NE. Relaxation induced optical anisotropy during dynamic overshoot swelling of zwitterionic polymer films. *Thin Solid Films* 2013;545:320–6.
- [18] Manjikow J, Papanu JS, Hess DW, Soane DS, Bell AT. Influence of processing and molecular parameters on the dissolution rate of poly-(methyl methacrylate) thin films. *J Electrochem Soc* 1987;134:2003–7.
- [19] Manjikow J, Papanu JS, Soong DS, Hess DW, Bell AT. An in situ study of dissolution and swelling behavior of poly-(methyl methacrylate) thin films in solvent/nonsolvent binary mixtures. *J Appl Phys* 1987;62:682–8.
- [20] Papanu JS, Hess DW, Bell AT, Soane DS. In situ ellipsometry to monitor swelling and dissolution of thin polymer films. *J Electrochem Soc* 1989;136:1195–200.
- [21] Papanu JS, Hess DW, Soane DS, Bell AT. Dissolution of thin poly(methyl methacrylate) films in ketones, binary ketone/alcohol mixtures, and hydroxy ketones. *J Electrochem Soc* 1989;136:3077–83.
- [22] Papanu JS, Hess DW, Soane DS, Bell AT. Swelling of poly(methyl methacrylate) thin films in low molecular weight alcohols. *J Appl Polym Sci* 1990;39:803–23.
- [23] Papanu JS, Soane DS, Bell AT, Hess DW. Transport models for swelling and dissolution of thin polymer films. *J Appl Polym Sci* 1989;38:859–85.
- [24] Ogieglo W, Wormeester H, Wessling M, Benes NE. Temperature-induced transition of the diffusion mechanism of n-hexane in ultra-thin polystyrene films, resolved by in-situ spectroscopic ellipsometry. *Polymer* 2013;54:341–8.
- [25] Ogieglo W, Wormeester H, Wessling M, Benes NE. Probing the surface swelling in ultra-thin supported polystyrene films during case II diffusion of n-hexane. *Macromol Chem Phys* 2013;214:2480–8.
- [26] Reichelt S, Eichhorn KJ, Aulich D, Hinrichs K, Jain N, Appelhans D, Voit B. Functionalization of solid surfaces with hyper-branched polyesters to control protein adsorption. *Colloids Surf B* 2009;69:169–77.
- [27] Sturm J, Tasch S, Niko A, Leising G, Toussaere E, Zyss J, Kowalczyk TC, Singer KD, Scherf U, Huber J. Optical anisotropy in thin films of a blue electroluminescent conjugated polymer. *Thin Solid Films* 1997;298:138–42.
- [28] Pettersson LAA, Ghosh S, Inganäs O. Optical anisotropy in thin films of poly(3,4-ethylenedioxythiophene)-poly(4-styrenesulfonate). *Org Electron* 2002;3:143–8.
- [29] Campoy-Quiles M, Nelson J, Etchegoin PG, Bradley DDC, Zhokhavets V, Gobsch G, Vaughan H, Monkman A, Inganäs O, Person NK, Arwin H, Garriga M, Alonsos MI, Herrmann G, Becker M, Scholdei W, Jahja M, Bubeck C. On the determination of anisotropy in polymer thin films: a comparative study of optical techniques. *Phys Status Solidi C* 2008;5:1270–3.
- [30] Campoy-Quiles M, Etchegoin PG, Bradley DDC. On the optical anisotropy of conjugated polymer thin films. *Phys Rev B* 2005;72, 045209/1–16.
- [31] Laskarakis A, Logothetidis S. On the optical anisotropy of poly(ethylene terephthalate) and poly(ethylene naphthalate) polymeric films by spectroscopic ellipsometry from visible–far ultraviolet to infrared spectral regions. *J Appl Phys* 2006;99, 066101–3.
- [32] Winfield JM, Donley CL, Kim J-S. Anisotropic optical constants of electroluminescent conjugated polymer thin films determined by variable-angle spectroscopic ellipsometry. *J Appl Phys* 2007;102, 063505–7.
- [33] Patil N, Soni J, Ghosh N, De P. Swelling-induced optical anisotropy of thermoresponsive hydrogels based on poly(2-(2-methoxyethoxy)ethyl methacrylate): deswelling kinetics probed by quantitative mueller matrix polarimetry. *J Phys Chem B* 2012;116:13913–21.
- [34] Buchhold R, Nakladal A, Gerlach G, Herold M, Gauglitz G, Sahre K, Eichhorn KJ. Swelling behavior of thin anisotropic polymer layers. *Thin Solid Films* 1999;350:178–85.
- [35] Kleinfeld ER, Ferguson GS. Rapid, reversible sorption of water from the vapor by a multilayered composite film: a nanostructured humidity sensor. *Chem Mater* 1995;7:2327–31.
- [36] Herzinger CM, Johns B, McGahan WA, Woollam JA, Paulson W. Ellipsometric determination of optical constants for silicon and thermally grown silicon dioxide via a multi-sample, multi-wavelength, multi-angle investigation. *J Appl Phys* 1998;83:3323–36.
- [37] Aspnes DE, Studna AA, Kinsbron E. Dielectric properties of heavily doped crystalline and amorphous silicon from 1.5 to 6.0 eV. *Phys Rev B* 1984;29:768–79.
- [38] Rehfeldt F, Tanaka M. Hydration forces in ultrathin films of cellulose. *Langmuir* 2003;19:1467–73.
- [39] Mikhaylova Y, Dutschk V, Bellmann C, Grundke K, Eichhorn KJ, Voit B. Study of the solid–liquid interface of hydroxyl-terminated hyperbranched aromatic polyesters (HBP-OH) in aqueous media. I. Characterisation of the properties and swelling behaviour of HBP-OH thin films. *Colloids Surf A* 2006;279:20–7.
- [40] Mathe G, Albersdorfer A, Neumaier KR, Sackmann E. Disjoining pressure and swelling dynamics of thin adsorbed polymer films under controlled hydration conditions. *Langmuir* 1999;15:8726–35.

- [41] Chen WL, Shull KR, Papapetrou T, Styrkas DA, Keddie JL. Equilibrium swelling of hydrophilic polyacrylates in humid environments. *Macromolecules* 1999;32:136–44.
- [42] Dinh HN, Birss VI. Characteristics of the polyaniline anodic pre-peak. *Electrochim Acta* 1999;44:4763–71.
- [43] Nabok AV, Hassan AK, Ray AK. Condensation of organic vapours within nanoporous calixarene thin films. *J Mater Chem* 2000;10:189–94.
- [44] Nabok AV, Lavrik NV, Kazantseva ZI, Nesterenko BA, Markovskiy LN, Kalchenko VI, Shvaniuk AN. Complexing properties of calix[4]resorcinolarene LB films. *Thin Solid Films* 1995;259:244–7.
- [45] Arwin H. TIRE and SPR-enhanced SE for adsorption processes. In: Hinrichs K, Eichhorn KJ, editors. *Ellipsometry of functional organic surfaces and films*. Springer series in surface sciences, vol. 52. Heidelberg: Springer-Verlag; 2014. p. 249–64.
- [46] Harris JJ, Bruening ML. Electrochemical and *in situ* ellipsometric investigation of the permeability and stability of layered polyelectrolyte films. *Langmuir* 2000;16:2006–13.
- [47] Forzani ES, Pérez MA, Teijelo ML, Calvo Ej. Redox driven swelling of layer-by-layer enzyme-polyelectrolyte multilayers. *Langmuir* 2002;18:9867–73.
- [48] Tagliazucchi M, Grumelli D, Calvo Ej. Nanostructured modified electrodes: role of ions and solvent flux in redox active polyelectrolyte multilayer films. *PCCP* 2006;8:5086–95.
- [49] Crossland EJW, Rahimi K, Reiter G, Steiner U, Ludwigs S. Systematic control of nucleation density in poly(3-hexylthiophene) thin films. *Adv Funct Mater* 2011;21:518–24.
- [50] Simons K, Nijmeijer K, Sala JG, van der Werf H, Benes NE, Dingemans TJ, Wessling M. CO₂ sorption and transport behavior of ODPA-based polyetherimide polymer films. *Polymer* 2010;51:3907–17.
- [51] Müller Y, Tot I, Potthast A, Rosenau T, Zimmermann R, Eichhorn KJ, Nitschke C, Scherr G, Freudenberg U, Werner C. The impact of esterification reactions on physical properties of cellulose thin films. *Soft Matter* 2010;6:3680–4.
- [52] Hegewald J, Schmidt T, Eichhorn KJ, Kretschmer K, Kuckling D, Arndt KF. Electron beam irradiation of poly(vinyl methyl ether) films. 2. Temperature-dependent swelling behavior. *Langmuir* 2006;22:5152–9.
- [53] Pantelić N, Wansapura CM, Heineman WR, Seliskar CJ. Dynamic *in situ* spectroscopic ellipsometry of the reaction of aqueous iron(II) with 2,2'-bipyridine in a thin nafion film. *J Phys Chem B* 2005;109:13971–9.
- [54] Zudans I, Heineman WR, Seliskar CJ. In situ dynamic measurements of sol-gel processed thin chemically selective PDMAAC-silica films by spectroscopic ellipsometry. *Chem Mater* 2004;16:3339–47.
- [55] Richardson H, López-García f, Sferrazza M, Keddie JL. Thickness dependence of structural relaxation in spin-cast, glassy polymer thin films. *Phys Rev E* 2004;70, 051805/1–8.
- [56] Ogieglo W, Wormeester H, Wessling M, Benes NE. Spectroscopic ellipsometry analysis of a thin film composite membrane consisting of polysulfone on a porous α -alumina support. *ACS Appl Mater Interfaces* 2012;4:935–43.
- [57] Sirard SM, Ziegler KJ, Sanchez IC, Green PF, Johnston KP. Anomalous properties of poly(methyl methacrylate) thin films in supercritical carbon dioxide. *Macromolecules* 2002;35:1928–35.
- [58] Woollam JA, Johs B, Herzinger CM, Hilfiker J, Synowicki R, Bungay CL. Overview of variable angle spectroscopic ellipsometry (VASE), Part I: Basic theory and typical applications. *Proc SPIE Opt Metrol 1999;CR72:3–28.*
- [59] Press WH, Teukolsky SA, Vetterling WT, Flannery BP. *Numerical recipes in C*. Cambridge: Cambridge University Press; 1992, 994 pp.
- [60] Jellison Jr GE. Data analysis for spectroscopic ellipsometry. *Thin Solid Films* 1993;234:416–22.
- [61] Jenkins RA, White HE. *Fundamentals of optics*. New York: McGraw-Hill; 1976, 637 pp.
- [62] Johs B, Hale JS. Dielectric function representation by B-splines. *Phys Status Solidi A* 2008;205:715–9.
- [63] Anonymous. Complete EASE™ data analysis manual. Version 4.05. Lincoln, NE: J. A. Woollam Co. Inc.; 2009, 274 pp.
- [64] Richardson H, Sferrazza M, Keddie JL. Influence of the glass transition on solvent loss from spin-cast glassy polymer thin films. *Eur Phys J E* 2003;12:87–91.
- [65] López García f, Keddie JL, Sferrazza M. Probing the early stages of solvent evaporation and relaxation in solvent-cast polymer thin films by spectroscopic ellipsometry. *Surf Interface Anal* 2011;43:1448–52.
- [66] Hennig A, Eichhorn KJ, Staudinger U, Sahre K, Rogalli M, Stamm M, Neumann AW, Grundke K. Contact angle hysteresis: study by dynamic cycling contact angle measurements and variable angle spectroscopic ellipsometry on polyimide. *Langmuir* 2004;20:6685–91.
- [67] Sechrist KE, Nolte AJ. Humidity swelling/deswelling hysteresis in a polyelectrolyte multilayer film. *Macromolecules* 2011;44:2859–65.
- [68] Sirard SM, Green PF, Johnston KP. Spectroscopic ellipsometry investigation of the swelling of poly(dimethylsiloxane) thin films with high pressure carbon dioxide. *J Phys Chem B* 2001;105:766–72.
- [69] Schmidt DJ, Cebeci FC, Kalcioğlu ZI, Wyman SG, Ortiz C, Van Vliet KJ, Hammond PT. Electrochemically controlled swelling and mechanical properties of a polymer nanocomposite. *ACS Nano* 2009;3:2207–16.
- [70] Wormeester H, Kooij ES, Mewe A, Rekveld S, Poelsema B. Ellipsometric characterisation of heterogeneous 2D layers. *Thin Solid Films* 2004;455–456:323–34.
- [71] Michels A, Hamers J. The effect of pressure on the refractive index of CO₂: the Lorentz–Lorenz formula. *Physica* 1937;4:995–1006.
- [72] Xiao GZ, Adnet A, Zhang Z, Sun FC, Grover CP. Monitoring changes in the refractive index of gases by means of a fiber optic Fabry–Perot interferometer sensor. *Sens Actuators A* 2005;118:177–82.
- [73] Besserer GJ, Robinson DB. Refractive indexes of ethane, carbon dioxide, and isobutane. *J Chem Eng Data* 1973;18:137–40.
- [74] Pham JQ, Sirard SM, Johnston KP, Green PF. Pressure, temperature, and thickness dependence of CO₂-induced devitrification of polymer films. *Phys Rev Lett* 2003;91:175503.
- [75] Wind JD, Sirard SM, Paul DR, Green PF, Johnston KP, Koros WJ. Relaxation dynamics of CO₂ diffusion, sorption, and polymer swelling for plasticized polyimide membranes. *Macromolecules* 2003;36:6442–8.
- [76] Wind JD, Sirard SM, Paul DR, Green PF, Johnston KP, Koros WJ. Carbon dioxide-induced plasticization of polyimide membranes: pseudo-equilibrium relationships of diffusion, sorption, and swelling. *Macromolecules* 2003;36:6433–41.
- [77] Carla V, Wang K, Hussain Y, Efimenko K, Genzer J, Grant C, Sarti GC, Carbonell RG, Doghieri F. Nonequilibrium model for sorption and swelling of bulk glassy polymer films with supercritical carbon dioxide. *Macromolecules* 2005;38:10299–313.
- [78] Horn NR, Paul DR. Carbon dioxide sorption and plasticization of thin glassy polymer films tracked by optical methods. *Macromolecules* 2012;45:2820–34.
- [79] Li Y, Park Ej, Lim KT, Johnston KP, Green PF. Role of interfacial interactions on the anomalous swelling of polymer thin films in supercritical carbon dioxide. *J Polym Sci B Polym Phys* 2007;45:1313–24.
- [80] Chandler CM, Vogt BD, Francis TJ, Watkins JJ. Unexpected scaling behavior of the order–disorder transition of nearly symmetric polystyrene-block-polysoprene diblock copolymers diluted with a nominally neutral solvent at very low dilution. *Macromolecules* 2009;42:4867–73.
- [81] Struik LCE. Physical aging in amorphous glassy polymers. *Ann NY Acad Sci* 1976;279:78–85.
- [82] Filippova NL. Interdiffusion in polymer film by ellipsometry. *J Colloid Interface Sci* 1999;212:589–92.
- [83] Elbs H, Krausch G. Ellipsometric determination of Flory–Huggins interaction parameters in solution. *Polymer* 2004;45:7935–42.
- [84] Pham JQ, Johnston KP, Green PF. Retrograde vitrification in CO₂/polystyrene thin films. *J Phys Chem B* 2004;108:3457–61.
- [85] Nolte AJ, Treat ND, Cohen RE, Rubner MF. Effect of relative humidity on the young's modulus of polyelectrolyte multilayer films and related nonionic polymers. *Macromolecules* 2008;41:5793–8.
- [86] Filippov LK. Study of diffusion in films on planar substrates by ellipsometry. *J Chem Soc Faraday Trans* 1993;89:4053–7.
- [87] Atarashi H, Hirai T, Horii K, Hino M, Morita H, Serizawa T, Tanaka K. Uptake of water in as-spun poly (methyl methacrylate) thin films. *RSC Adv* 2013;3:3516–9.
- [88] Freudenberg U, Zimmermann R, Schmidt K, Behrens SH, Werner C. Charging and swelling of cellulose films. *J Colloid Interface Sci* 2007;309:360–5.
- [89] Eichhorn KJ, Sahre K, Günther M, Suchanek G, Gerlach G. Swelling of a thin B⁺ implanted polyimide layer – a dynamic spectroscopic ellipsometry study. *Thin Solid Films* 2004;455–456:292–4.
- [90] Sahre K, Eichhorn KJ, Günther M, Suchanek G, Gerlach G. Water sorption properties of carbonized layers produced by controlled B⁺ bombardment of thin polyimide and polysulfone films. *Anal Bioanal Chem* 2004;378:396–401.

- [91] Rowe BW, Freeman BD, Paul DR. Effect of sorbed water and temperature on the optical properties and density of thin glassy polymer films on a silicon substrate. *Macromolecules* 2007;40:2806–13.
- [92] Spaeth K, Gauglitz G. Characterisation of the optical properties of thin polymer films for their application in detection of volatile organic compounds. *Mater Sci Eng C* 1998;5: 187–91.
- [93] Spaeth K, Kraus G, Gauglitz G. In-situ characterization of thin polymer films for applications in chemical sensing of volatile organic compounds by spectroscopic ellipsometry. *Fresenius J Anal Chem* 1997;357:292–6.
- [94] Rathgeb F, Reichl D, Herold M, Mader O, Mutschler T, Gauglitz G. Dyeless optical detection of ammonia in the gaseous phase using a pH-responsive polymer – characterization of the sorption process. *Fresenius J Anal Chem* 2000;368:192–5.
- [95] Schmidt S, Motschmann H, Hellweg T, von Klitzing R. Thermoresponsive surfaces by spin-coating of PNIPAM-co-PAA microgels: a combined AFM and ellipsometry study. *Polymer* 2008;49:749–56.
- [96] Gensel J, Liedel C, Schoberth HG, Tsarkova L. Microstructure-macro-response relationship in swollen block copolymer films. *Soft Matter* 2009;5:2534–7.
- [97] Zettl U, Knoll A, Tsarkova L. Effect of confinement on the mesoscale and macroscopic swelling of thin block copolymer films. *Langmuir* 2010;26:6610–7.
- [98] Pantelić N, Andria SE, Heineman WR, Seliskar CJ. Characterization of partially sulfonated polystyrene-block-poly(ethylene-ran-butylene)-block-polystyrene thin films for spectroelectrochemical sensing. *Anal Chem* 2009;81:6756–64.
- [99] Yagüe JL, Gleason KK. Systematic control of mesh size in hydrogels by initiated chemical vapor deposition. *Soft Matter* 2012;8: 2890–4.
- [100] Lau KKS, Gleason KK. All-dry synthesis and coating of methacrylic acid copolymers for controlled release. *Macromol Biosci* 2007;7:429–34.
- [101] Decher G. Fuzzy nanoassemblies: toward layered polymeric multicomposites. *Science* 1997;277:1232–7.
- [102] Hiller J, Rubner MF. Reversible molecular memory and pH-switchable swelling transitions in polyelectrolyte multilayers. *Macromolecules* 2003;36:4078–83.
- [103] Halthur TJ, Claesson PM, Eloffson UM. Stability of polypeptide multilayers as studied by *in situ* ellipsometry: effects of drying and post-buildup changes in temperature and pH. *J Am Chem Soc* 2004;126:17009–15.
- [104] Tanchak OM, Barrett CJ. Swelling dynamics of multilayer films of weak polyelectrolytes. *Chem Mater* 2004;16:2734–9.
- [105] Wong JE, Rehfeldt F, Hänni P, Tanaka M, Klitzing RV. Swelling behavior of polyelectrolyte multilayers in saturated water vapor. *Macromolecules* 2004;37:7285–9.
- [106] Burke SE, Barrett CJ. Swelling behavior of hyaluronic acid/polyallylamine hydrochloride multilayer films. *Biomacromolecules* 2005;6:1419–28.
- [107] Itano K, Choi J, Rubner MF. Mechanism of the pH-induced discontinuous swelling/deswelling transitions of poly(allylamine hydrochloride) – containing polyelectrolyte multilayer films. *Macromolecules* 2005;38:3450–60.
- [108] Miller MD, Bruening ML. Correlation of the swelling and permeability of polyelectrolyte multilayer films. *Chem Mater* 2005;17:5375–81.
- [109] Olugebefola SC, Ryu SW, Nolte AJ, Rubner MF, Mayes AM. Photo-cross-linkable polyelectrolyte multilayers for 2-D and 3-D patterning. *Langmuir* 2006;22:5958–62.
- [110] Blacklock J, Sievers TK, Handa H, You YZ, Oupicky D, Mao G, Mohwald H. Cross-linked bioreducible layer-by-layer films for increased cell adhesion and transgene expression. *J Phys Chem B* 2010;114:5283–91.
- [111] Fiche JB, Laredo T, Tanchak O, Lipkowski J, Dutcher JR, Yada RY. Influence of an electric field on oriented films of DMPC/gramicidin bilayers: a circular dichroism study. *Langmuir* 2010;26: 1057–66.
- [112] Tan WS, Cohen RE, Rubner MF, Sukhishvili SA. Temperature-induced, reversible swelling transitions in multilayers of a cationic triblock copolymer and a polyacid. *Macromolecules* 2010;43:1950–7.
- [113] Xu L, Zhu Z, Sukhishvili SA. Polyelectrolyte multilayers of diblock copolymer micelles with temperature-responsive cores. *Langmuir* 2011;27:409–15.
- [114] Doodo S, Balzer BN, Hugel T, Laschewsky A, Von Klitzing R. Effect of ionic strength and layer number on swelling of polyelectrolyte multilayers in water vapour. *Soft Mater* 2013;11:157–64.
- [115] Han L, Mao Z, Wu J, Guo Y, Ren T, Gao C. Directional cell migration through cell-cell interaction on polyelectrolyte multilayers with swelling gradients. *Biomaterials* 2013;34:975–84.
- [116] Murphy EF, Lu JR, Lewis AL, Brewer J, Russell J, Stratford P. Characterization of protein adsorption at the phosphoryl-choline incorporated polymer–water interface. *Macromolecules* 2000;33:4545–54.
- [117] Murphy EF, Lu JR, Brewer J, Russell J, Penfold J. The reduced adsorption of proteins at the phosphoryl choline incorporated polymer–water interface. *Langmuir* 1999;15: 1313–22.
- [118] Shirshov YM, Zynio SA, Matsas EP, Beketov GV, Prokhorovich AV, Venger EF, Markovskiy LN, Kalchenko VI, Soloviov AV, Merker R. Optical parameters of thin calixarene films and their response to benzene, toluene and chloroform adsorption. *Supramol Sci* 1997;4:491–4.
- [119] Nerapsuri V, Keddie JL, Vincent B, Bushnak IA. Swelling and deswelling of adsorbed microgel monolayers triggered by changes in temperature, pH, and electrolyte concentration. *Langmuir* 2006;22:5036–41.
- [120] Burkert S, Schmidt T, Gohs U, Dorschner H, Arndt KF. Cross-linking of poly(N-vinyl pyrrolidone) films by electron beam irradiation. *Radiat Phys Chem* 2007;76:1324–8.
- [121] Pathak SC, Hess DW. Dissolution and swelling behaviour of plasma-polymerized polyethylene glycol-like hydrogel films for use as drug delivery reservoirs. *ECS Trans* 2008;6(20):1–12.
- [122] Richter A, Janke A, Zschoche S, Zimmermann R, Simon F, Eichhorn KJ, Voit B, Appelhans D. PH-stable hyperbranched poly(ethyleneimine)-maltoose films for the interaction with phosphate containing drugs. *New J Chem* 2010;34:2105–8.
- [123] Beyerlein D, Belge G, Eichhorn K-J, Gauglitz G, Grundke K, Voit B. Preparation and properties of thin films of hyperbranched polyesters with different end groups. *Macromol Symp* 2001;164:117–32.
- [124] Van Der Zeeuw EA, Sagis LMC, Koper GJM, Mann EK, Haarmans MT, Bedaux D. The suitability of scanning angle reflectometry for colloidal particle sizing. *J Chem Phys* 1996;105: 1646–53.
- [125] Emmerzael R, van der Zeeuw E, Koper G. The use of reflectometry for the study of swelling of latex particles at a silica surface. *Prog Colloid Polym Sci* 1997;104:107–9.
- [126] Ciuffi N, Torsi L, Farella I, Altamura D, Valentini A, Ditaranto N, Sabatini L, Zambonin PG, Bleve-Zacheo T. Deposition and analytical characterization of fluoropolymer thin films modified by palladium nanoparticles. *Thin Solid Films* 2004;449:25–33.
- [127] Chan K, Gleason KK. Initiated chemical vapor deposition of linear and cross-linked poly(2-hydroxyethyl methacrylate) for use as thin-film hydrogels. *Langmuir* 2005;21:8930–9.
- [128] Horcajada P, Serre C, Grosso D, Boissiere C, Perruchas S, Sanchez C, Ferey G. Colloidal route for preparing optical thin films of nanoporous metal-organic frameworks. *Adv Mater* 2009;21:1931–5.
- [129] Abuin GC, Cecilia Fuertes M, Corti HR. Substrate effect on the swelling and water sorption of Nafion nanomembranes. *J Membr Sci* 2013;428:507–15.
- [130] Warendra M, Richter A, Schmidt D, Janke A, Muller M, Simon F, Zimmermann R, Eichhorn KJ, Voit B, Appelhans D. Fabricating pH-stable and swellable very thin hyperbranched poly(ethylene imine)-oligosaccharide films fabricated without precoating: first view on protein adsorption. *Macromol Rapid Commun* 2012;33:1466–73.
- [131] Schiebener P, Straub J, Sengers JL, Gallagher J. Refractive index of water and steam as function of wavelength, temperature and density. *J Phys Chem Ref Data* 1990;19:677–717.
- [132] Thormählen I, Straub J, Grigull U. Refractive index of water and its dependence on wavelength, temperature, and density. *J Phys Chem Ref Data* 1985;14:933–45.
- [133] Wohlfarth C. Refractive index of hexane. In: Lechner MD, editor. *Refractive indices of pure liquids and binary liquid mixtures (supplement to III/38)*. Condensed matter series, vol. 47. Berlin, Heidelberg; 2008. p. 348–54.
- [134] Aminabhavi TM, Patil VB, Aralaguppi MI, Phayde HTS. Density, viscosity, and refractive index of the binary mixtures of cyclohexane with hexane, heptane, octane, nonane, and decane at (298.15, 303.15, and 308.15) K. *J Chem Eng Data* 1996;41:521–5.
- [135] Wohlfarth C. Refractive index of toluene. In: Lechner MD, editor. *Refractive indices of pure liquids and binary liquid mixtures (supplement to III/38)*. Condensed matter series., vol. 47. Berlin, Heidelberg; 2008. p. 390–5.

- [136] Aminabhavi TM, Patil VB. Density, viscosity, refractive index, and speed of sound in binary mixtures of ethenylbenzene with N,N-dimethylacetamide, tetrahydrofuran, N,N-dimethylformamide, 1,4-dioxane, dimethyl sulfoxide, chloroform, bromoform, and 1-chloronaphthalene in the temperature interval (298.15–308.15) K. *J Chem Eng Data* 1998;43:497–503.
- [137] Wohlfarth C. Refractive index of ethanol. In: Lechner MD, editor. Refractive indices of pure liquids and binary liquid mixtures (supplement to III/38). Condensed matter series, vol. 47. Berlin, Heidelberg; 2008. p. 108–15.
- [138] Kamiya Y, Naito Y, Hirose T, Mizoguchi K. Sorption and partial molar volume of gases in poly (dimethyl siloxane). *J Polym Sci B Polym Phys* 1990;28:1297–308.
- [139] Horn NR, Paul DR. Carbon dioxide plasticization and conditioning effects in thick vs. thin glassy polymer films. *Polymer* 2011;52:1619–27.
- [140] Carlà V, Hussain Y, Carbonell R, Doghieri F. Modeling solubility isotherms and sorption kinetics of supercritical carbon dioxide in initially glassy polymers using non-equilibrium thermodynamics. In: AIChE Ann Meeting Conf Proc. 2006, 6 pp.
- [141] Carlà V, Hussain Y, Grant C, Sarti GC, Carbonell RG, Doghieri F. Modeling sorption kinetics of carbon dioxide in glassy polymeric films using the nonequilibrium thermodynamics approach. *Ind Eng Chem Res* 2009;48:3844–54.
- [142] Collins RW, Yang BY. In situ ellipsometry of thin film deposition: Implications for amorphous and microcrystalline Si growth. *J Vac Sci Technol B* 1989;7:1155–64.
- [143] Jellison Jr GE, Chisholm MF, Gorbatkin SM. Optical functions of chemical vapor deposited thin film silicon determined by spectroscopic ellipsometry. *Appl Phys Lett* 1993;62:3348–50.
- [144] Elwing H. Protein absorption and ellipsometry in biomaterial research. *Biomaterials* 1998;19:397–406.
- [145] Spuller MT, Perchuk RS, Hess DW. Evaluating photoresist dissolution, swelling, and removal with an in situ film refractive index and thickness monitor. *J Electrochem Soc* 2005;152: G40–G4.
- [146] Foose LL, Blanch HW, Radke CJ. Effect of sodium dodecylbenzene sulfonate on subtilisin carlsberg proteolysis of an immobilized ovalbumin film. *Biotechnol Bioeng* 2009;102:1273–7.
- [147] Wessling M, Schoeman S, van der Boomgaard T, Smolders CA. Plasticization of gas separation membranes. *Gas Sep Purif* 1991;5: 222–8.
- [148] Wessling M, Huisman I, Boomgaard Tvd, Smolders CA. Dilution kinetics of glassy, aromatic polyimides induced by carbon dioxide sorption. *J Polym Sci B Polym Phys* 1995;33:1371–84.
- [149] Berens AR, Hopfenberg HB. Diffusion and relaxation in glassy polymer powders: 2. Separation of diffusion and relaxation parameters. *Polymer* 1978;19:489–96.
- [150] Aspnes DE. Optical properties of thin films. *Thin Solid Films* 1982;89:249–62.
- [151] Aspnes DE. Local-field effects and effective-medium theory: a microscopic perspective. *Am J Phys* 1982;50:704–9.
- [152] Born M, Wolf E, Bhatia AB. Principles of optics. Electromagnetic theory of propagation, interference and diffraction of light. Cambridge, UK: Cambridge University Press; 2000, 936 pp.
- [153] Sirard SM, Castellanos H, Green PF, Johnston KP. Spectroscopic ellipsometry of grafted poly(dimethylsiloxane) brushes in carbon dioxide. *J Supercrit Fluids* 2004;32:265–73.
- [154] Ogieglo W, Wormeester H, Wessling M, Benes NE. Effective medium approximations for penetrant sorption in glassy polymers accounting for excess free volume. *Polymer* 2014;55: 1737–44.
- [155] Flory PJ. Principles of polymer chemistry. Ithaca, NY: Cornell University Press; 1953, 672 pp.
- [156] Flory PJ, Rehner JJ. Statistical mechanics of cross-linked polymer networks II. Swelling. *J Chem Phys* 1943;11:521–6.
- [157] Schneider MF, Mathe G, Tanaka M, Gege C, Schmidt RR. Thermodynamic properties and swelling behavior of glycolipid monolayers at interfaces. *J Phys Chem B* 2001;105:5178–85.
- [158] Rehfeldt F, Tanaka M, Pagnoni L, Jordan R. Static and dynamic swelling of grafted poly(2-alkyl-2-oxazoline)s. *Langmuir* 2002;18:4908–14.
- [159] Lavalle P, Gergely C, Cuisinier FJG, Decher G, Schaaf P, Voegel JC, Picart C. Comparison of the structure of polyelectrolyte multilayer films exhibiting a linear and an exponential growth regime: an in situ atomic force microscopy study. *Macromolecules* 2002;35:4458–65.
- [160] Dubas ST, Schlenoff JB. Swelling and smoothing of polyelectrolyte multilayers by salt. *Langmuir* 2001;17:7725–7.
- [161] Suárez MF, Compton RG. In situ atomic force microscopy study of polypyrrole synthesis and the volume changes induced by oxidation and reduction of the polymer. *J Electroanal Chem* 1999;462:211–21.
- [162] Takada K, Diaz DJ, Abruna HD, Cuadrado I, Casado C, Alonso B, Moran M, Losada J. Redox-active ferrocenyl dendrimers: thermodynamics and kinetics of adsorption. In-situ electrochemical quartz crystal microbalance study of the redox process and tapping mode AFM imaging. *J Am Chem Soc* 1997;119:10763–73.
- [163] Liu G, Zhang G. Collapse and swelling of thermally sensitive poly(N-isopropylacrylamide) brushes monitored with a quartz crystal microbalance. *J Phys Chem B* 2004;109:743–7.
- [164] Rodenhausen KB, Kasputis T, Pannier AK, Gerasimov JY, Lai RY, Solinsky M, Tiwald TE, Wang H, Sarkar A, Hofmann T, Ianno N, Schubert M. Combined optical and acoustical method for determination of thickness and porosity of transparent organic layers below the ultra-thin film limit. *Rev Sci Instrum* 2011;82: 10311.
- [165] Richter R, Rodenhausen KB, Eisele N, Schubert M. Coupling spectroscopic ellipsometry and quartz crystal microbalance to study organic films at the solid–liquid interface. In: Hinrichs K, Eichhorn KJ, editors. Ellipsometry of functional organic surfaces and films. Springer series in surface sciences, vol. 52. Heidelberg: Springer-Verlag; 2014. p. 223–48.
- [166] Rouessac V, van der Lee A, Bosc F, Durand J, Ayral A. Three characterization techniques coupled with adsorption for studying the nanoporosity of supported films and membranes. *Micropor Mesopor Mater* 2008;111:417–28.
- [167] Lee D, Nolte AJ, Kunz AL, Rubner MF, Cohen RE. pH-induced hysteretic gating of track-etched polycarbonate membranes: swelling/deswelling behavior of polyelectrolyte multilayers in confined geometry. *J Am Chem Soc* 2006;128:8521–9.
- [168] Furchner A, Bittrich E, Uhlmann P, Eichhorn KJ, Hinrichs K. In-situ characterization of the temperature-sensitive swelling behavior of poly(N-isopropylacrylamide) brushes by infrared and visible ellipsometry. *Thin Solid Films* 2013;541:41–5.